# GEOPHYSICAL SITE INVESTIGATION OF THE FEDERAL COLLEGE OF EDUCATION, ZARIA, NIGERIA

**BY**

**SAMINU OLATUNJI, B.Sc. (Ed),**
**UNIVERSITY OF ILORIN**

•

**A THESIS SUBMITTED TO THE POSTGRADUATE SCHOOL, AHMADU BELLO UNIVERSITY, ZARIA IN PARTIAL FULFILMENT, OF THE REQUIREMENTS FOR THE AWARD OF THE DEGREE OF MASTER OF SCIENCE IN APPLIED GEOPHYSICS**

**DEPARTMENT OF PHYSICS**
**FACULTY OF SCIENCE**
**AHMADU BELLO UNIVERSITY**
**ZARIA**

***AUGUST, 1999***

# DECLARATION

The author of this work hereby declare that this is the original report of the research carried out by him under the supervision of Professor I. B. Osazuwa. Any part or the whole of this work has never been presented in whatever form to any institution apart from Ahmadu Bello University, Zaria, Nigeria for the award of any degree other than this.

The works of others cited are duly acknowledged by means of references.

S. OLATUNJI
(AUTHOR)

# CERTIFICATION

This thesis titled "Geophysical site Investigation of the Federal College of Education Zaria, Nigeria" by Saminu Olatunji meets the regulation governing the award of the degree of Master of Science in Applied Geophysics of Ahmadu Bello University and is approved for its contribution to knowledge and library presentation.

Prof. I. B. Osazuwa
Chairman, Supervisory Committee

13/9/99
Date

Dr. M. N. Umego
Member, Supervisory Committee

13/9/99
Date

Prof. I. B. Osazuwa
Head of Department

13/9/99
Date

Prof. S.B Ojo
Dean, Postgraduate School

26/05/00
Date

# DEDICATION

Dedicated to my family.

# ACKNOWLEDGEMENT

I thank the Almighty God, for successfully sailing me through the rigour of this resourceful and promising research work.

My special thanks to Prof. I. B. Osazuwa, for encouraging me to study Applied Geophysics, assisting to secure the admission, suggesting the research topic to me and at the golden end of it all, supervising the research. I appreciate not only his assiduity, painstaking and enduring attitudes to my disturbing 'learner type' questioning habits in order to ensure the successful completion of this work, but for his daily helps both in deed and in need to me. May God reward him accordingly.

I equally thank Dr. M. N. Umego for his easy going and always approachable attitudes to me with numerous suggestions and academic contributions in the course of this study.

Prof. C. O. Ajayi, and Prof. S. B. Ojo can never be forgotten for their fatherly contributions in various forms to make my success in this study a reality.

I sincerely acknowledge the assistance offered me by the International Programme in the Physical Sciences (IPPS) of Uppsala University Sweden, by providing scientific facilities to the physics Department, Geophysics programme unit, which aided the smooth and timely completion of this work and also by providing the research grants for the field work and the final production of this thesis.

The efforts of the following eminent individuals are equally cherished. They are: Dr. V. Makinde of Physics Department, Federal College of Education (F.C.E.) Zaria; Mr. Alagbe of the Geology Department A. B. U., Zaria; Messrs. H.O. Aboh and C. Z. Akaolisa both of Kaduna Polytechnic, Kaduna and Mr. Emmanuel, K. Ogunleye, the Cartographer for Geography Department, A. B. U., Zaria.

I am grateful to the Provost, Federal College of Education, Zaria, Alhaji Mohammed Aliyu Shika, and the Management of the College for supporting me sincerely to ensure the completion of this work.

That a name is not mentioned here is not meant to disregard many others that contributed in whatever form, but the omission is as a result of space constraint. Please, pardon me and thank you all.

# ABSTRACT

A comprehensive geophysical survey was carried out over the premises of the Federal College of Education, Zaria, with a view to investigating the depth to basement, depth to and thickness of aquifer, depth to and thickness of the weathered basement as well as the subsurface structural systems such as the fractures and faults. The D.C. Resistivity and VLF methods were employed to accomplish the study. The conventional vertical Electrical Sounding (VES) using Schlumberger array was carried out at 40 stations, 8 of which were Radial stations with 4 profiles per station. So a total of 64 profiles were sounded. VLF data were taken from all the VES stations as well. ABM Terrameter (SAS 300P) was used to collect resistivity data while EM/6 VLF equipment was used to collect the VLF data. Results from the interpretation of the data collected suggest 3 layers in most parts of the area studied. However, there are cases of 2 layers. The resistivity value for the first layer (topsoil) varies from 30 to 300 ohm-meters with thickness ranging between 3.5 and 14 m. The second layer (weathered basement) has resistivity values of 84 to 480 ohm-meters and thickness of between 9 and 36.5 meters. Its depth varies from 5 to 14 meters. The third layer appeared to be the bedrock with the resistivity value as much as 3000 ohm-meters in some locations. Towards the eastern part of the study area, the fresh bedrock records the greatest depth of about 40.1 m. The depth of aquifer ranges from 1.5 to 4.0 meters while its thickness ranges from 5 to 14 m. Further, the geologic sections derived in this work together with the aquifer plots suggest that weathered basement in the area does not entirely represent a promising aquifer for the fact that in some cases, aquifers occurred both in the topsoil and in the weathered basement while it disappeared in some areas of weathered basement. Radial sounding plots revealed the existence of anisotropics, trending NE-SW, NVV-SE and E - W directions. The VLF interpretations similarly indicated the

presence of vertical contact or fractures zones which is more pronounced towards the western part of the survey area. The highest conductivity in the area occurs towards the west as can be seen from VLF plots. There is hence a strong water-bearing potential within the subsurface rocks in this part of the study area.

## TABLE OF CONTENTS

# LIST OF TABLES

# LIST OF FIGURES

# ABBREVIATIONS AND SYMBOLS USED

| | |
|---|---|
| F.C.E | Federal College of Education |
| VES | Vertical Electrical Sounding. |
| M | Metre |
| KM | Kilometre |
| NW-SE | Northwest-Southeast |
| NE-SW | Northeast-Southwest |
| N-E | North-East |
| E-W | East-West |
| ° | Degree |
| ' | Minute |
| " | Second |
| mV | Millivolt |
| Δ | Change |
| I | Electric Current |
| ρ | True Resistivity |
| $\rho_a$ | Apparent resistivity |
| A | Cross Sectional area, |
| V | Electric Potential |
| L | Length |
| % | Percentage |
| θ | Angle |
| K | Geometric Factor |
| VLF | Very Low Frequency |

| | |
|---|---|
| **MN** | Potential Electrode separation |
| **AB** | Current electrode separation |
| **π** | Pi (= 3.1416) |
| L.G.A. | Local Government Area |
| kHz | Kilohertz |
| **Hs** | Vertical Magnetic Field |
| **Hp** | Horizontal Magnetic Field |
| ***i.e.*** | That is |
| ***et al*** | And others |
| **Ω** | Ohms |

# CHAPTER ONE

## INTRODUCTION

### 1.1 Preamble

In carrying out the geophysical investigation of a site different methods can be employed. The one to be used depends on the nature and parameters to be investigated. Methods such as gravity and magnetic which are potential methods have been found to be greatly adequate in investigating the nature of underlying earth materials and in determining depth to bedrock (basement). Other methods such as the direct current (d.c.) resistivity methods and very low frequency (VLF) method have been found sufficient and cheap in investigating parameters like depth to water-table (aquifer), aquifer thickness, depth to basement, identification of weathered basement and fracture systems in rocks among others.

In this work the d.c. resistivity and VLF methods were used in carrying out the geophysical site investigation of the area covered by the Federal College of Education (F.C.E.), Zaria. The parameters investigated include depth to bedrock, aquifer thickness, depth to basement and distribution of weathered basement and fracture systems of the area.

### 1.2 Climate And Geomorphology of the Study Area

The Federal College of Education, Zaria is located North-East of Zaria Local Government Area (Fig. 1.1) in Kaduna State of Nigeria (Fig. 1.2). Substantial area of the site have been developed as shown in Figure 1.3. The College is bounded approximately by longitudes 7°43'21"E and 7°43'49"E and latitudes 11°5'10"N and 11°5'28"N within the

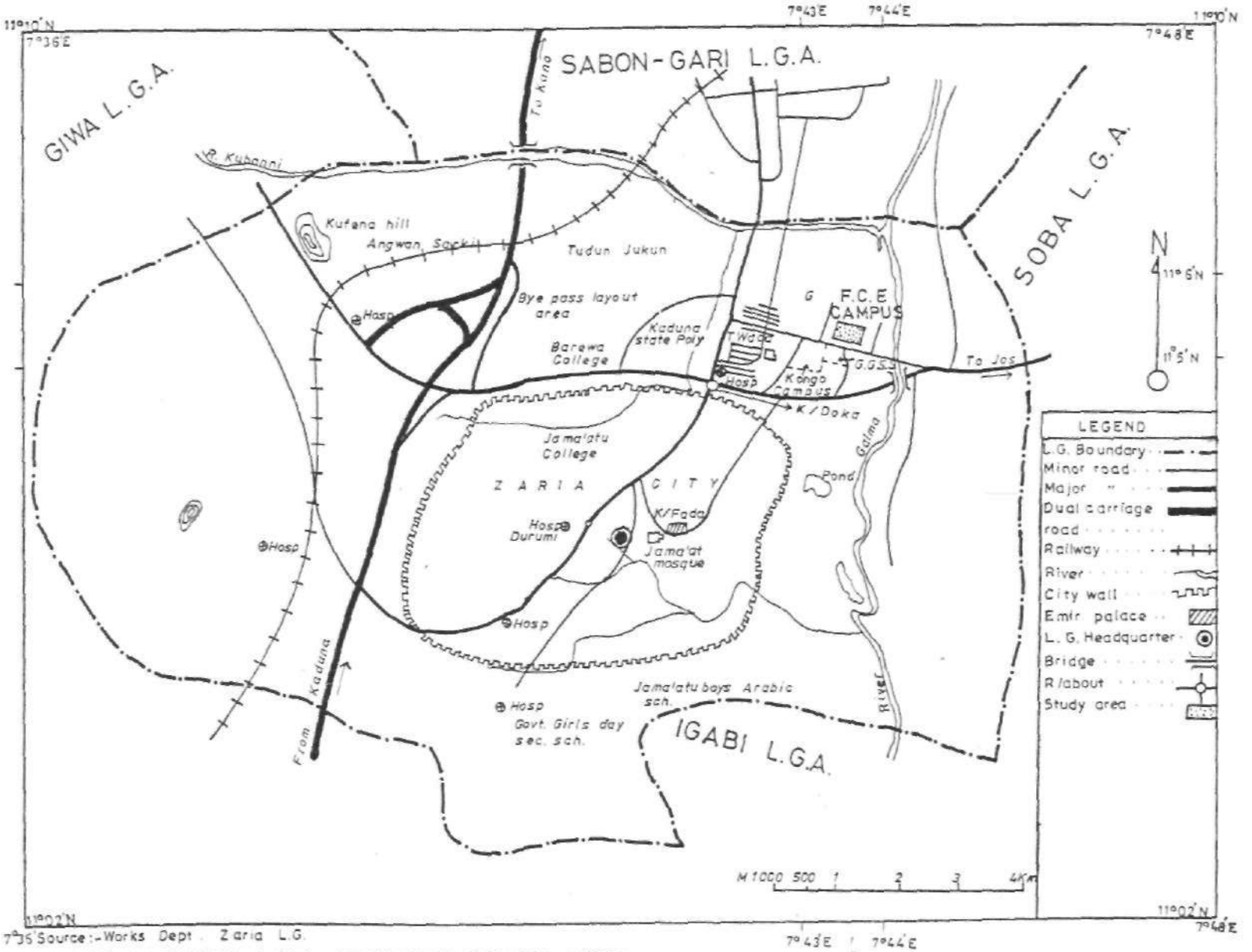


FIG. 1·1 ZARIA L.G.A. SHOWING STUDY AREA

Source :- Works Dept. Zaria L.G.

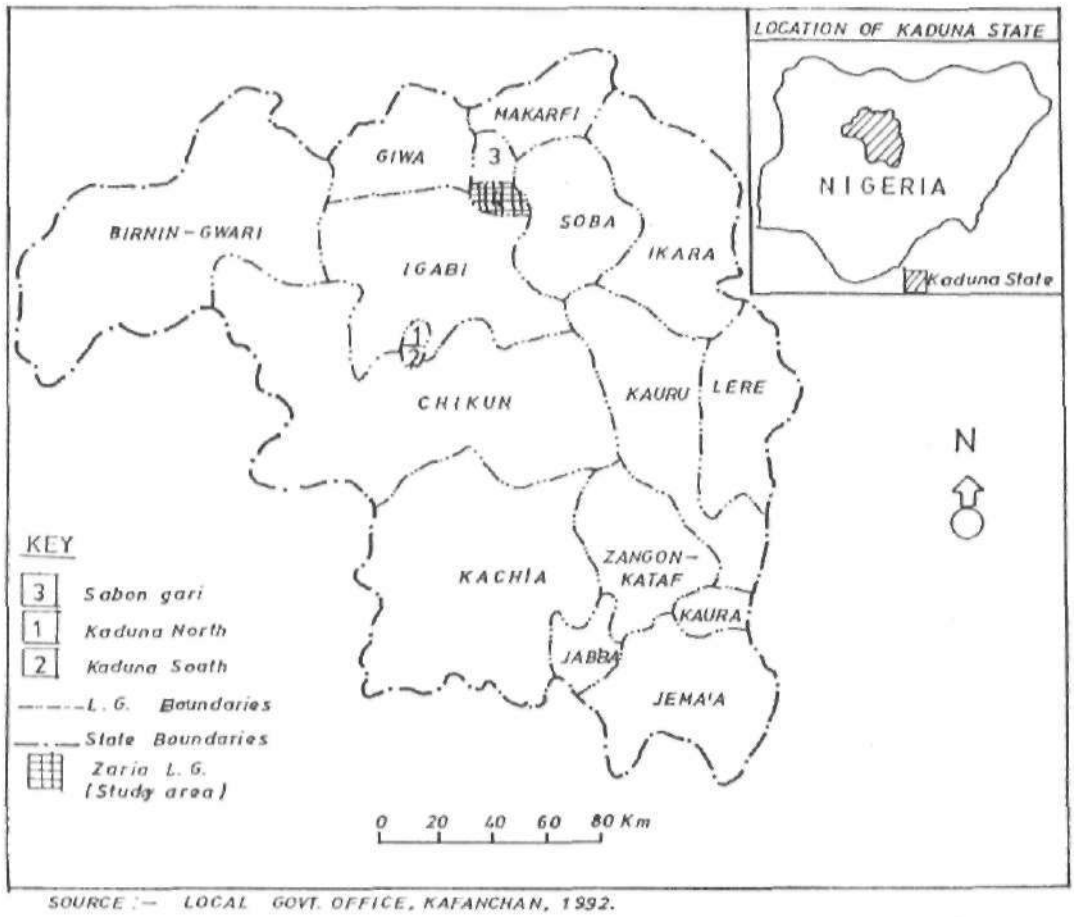


SOURCE :- LOCAL GOVT. OFFICE, KAFANCHAN, 1992.

FIG.1.2 KADUNA STATE SHOWING ZARIA L.G.A.

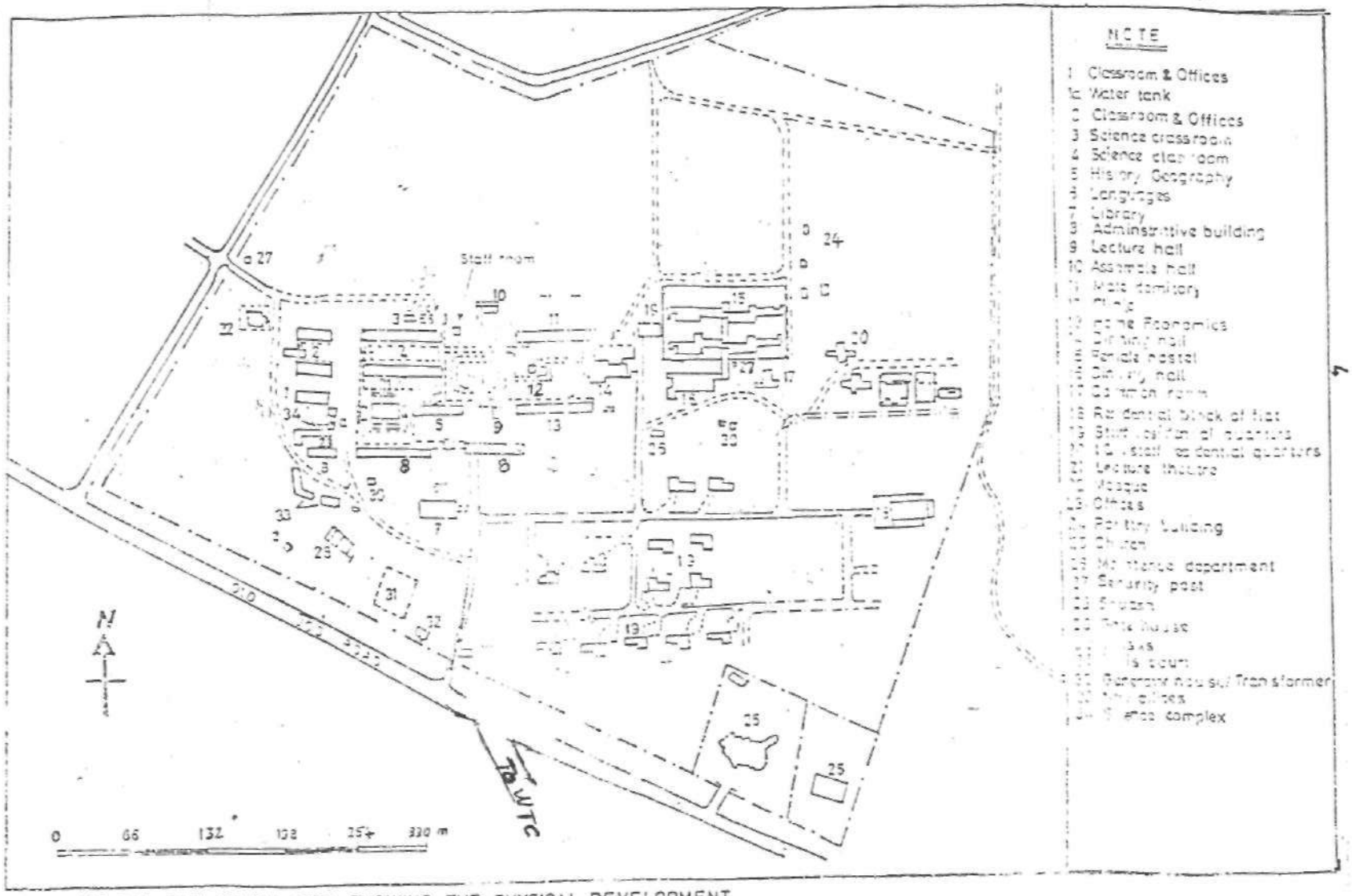


FIG. 1·3 THE STUDY AREA SHOWING THE PHYSICAL DEVELOPMENT

Zaria topographic map Sheet 102 SW. The entire Zaria area is located on a plateau at a height 570 m above sea-level possessing a tropical continental climate (Ologe, 1971).

The area can be reached through a federal high way from Kaduna through Zaria to Jos. The site is linked with a state tarried owned road branching to the west side when about reaching the outskirt of Zaria township via Jos, Plateau State (Fig. 1.1). The area is located at the extreme end of the southtern part of Kubanni River Basin.

The study area falls within the semi-arid zone of Nigeria (Harold, 1970). The mean annual rainfall over a period of 40 years for Zaria is 109.2 mm (Olufemi, 1985). Middle to the end of April marks the beginning of perennial rain and ends late October to early November. The greatest rainfall comes usually by August. The harmattan period, marking the coldest period with temperatures between 20°C and 30°C, starts in late December. The hottest period is in March with temperature rising above 35°C. Groundwater occurrence in this area is therefore,not only a consequence of hydrologic and geologic events, but also climatic in origin. The area also witnesses the invasion of two air masses: the nothern air mass that is dry and continental in origin, and the southern air mass which is moist, and comes from the Atlantic. This airmass which is cold and equitorial maritime in nature (Thorp, 1970).

Zaria area lies on the vast plain scenery gently undulating which extends East-west from lake Chad to Sokoto and Northwards from the southern parts of Kaduna to the Tigueddi scarp near Agades in Niger Republic (Thorp, 1970). The area has a rugged topography with two types of hilly features. Inselbergs which are massive granitic bodies like Kufena hill which is about 820 m above sea-level; an outcrop of sort which is prominent

at the extreme south-western part of the study area, mark the first type. The second type is whale backs which is numerous, but inconspicuous (McCurry, 1970).

The drainage system of Zaria area focuses on the River Galma, a major tributary to River Kaduna. It flows towards north, about 900m away from the Eastern fence of the study area. Kubanni river flows Eastward, about 500m away from the Northern fence of the study area. The confluence of Galma and Kubanni is about 1.0km away from the fence of the study area at North-Eastern direction (Fig. 1.1). Galma and Kubanni rivers carry water throughout the year unlike their smaller tributaries that are seasonal (Thorp, 1970).

## 1.3 Aim and Scope of this Study

The study site lacks detailed geophysical investigation as all previous geophysical works carried out around this site are regional in nature. The aim was to determine the depth to bedrock, aquifer thickness and depth, distribution of weathered basement and the fracture systems at the study area.

The work involved the use of Schlumberger array in d.c. resistivity and VLF methods which are considered sufficient to supply all the necessary information about the parameters of interest when appropriate computer programs were used to aid interpretations. Since the work covered the entire land of the college, hence it will also identify the the strategic and potential positions for the locations of boreholes, siting of high-rise buildings and possible depth of sewage system in order to avoid contamination of ground water.

## 1.4 Limitations

It was not possible to lay out regular grid because the study area has been developed with buildings and fences (Fig. 1.3). However, random stations were selected all over the area as much as the physical developments could afford and the program employed readily grided the area for easy interpretation.

Radial type of VES soundings at selected sites, with profiles spreading in the N-S, E-W, NE-SW and NW-SE directions, were carried out. The radial soundings were aimed at estimating the extent of anisothropy in the area. Radial sounding was impossible at all stations due to the presence of buildings and fences coupled with limited time available for the survey. However, radial soundings were carried out at 8 stations distributed over the area.

# CHAPTER TWO

# LITERATURE REVIEW

## 2.1 Review of Previous Studies in the Survey area.

### 2.1.1 Previous Geophysical Investigations

In spite of the fact that their locations were not specified, the presence of prominent, steeply dipping joints in some outcrops of granite in the Kubanni basin was reported (DU Preez, 1952). Some of the joints were found to contain ground- water (DU Preez, 1952). A remarkable work in the area is the aeromagnetic survey project carried out throughout the country by the geological survey of Nigeria. This culminated in the production of nation-wide aeromagnetic maps for uses in geophysical studies.

Danladi (1985) equally confirmed the presence of water- bearing fractures, but that aquifers are isolated and located at shallow basement areas of Zaria. This study site is located SE of the area surveyed by Hassan (1987). He reported that the bedrock is undulating, with depths of burial increasing towards the southern part of the present survey area. Hassan (1987) estimated the depths to vary between 5 and 60m in the north-south direction and that the area is likely to have been faulted or down-thrown.

### 2.1.2 Related Previous Studies

A regional study of Sheet 102 SW by Olowu (1967) revealed that with the exception of Galma river all streams in the area are seasonal and that the depth to water-table

increased progressively away from the banks of the river during dry season. He also reported the occurrence of ground- water in joints, weathered portion of basement complex and in overlying alluvium. Eigbefo (1978) not only confirmed that the depths to water-table at various points in Kubanni basin range between 3 and 10 m, he also found out the range of thickness of weathered basement to be 1 to 30m.

McCurry (1970) studied basement geology of Zaria and established that basement complex rock is made up of Older Granite and Biotite Granite Gneiss. Klinkenbera (1970) classified soils in Zaria under leached ferruginous tropical soils. According to him, the soil is weakly developed near the inselbergs and hydromorphic soils and formed fadama soils (i.e. subject to periodic flooding) and that the soils contain about 40 per cent clay at some depths.

On the weather and climatic studies of Zaria environs Hore (1970) informed that Zaria has tropical continental climate which he claimed to be most prominent in the dry seasons - around December and January. He confirmed the mean daily temperature of 31°C with maximum value of about 36°C which usually occurs around April. He concluded by giving 108.8 mm as the mean annual rainfall in Zaria.

## 2.2 Geology of the Survey Area

### 2.2.1 General

Nigeria lies in the Pan-African mobile belt, which has been affected by Pan-Africa events whose stages are Orogenic, Expierogenic, Tectonic and Metamorphic cycles. In Nigeria the geology comprises of Basement Complex and sedimentary basins. The

basement complex covers over 50% of the total land surface of Nigeria. The study area is located on the northern sector of the Nigerian Basement Complex (Fig. 2.1). The Basement Complex is divided into four broad types:

i) the Older metasediment

ii) the Younger metasediment

iii) the Older Granite and

iv) the Younger Granite and, both metavolcanics and Volcanics or Basement gneiss and Migmatite.

McCurry (1970) mapped 1200 $km^2$ area of Northern Nigeria which was later reviewed by Webb (1972) within which the study area falls. He presented a comprehensive location map of rock units in the area (Fig. 2.2). The map shows that the survey area lies on the Older Granite of the Basement Complex.

### 2.2.2 The Older Granite

Older Granite refers to rock series ranging in composition from Granite to Granodiorite Oyawoye (1964). Granite intrusion into the Nigeria basement occurred during the Eburnean and lower Cambrian ages. The Eburnean Granites are fine-grained Granites that represent a group of minor discordant intrusion of small aerial extent; occurring as dykes and irregular bodies. The group include Biotite and Muscovite Granite and Adamelites. They are pale brown equigranular and usually foliated. Their contact with the later Granite is complex, but in some places degradational and in some places replaced by the later Granites. The most common types of Older Granites are:

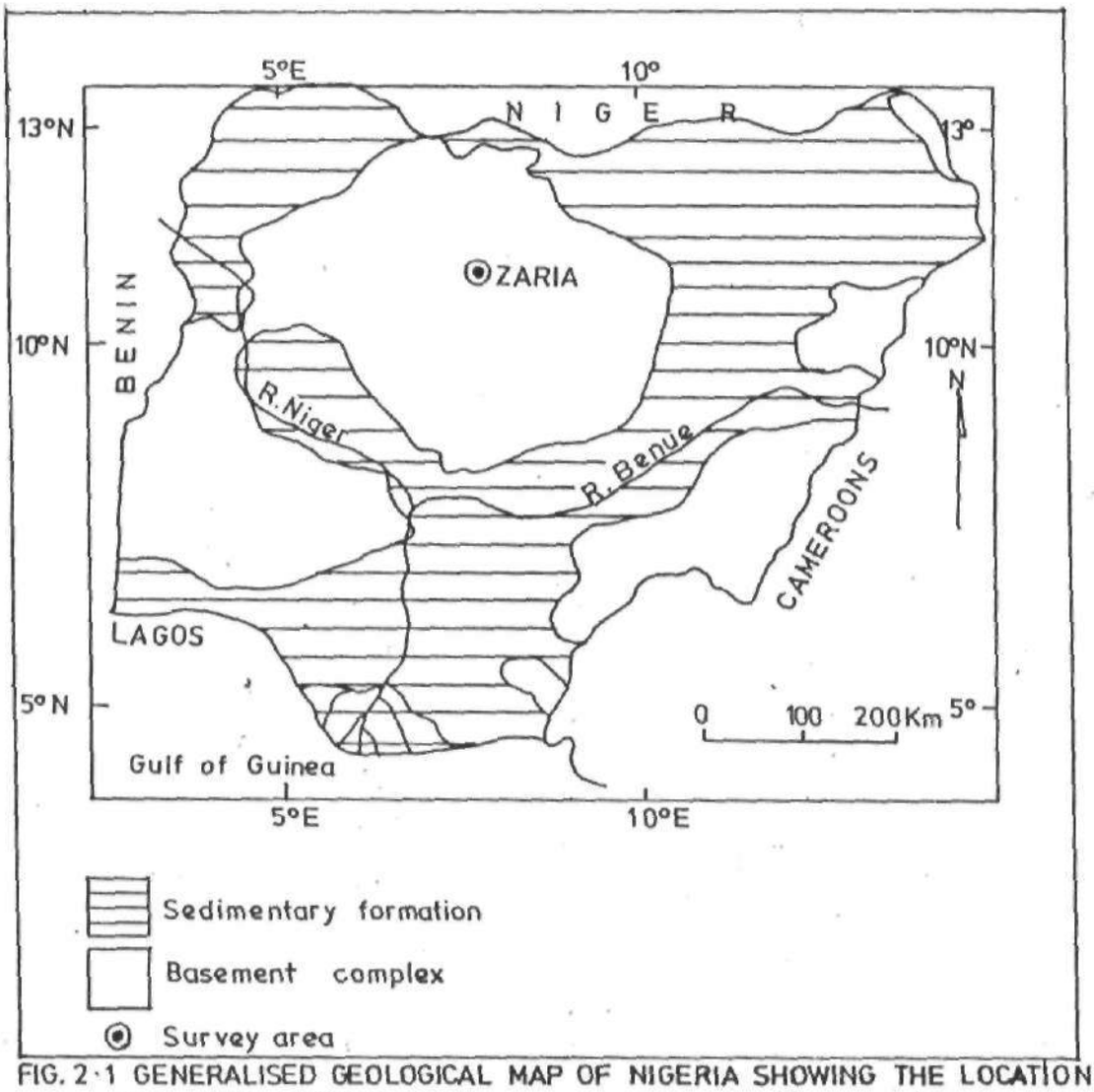


FIG. 2·1 GENERALISED GEOLOGICAL MAP OF NIGERIA SHOWING THE LOCATION OF THE SURVEY AREA.

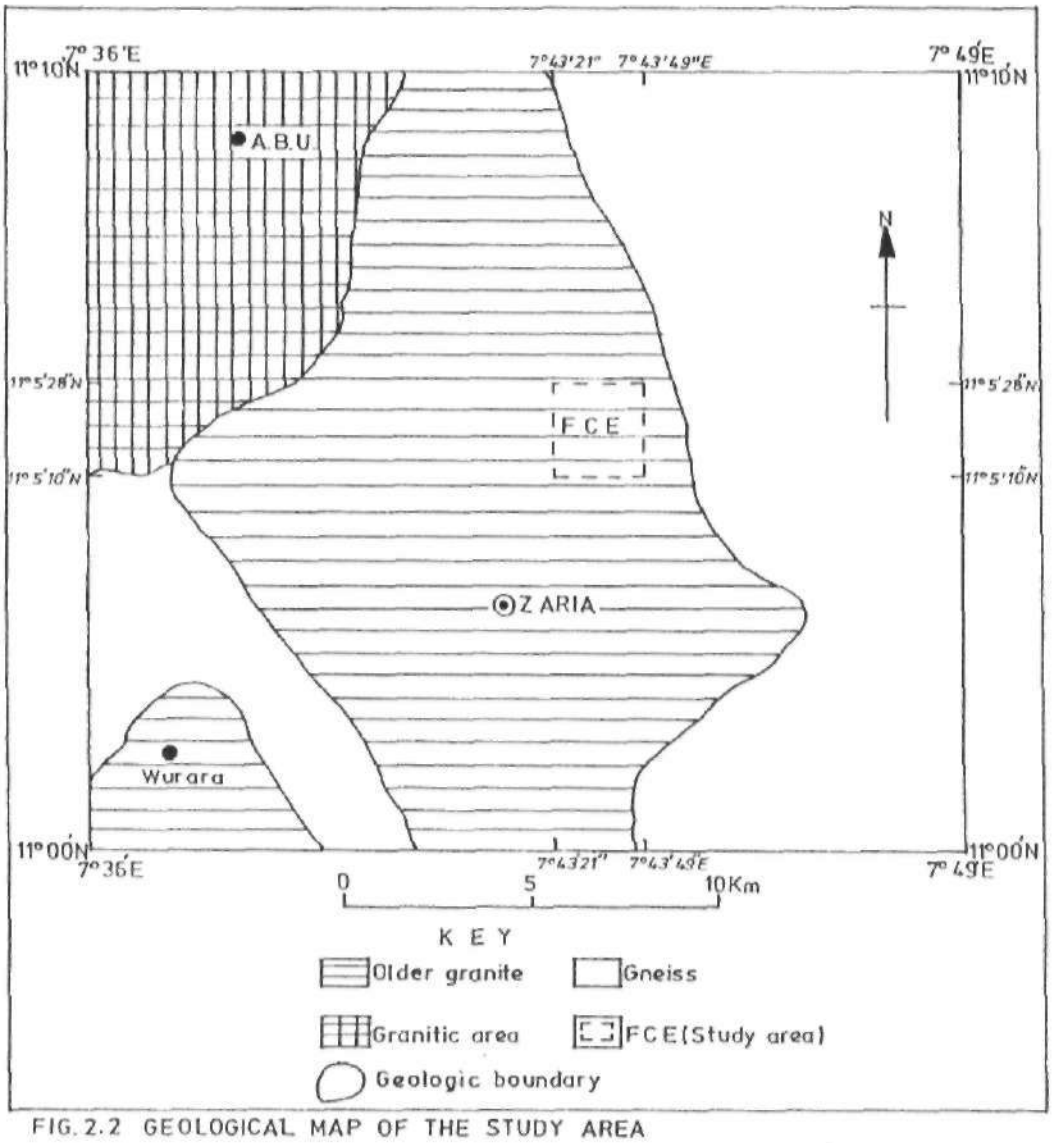


FIG. 2.2 GEOLOGICAL MAP OF THE STUDY AREA

i) Porphyritic Biotite Granite,

ii) Granodiorite Granite,

iii) Syenites Granite,

iv) Aegerine Augen Granite,

v) Fayalite quartz Monzolite and

vi) Quartz - diorite Granite

Eigbefo (1978), in his work on Kubanni basin in general listed the different basement rocks found in the area, the present study area inclusive, *viz*:

i) Coarse porphyritic-biotite granite

ii) Medium-Coarse grained biotite granite gneiss

iii) Applite granite; Pegmatites and Quartz veins intrude most of the bodies, and

vi) Weathered basement. This is about 14% of the basin's total area and forms a storage aquifer; he reported.

The surface of the Older Granite Basement in the study area was found to be overlain by a deposit which Wright & McCurry (1970) listed as Older laterite, Younger laterite, Older alluvium and Younger alluvium; the last two being Quaternary deposits. They added that the Older laterite is characterised by high topography, thickness of up to 7 meters, reddish-brown, cellular in nature and purer than the Younger laterite. The Younger laterite has lower topography, thickness is less than 6 meters, browner, and are mostly exposed along streams. The alluvia are formed almost at the same time with younger laterite and are seen everywhere in the area. They result in the accumulations of

fine grey-brown sands, clays, red sand silt and gravel to a thickness as much as 15 meters in some places (Wright and McCurry, 1970).

This superficial deposits finds its value in the area not only serve as a recharging medium to the aquifer but also as a shield to storage when it is underlain by a weathered basement (Eigbefo, 1978).

### 2.2.3 Structural Geology of the Study Area

Structures like fractures, faults and joints play prominent roles in groundwater studies. They can control the flow, recharge and discharge modes of ground water in an area especially when dealing with crystalline rocks as is the case of this study area. A prominent joint can store water especially when it is overlain by a weathered basement (Akpoborie, 1973). In his study on Kubanni basin, Akpoborie (1973) reported that the Older granite inselbergs are intensively fractured giving ways for easy recharge of weathered basement aquifer with rain water.

Two major deformations were reported by Eigbefo (1978) in his study of the area; the greater one is along N-S while a less prominent one is along E-W. These deformations are likely to arise in connection with the Nigeria basement complex faulting and fracture pattern caused by transcurrent movement. The deformation are oriented in the NW-SE and NE-SW directions (Oluyide and Udo, 1986).

The identified elements for groundwater storage in the study from the various studies are weathered basement, Older laterite and alluvial deposits. The characteristics of these elements include: high porosity and less consolidation.

# CHAPTER THREE

# METHODOLOGY

## 3.1 Data Acquisition

### 3.1.1 Field-Work Planning

The field work was accomplished between 24th of February and 3rd of March, 1998. This period was chosen because it was the peak of the dry season in the area when the ground-water table would presumably be at its maximum depth below the ground surface while the aquifer thickness would be at its minimum.

A total of 40 VES sounding points were used out of which 8 were radial sounding points with four profiles per point and 32 single profile points; making a total of 64 profiles. Regular directions of N-S and E-W were maintained in the orientation of the profiles, but NE-SW and NW-SE directions were included in all the radial soundings.

A total of 8 travel lines/survey lines with eleven data points on each, were chosen for VLF method; making a total of 88 data points. Figure 3.1 shows the distribution of points for resistivity and VLF surveys in the area. Filtered contour points were obtained by appropriate manipulation as suggested by Fraser (1969).

#### 3.1.2 Choice of Electrode Configuration

For the resistivity work Schlumberger array was chosen for the following reasons:

FIG 31 VES AND VLF SURVEY POINTS IN THE STUDY AREA

i) Only the two Current electrodes are moved at a time, thus, it is more convenient than Wenner array for sounding.

ii) Effect of shallow resistivity variation (noise) is constant with fixed potential electrodes, thus, minimising the error.

iii) Depth and lateral variation information can be obtained from the VES field data (by employing Zohdy's interpretation method).

iv) The electrode effect on the resistivity curve is greatly minimised. This effect comes about because of the perturbations caused by the passage of the potential electrodes over a superficial inhomogeneity which is much greater than those due to the current electrodes (Kunetz, 1966; Parasnis, 1962). Since the movements of the potential electrodes are minimised, this electrode effect is also minimised.

### 3.1.3 Data Collection

The choice of the sounding location (Fig. 3.1 and Table 3.1) were made so as to cover the whole area of F.C.E. land in order to achieve the set objectives. Either N-S or E-W profile was taken at each single VES point while 8 radial soundings containing four profiles were distributed evenly over the study area as the physical structures on the premises can accommodate. These structures (Figure 1.3) disallowed regular griding.

Previous geophysical surveys within areas of the northern part of Nigeria, Old Kaduna state in particular, show that the overburden in the basement area is not so thick as to warrant wider current electrode spacing for deeper penetration Oyawoye (1964).

**TABLE 3.1:** VES Locations in the Study area (a = N-S, b = E-W, C = NE-SW and d = NW-SE direction)

| SN | STN. NO. & DIR | | SN | STN. NO. & DIR. | | SN | STN. NO. & DIR. | | SN | STN. NO. & DIR. |
|---|---|---|---|---|---|---|---|---|---|---|
| 1 | 01a | | 17 | 12c | | 33 | 19c | | 49 | 25b |
| 2 | 01b | | 18 | 12d | | 34 | 19d | | 50 | 26a |
| 3 | 01c | | 19 | 13a | | 35 | 20a | | 51 | 27b |
| 4 | 01d | | 20 | 14b | | 36 | 20b | | 52 | 28b |
| 5 | 02b | | 21 | 15a | | 37 | 20c | | 53 | 29b |
| 6 | 03b | | 22 | 16a | | 38 | 20d | | 54 | 30a |
| 7 | 04b | | 23 | 16b | | 39 | 21a | | 55 | 31a |
| 8 | 05b | | 24 | 16c | | 40 | 21b | | 56 | 32a |
| 9 | 06a | | 25 | 16d | | 41 | 21c | | 57 | 33a |
| 10 | 07b | | 26 | 17a | | 42 | 21d | | 58 | 34b |
| 11 | 08b | | 27 | 17b | | 43 | 22a | | 59 | 35b |
| 12 | 09a | | 28 | 17c | | 44 | 22b | | 60 | 36a |
| 13 | 10b | | 29 | 17d | | 45 | 22c | | 61 | 37b |
| 14 | 11b | | 30 | 18a | | 46 | 22d | | 62 | 38a |
| 15 | 12a | | 31 | 19a | | 47 | 23b | | 63 | 39a |
| 16 | 12b | | 32 | 19b | | 48 | 24b | | 64 | 40b |

Therefore, the widest current electrode spacing used was 200 m, that is, ½AB = 100 m (Table 3.2). According to Barker (1989), the maximum depth of penetration in Schlumberger array is 0.19 AB. Thus, the maximum depth probed was about 36 to 40 m. Sounding depths not exceeding 40 m in this area is considered enough for groundwater study and other parameters of interest. The potential electrode separation, MN, was also increased intermittently in order to maintain a measurable potential, but it did not exceed one-fifth of the half-current electrode separation, ½AB, as suggested by Dobrin and Savit (1988).

TABLE 3.2: VES Electrodes Spacings and K-Factor Used in the Study

| S/N | MN(m) | ½AB(m) | K-Factor |
|---|---|---|---|
| 1 | 1.0 | 1.00 | 2.2562 |
| 2. | 1.0 | 1.50 | 6.2832 |
| 3 | 1.0 | 2.50 | 18.8500 |
| 4 | 1.0 | 3.75 | 43.3932 |
| 5 | 1.0 | 5.00 | 77.7544 |
| 6. | 1.0 | 7.50 | 175.9292 |
| 7. | 1.0 | 10.00 | 313.3739 |
| 8. | 3.0 | 7.50 | 56.5487 |
| 9. | 3.0 | 10.00 | 102.3636 |
| 10. | 3.0 | 15.00 | 233.2636 |
| 11. | 3.0 | 25.00 | 152.1423 |
| 12. | 3.0 | 37.50 | 1470.2654 |
| 13. | 3.0 | 50.00 | 2615.6377 |
| 14. | 10.0 | 37.50 | 433.9325 |
| 15. | 10.0 | 50.00 | 777.5442 |
| 16. | 10.0 | 75.00 | 1759.2919 |
| 17. | 10.0 | 100.00 | 3133.7387 |

Fraser (1969) recommended that the VLF reading should be taken on a regular grid of 50 by 50 ft along a survey/travel line perpendicular to the strike of the ore/geological structure and also perpendicular to the station used. For this reason, a grid size of 66 m was used and a GBR European VLF transmitting station located at Rugby, England transmitting at frequency 16.0 KHz having co-ordinate OIWII - 52N22 was used along an E-W direction of travel line on the study area, the direction which is roughly perpendicular to the station location used.

### 3.1.4 Instrumentation

In this survey, the resistivity and VLF equipment were used for the principal measurements. The Terrameter Signal Averaging system (SAS) model 300 was used for the resistivity survey. No booster was used because the expected depth-to-basement in the area is within the range of penetration of instrument. In this instrument consecutive readings are taken automatically and the results are averaged continuously and the updated running value is automatically presented on its digital read out screen. SAS 300 can operate in two modes:

i) Resistivity Survey mode: It contains resistivity meter, suitable for current electrode spacing of up to 2000 m under good surveying conditions. The change in potential per unit current ($\Delta V/I$) is automatically calculated and displayed in digital form (in ohms or milli ohms). The overall range is from 0.5 milli Ohms to 1999 kilo - Ohms. This mode was chosen for this work. However, the range can be extended down to 0.02 milli-Ohms by means of the SAS 200 Booster, but this is not necessary in this survey.

ii) Voltage measuring mode; The SAS 300 comprises of self potential instrument that measures natural DC potentials. The result is displayed in Volts or milli volts. The overall range extends from 0.01 mV to 500 V.

EM-6 VLF equipment was used for the electromagnetic study. A GBR European VLF transmitting station located at Rughby, England and transmitting at frequency 16.0 KHz was used. The station co-ordinate is 01WWII - 52N22. EM-6 measures the inphase and

quadrature component of the vertical magnetic field (Hs) as a percentage of horizontal primary field (Hp) (i.e. tilt/dip-angle and elipticity).

Inphase reading is taken from mechanical inclinometer while quadrature reading is taken from a graduated dial located at the lower end of the VLF instrument.

## 3.2 Bases and Theories of the Methods Used

### 3.2.1 Basis of D.C. Resistivity Methods

This method is based on the fact that when electric current is driven into the earth, any variation of the subsurface resistivity will alter the current flow which will in turn affect the distribution of the electric potential. The measurement of the electrical potential and the current especially on the earth's surface will make it possible to obtain information about the resistivity variation of the subsurface in the area concerned (Telford et al., 1976).

The regular pattern of current flow will be distorted by buried bodies or geological structures. For instance a conductive body will concentrate the electric field flow lines towards itself, while a resistive body will cause the current to flow around it and less concentrated in it. The potential fields, are hence deflected, the deflections which can be observed by the potential electrodes at the surface of the earth. The ratio of potential difference/deflection to the electric current present gives the resistance from which resistivity of the target subsurface body can be got.

## 3.2.2 Theory of D.C. Resistivity Method

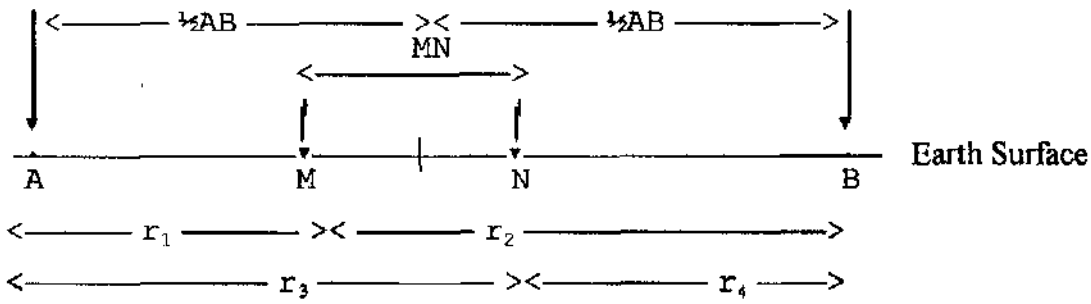


Fig. 3.2: Schlumberger Array

Fig. 3.2 is a schematic illustration of the Schlumberger array which was adopted in the survey. A and B are current Electrodes through which current is driven into the ground while M and N are two potential electrodes to record the potential distribution in the subsurface within the two current electrodes.

From the Ohm's law, the current I and potential V in a metal conductor at constant temperature are related as follows:

$$V = IR \qquad \ldots\ldots\ldots\ldots\ldots\ldots\ldots\ldots \quad (1)$$

where R is the constant of proportionality termed resistance and it is measured in ohms.

The resistance R, of a conductor is related to its length L and cross sectional area A by

$$R = \frac{\rho L}{A} \qquad \ldots\ldots\ldots\ldots\ldots\ldots\ldots\ldots\ldots\ldots\ldots\ldots\ldots\ldots \quad (2)$$

Where ρ is resistivity and it is a property of the material considered.

From equation (1) and (2)

$$V = \frac{I\rho L}{A} \quad \text{.....(3)}$$

The vertical electrical sounding (VES) with Schhumberger array involves fixing the potential electrodes at points M and N, and symmetrically increasing the current electrode separation AB about the centre by displacing A and B outwardly in steps. This will increase the depth of penetration of the current supplied to the ground. Therefore any anomalous body at depth within the separation AB will have influence on the potential field. Such influencing structures will make for the inhomogenuity of the earth materials. Thus the varying resistivity measured when electrode array position is varied in an inhomogeneous medium is termed Apparent resistivity.

For simple treatment, a semi-infinite solid with uniform resistivity, ρ, is considered. A potential gradient is measured at M and N when current I is introduced into the material through A and B on the surface. If A and B are point current electrodes located on the surface the equipotential surface is semi-spheral downward into the ground at each electrode. The surface area will then be $2\pi L^2$, where L is the radius of the sphere. Thus

$$V = \frac{I\rho}{2\pi L} \quad \text{.....(4)}$$



By deduction then, the potential at M ($V_M$), due to the two current electrodes, is

$$V_M = \frac{I\rho}{2\pi}\left(\frac{1}{r_1} - \frac{1}{r_2}\right) \quad \ldots\ldots\ldots\ldots\ldots\ldots \quad (5)$$

Similarly, the potential at electrode N ($V_N$) is given by

$$V_N = \frac{I\rho}{2\pi}\left(\frac{1}{r_1} - \frac{1}{r_4}\right) \quad \ldots\ldots\ldots\ldots\ldots\ldots \quad (6)$$

where $r_1$, $r_2$, $r_3$ and $r_4$ are as shown in figure 3.2.

The potential difference, $\Delta V$, across electrodes M and N is $V_M - V_N$. Now, if body is inhomogeneous, apparent resistivity is considered $\rho_a$, say, and thus:

$$\rho_a = K\left(\frac{\Delta V}{I}\right) \quad \ldots\ldots\ldots\ldots\ldots\ldots\ldots \quad (7)$$

Where $\rho_a$ is apparent resistivity in Ohm-meters, and

$$K = 2\pi\left[\left(\frac{1}{r_1} - \frac{1}{r_2}\right) - \left(\frac{1}{r_3} - \frac{1}{r_4}\right)\right]^{-1} \quad \ldots\ldots\ldots \quad (8)$$

K is called the geometrical factor whose value depends on the sort of electrode array used.

For Schlumberger array, if MN = b and ½AB = a then,

$$K = \pi\left(\frac{a^2}{b} - \frac{b}{4}\right) \quad \ldots\ldots\ldots\ldots\ldots\ldots\ldots \quad (9)$$

### 3.2.3 Basis of the V.L.F. Methods

The principle of the very Low Frequency (V.L.F.) Electromagnetic methods, is based on the fact that (eddy) current is induced in subsurface conductors (rock materials) when primary electromagnetic field from an oscillating current is applied on the rock from the surface. Secondary electromagnetic field which will distort the primary field is produced. This will flow in opposite direction to the primary field.

Resultant of the primary and secondary fields is picked up by a receiver coil at any observation point in the form of variation in amplitude or intensity and phase of the field (Dobrin and Savit, 1988).

A powerful radio transmitter sourced the time varying electromagnetic fields (primary field) in this work. The station is located in England and transmits unmodulated carrier waves at low frequency - 16.0 kHz (Fraser, 1969). A vertical current is generated from a vertical antenna at the said transmitting station. A concentric horizontal magnetic fields due to the current serving as the primary field is created. The V.L.F. equipment then measures the resultant fields due to the primary and that from the induced eddy current in the subsurface structures at the survey area. These two waves are of the same frequency but of different amplitudes and phases.

### 3.2.4 Theory of the V.L.F. Methods

The resultant waves measured with V.L.F. machine are of two types: that which is in-phase with the primary field whose amplitude is then called 'In-phase' or 'Real' component of the resultant field; and the second component is usually displaced 90°; thus

it is out of phase with the primary consequently its amplitude is termed the 'out-of-phase', 'Imaginary' or 'Quadrature' component of the resultant. For simple approach, inductive coupling is considered among a trio of coils - transmitter as coil 1, subsurface conductive body is coil 2 and Receiver (VLF machine) as coil 3. The inductive coupling between coil 1 and coil 2 is responsible for the 90° phase displacement or lag of secondary fields; and additional phase lag of θ depends on the conductivity property of the coils 2 (subsurface conductor or body) (Figure 3.3).

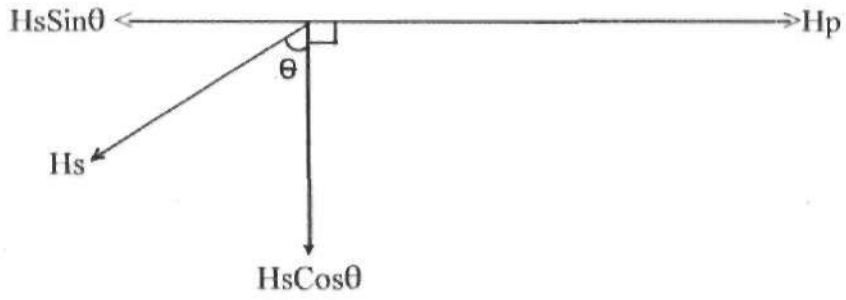


Fig. 3.3: Vector diagram of the Resultant Electromagnetic Fields

$H_s Sin\theta$ is 180° out of phase with the primary fields and thus it is the `Inphase' component of the resultant waves, $H_s Cos\theta$ is 90° out of phase with it and it is the `Quadrature' component. The closer θ is to 90° the more conductive is the subsurface rock material probed.

Actually, the present survey area is far (thousands of kilometers) from the transmitter used. Therefore, the primary field is considered uniform over the area. Consequently, the rock materials are subjected to a homogeneous horizontal primary field from the station, thereby allowing for simple mathematics to be employed in the comprehensive interpretation (Parasnis, 1962).

## 3.3 DATA REDUCTION

### 3.3.1 VES Data

Equation (7) was used to obtain apparent resistivity values for each profile. To do this the geometric factors, K, were first calculated for all the current electrode spacings using equation (9) (Table 3.2 shown earlier). These, together with the Resistance values got form the field data. Then the apparent resistivity values for each profile were plotted against the current electrode spacing (½ AB) (Table 3.2 shown earlier) on the log-log graph sheets to obtain the field and digitized curves using an appropriate computer software (Zohdy, 1989). The reduced values were used to obtain various contour maps as well.

The radial VES data were similarly reduced as above. Meanwhile, a linear plot, using linear scale, was obtained for apparent resistivity and electrode spacing (½ AB) along each of the four profiles at each radial VES point. Thus, resistivity anisotropy and geological deformation and trend were observed from the later plots above.

### 3.3.2 VLF Data

The In-phase and quadrature values were read and recorded side-by-side from the VLF instrument at each cross point of grid size 66 m by 66 m. The Inphase and quadrature components were plotted against distance along the survey line. This graph reveals areas of high and low conductivities in the study area. The VLF data are the ratio of the secondary to the primary field component expressed in percentage ($H_s/H_p$ %).

Fraser (1969) however suggested a simple numerical filtering technique aimed at eliminating erroneous interpretation of VLF data caused by large geological noise component generated from the transmitted frequency. This filtering method improves the resolution of anomalies which will ease their recognition.

The filter $F_{2,3}$ for instance, is given by

$$F_{2,3} = (M_3 + M_4) - (M_1 + M_2) \quad \ldots\ldots\ldots\ldots\ldots\ldots (10).$$

where $M_1$, $M_2$, $M_3$ and $M_4$ are four consecutive data points on the base map with $F_{2,3}$ fixed midway between $M_2$ and $M_3$. This is done for $M_4$, $M_5$, $M_6$ and $M_7$ to get $F_{5,6}$ midway between $M_5$ and $M_6$, similar filters were obtained for all other data points on all the travel lines. The filtered values are tabulated with their appropriate co-ordinates and then contoured. However, all negative F values were ignored during contouring. According to Fraser (1969) they are only caused by dip angle flanks and can distort the expected picture.

An inflection on the dip profile from a conductor (in this case a water bearing layer) yields a positive peak and hence indicating the presence of water bearing layer (Fraser, 1969). Thus the positive peaks reveal conductive area.

# CHAPTER FOUR

# INTERPRETATION OF RESULTS AND DEDUCTIONS

## 4.1 VES Data

### 4.1.1 General Statement

The interpretation of Vertical Electrical Sounding (VES) data involves expressing the information obtained from the surface measurements in geological terms. In so doing, the combination of some subsurface structure parameters like resistivities and layer thicknesses are determined.

For easy interpretation it is assumed that:

1. the various geoelectric layers encountered are electrically homogenous and isotropic. However, lateral variation in resistivity exists within a geoelectric layer. Thus any deviation from these ideal situations adds to the error in the final interpretation (Keary and Brooks, 1984).
2. the computed resistivity curves are based on the fact that the subsurface layers are horizontal. This may not be true in all cases expecially in a case of vertical contacts. Thus any vertical layer boundary encountered will introduce error into the interpretation.
3. each subsurface layer is unique as regards its curve. However, the interpretation suffers from non-uniqueness arising from problems of Equivalence and suppression' (Kunetz, 1966). Kunetz informed that problems of equivalence is the difficulty in distinguishing between two

resistive layers of different thicknesses and resistivities where products of these parameters are the same. Similarly, two consecutive layers may not be distinguished if the ratios of their thickness to resistivity are the same. The problem of suppression is associated with those layers whose resistivities are intermediate between the resistivities of the enclosing layers. Such layers (if their thicknesses are small) will have no practical influence on the resistivity curve for sounding.

### 4.1.2 Interpretation

The data analysis was performed using Zohdy's method which gives the automatic interpretation of the Schlumberger sounding curves to obtained the equivalent n-layer model from apparent resistivity curve of each sounding. Figures 4.1 and 4.2 are typical VES curves for stations FCE 01b and FCE 26b, while their resulting true resistivity layer models are shown in Figures 4.3 and 4.4. Similar plots and interpreted models were obtained for each of the 40 interpreted VES points whose layering are shown in Table 4.1

The interpretation of these curves is based on the principle that all points of maxima and minima, and points of inflection are indicators of existence of boundaries of different lithologies. Where the values tend to infinity is an indication of fresh basement rock (Zohdy, 1989 and Telford *et al.*, 1976).

Further, the equivalent time resistivity models of each sounding were used to produce a comprehensive subsurface isoresisivity contours at various preferred, predetermined depths. Conversely depth contours were plotted at various predetermined resistivity values.

FCE 01b (FIELD DATA)

| AB/2 | App. Res. | AB/2 | App. Res. |
|---|---|---|---|
| 1.00 | 475.95 | 10.00 | 1340.33 |
| 1.50 | 526.53 | 15.00 | 1513.58 |
| 2.50 | 550.51 | 25.00 | 1576.01 |
| 3.75 | 598.17 | 37.50 | 1658.25 |
| 5.00 | 689.43 | 50.00 | 1697.40 |
| 7.50 | 1030.32 | 75.00 | 1826.94 |
| | | 100.00 | 1900.40 |

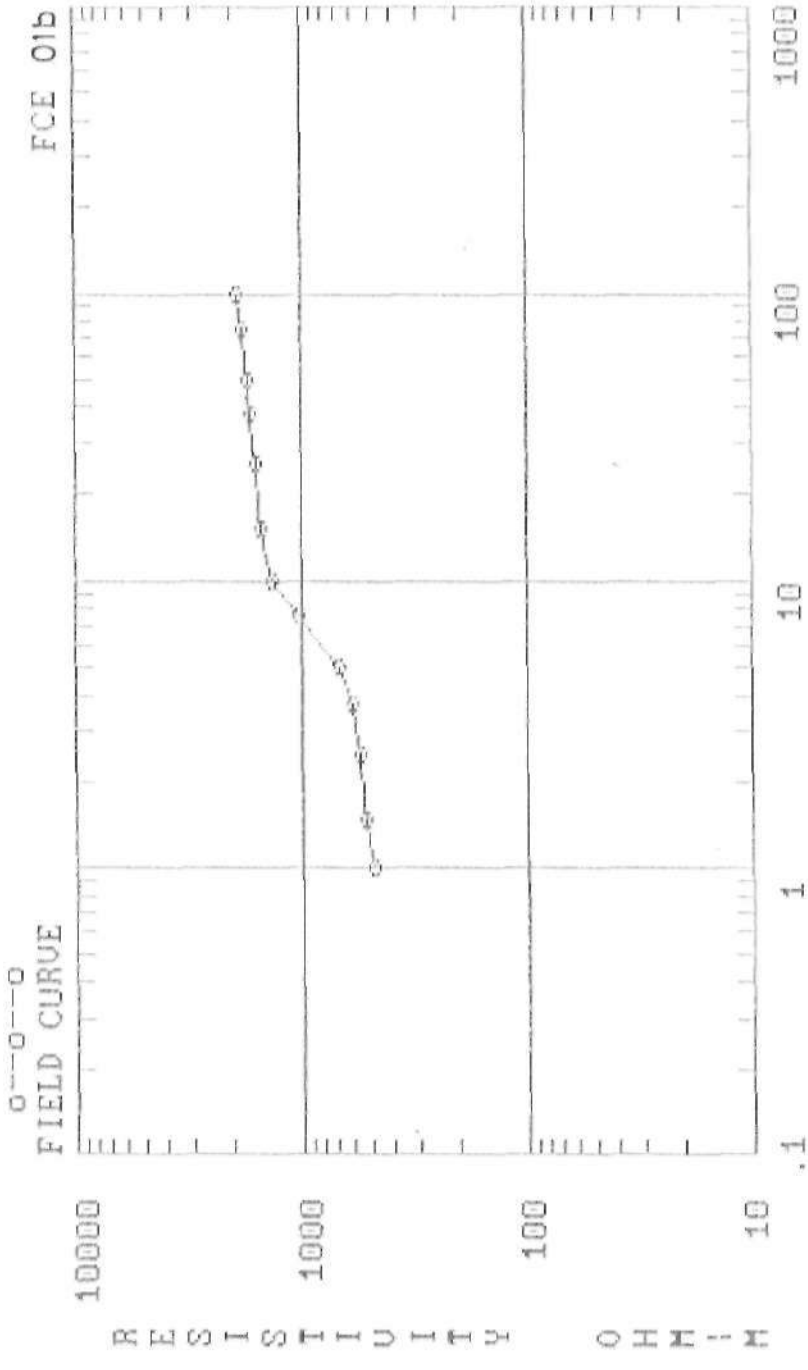


FIG. 4.1 VES CURVE AT STATION FCE 01b

FCE 26a (FIELD DATA)

| AB/2 | App. Res. | AB/2 | App. Res. |
|---|---|---|---|
| 1.00 | 110.98 | 10.00 | 79.91 |
| 1.50 | 85.10 | 15.00 | 99.14 |
| 2.50 | 65.22 | 25.00 | 139.56 |
| 3.75 | 58.31 | 37.50 | 173.79 |
| 5.00 | 54.97 | 50.00 | 214.80 |
| 7.50 | 64.78 | 75.00 | 304.71 |
| | | 100.00 | 349.41 |

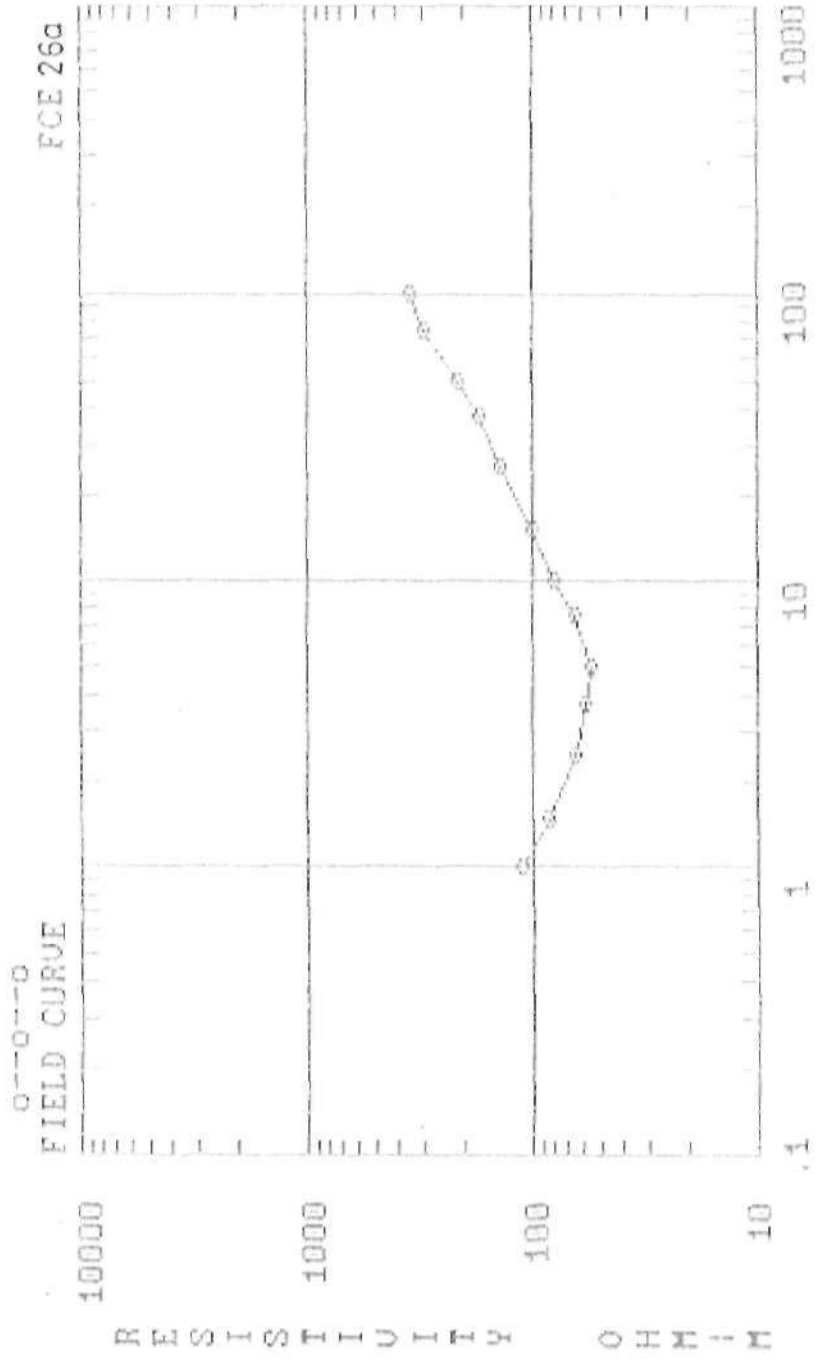


FIG. 4.2 VES CURVE AT STATION FCE 26a

FCE 01b (INTERPRETATION)

| DEPTH | RESIS. | DEPTH | RESIS. |
|---|---|---|---|
| 0.44 | 487.28 | 4.37 | 1964.76 |
| 0.64 | 522.51 | 6.42 | 2514.31 |
| 0.94 | 409.66 | 9.42 | 2421.97 |
| 1.38 | 363.12 | 13.83 | 1981.73 |
| 2.03 | 556.56 | 20.30 | 1665.25 |
| 2.98 | 1128.79 | 29.80 | 1674.74 |
| | | 99999.00 | 1985.95 |

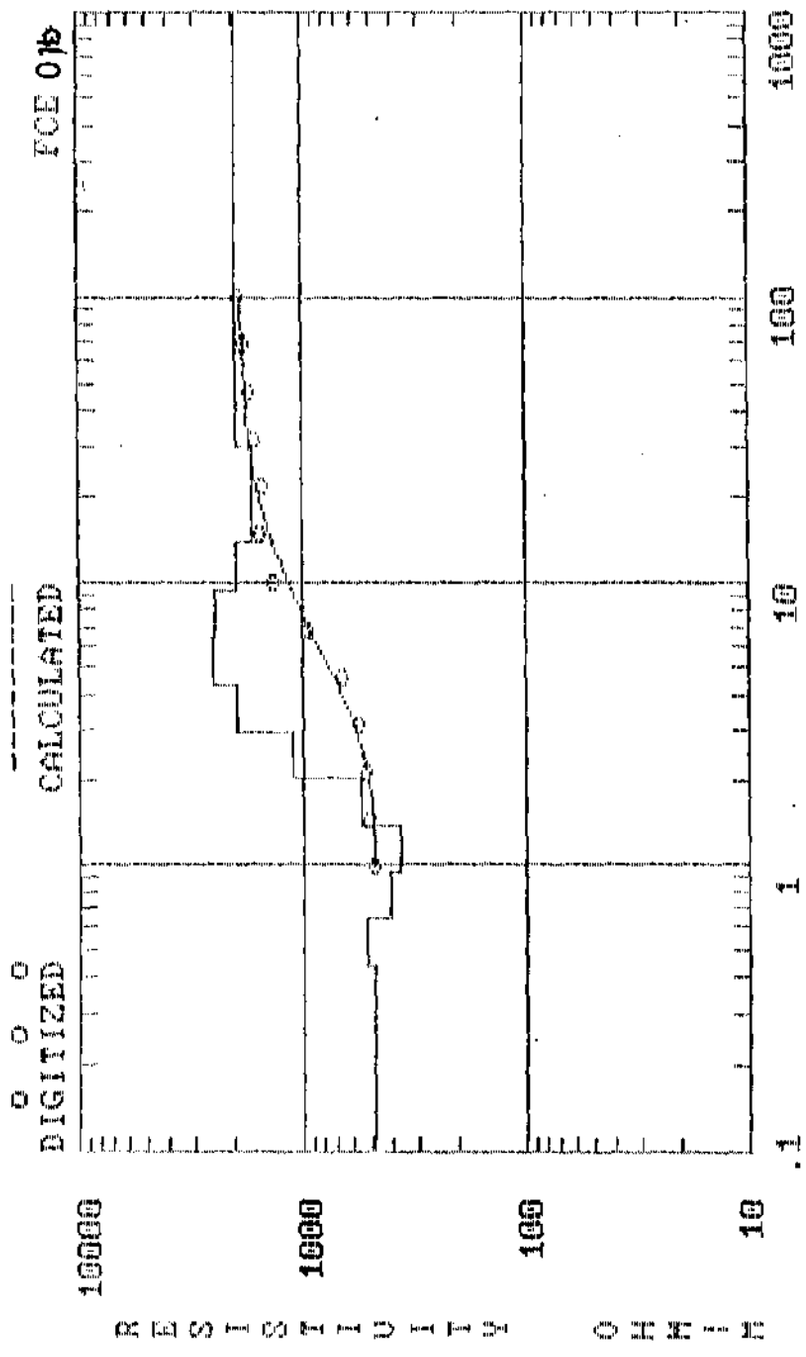


FIG. 4.3 MODEL INTERPRETATION OF THE VES FCE 01b

FCE 26a (INTERPRETATION)

| DEPTH | RESIS. | DEPTH | RESIS. |
|---|---|---|---|
| 0.44 | 143.92 | 4.37 | 66.09 |
| 0.64 | 103.54 | 6.42 | 94.42 |
| 0.94 | 75.83 | 9.42 | 130.70 |
| 1.38 | 48.30 | 13.83 | 188.12 |
| 2.03 | 36.24 | 20.30 | 288.98 |
| 2.98 | 44.47 | 29.80 | 454.40 |
| | | 99999.00 | 701.70 |

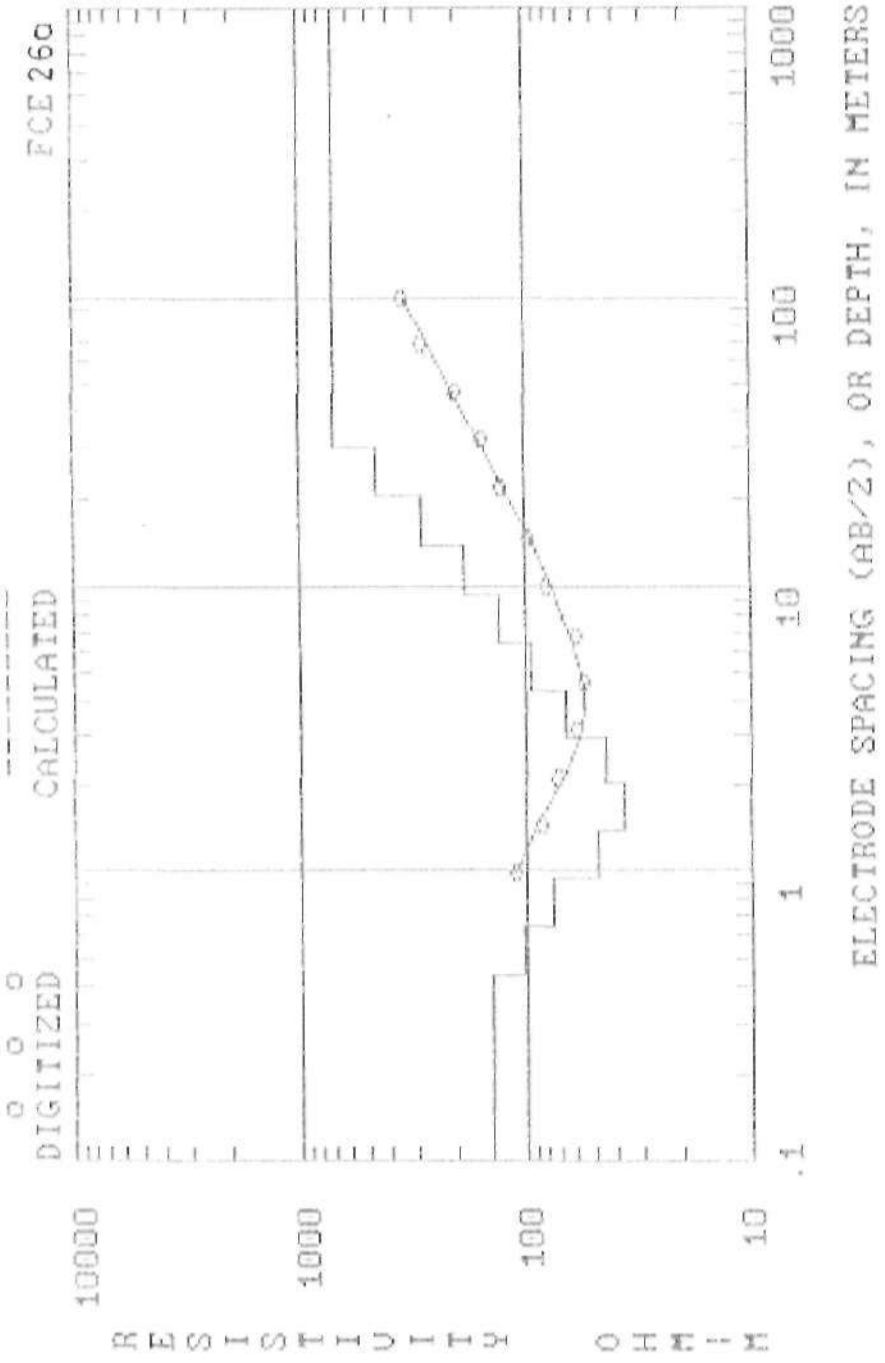


FIG. 4.4 MODEL INTERPRETATION OF THE VES FCE 26a

*Table 4.1: Number of Subsuface Layers at each VES Point*

| VES POINTS | NUMBER OF LAYERS | VES POINTS | NUMBER OF LAYERS |
|---|---|---|---|
| 1 | 2 | 21 | 3 |
| 2 | 4 | 22 | 3 |
| 3 | 3 | 23 | 3 |
| 4 | 3 | 24 | 3 |
| 5 | 3 | 25 | 3 |
| 6 | 3 | 26 | 3 |
| 7 | 3 | 27 | 2 |
| 8 | 3 | 28 | 2 |
| 9 | 2 | 29 | 3 |
| 10 | 2 | 30 | 3 |
| 11 | 3 | 31 | 3 |
| 12 | 3 | 32 | 3 |
| 13 | 2 | 33 | 3 |
| 14 | 2 | 34 | 3 |
| 15 | 2 | 35 | 3 |
| 16 | 3 | 36 | 2 |
| 17 | 3 | 37 | 3 |
| 18 | 3 | 38 | 3 |
| 19 | 3 | 39 | 3 |
| 20 | 3 | 40 | 3 |

The resistivity ranges of various rock materials in the area were compiled from past information (Tables 4.2 and 4.3) from which comprehensive contour sections were obtained for geologic analysis along profiles AB, CD, EF and GH, as shown in figure 3.1. Remarkable geologic deformation trends were observed on the radial VES plots.

*Table 4.2: Typical resistivity values of Rock Materials*

| ROCK TYPE | RESISTIVITY RANGE (Ohm-meters) |
|---|---|
| Fadama Loan | 30 - 90 |
| Weathered Laterite | 200 - 500 |
| Fresh Laterite | 501 - 800 |
| Sand Clay and Silt | 100 - 200 |
| Weathered basement | 20 - 400 |
| Natural Water (igneous rocks) | 0.5 - 150 |
| Natural Water sediments) | 1 - 100 |
| Alluvium and Sands | 10 - 800 |
| Fresh Basement | 1000 - $\alpha$ |

*Table 4.3: Resistivity Values Adopted for this work.*

| Rock Type | Resistivity Range (Ohm-Meters) |
|---|---|
| Fadama Loam | 30 - 90 |
| Clay, Silt and Sand | 70 - 300 |
| Weathered Basement | 100 - 500 |
| Fresh Basement | 501 - $\alpha$ |

### 4.1.3 Resistivity Values

Table 4.2 and 4.3 show the resistivity values of rock types in basement areas similar to the study area, compiled from previous works (Telford *et al.*, 1976; Hassan, 1987 and Shemang, 1990).

## 4.2 Results and Deductions From VES Data

For an analytical discussion of the results of the VES, the geologic equivalent of the geoelectric section for each of the profiles were drawn. Details are discussed below.

### 4.2.1 Geologic Sections Equivalent to Geoelectric sections

The interpretation of the collected geoelectrical sounding data is generally meaningless without some reliable geological control or some data relating to the intrinsic resistivities of the various geoelectric areas (Worthington, 1977).

To obtain geoelectric section along a profile, the profile of interest is first drawn as shown in figure 3.1. The position of each VES point is then marked out. Then the resistivity values beneath each VES point along with their depth positions which has been prefixed say at 1, 5, 10, 15 meters etc, are obtained using the interpretation data for the geoelectric cross sections automatically generated by the Zohdy's Program. Appropriate resistivity boundaries in form of contour are then drawn through points with equal resistivity values following the resistivity ranges obtained for various rock types. The resulting map shows the presence and extent (thickness) of a rock material at a point. Such outcome is termed geologic section.

The geologic sections in this work was drawn based on the following control:

1. Use of log data information from the borehole on the study site (Figure 4.5). Figure 4.6 shows the location of the borehole,
2. Typical Resistivity values from previous works in the area gave way to the acceptable values for various earth materials (Table 4.2 and 4.3). According to Hockney (1986), these values are reliable, bearing a little error variations of values,

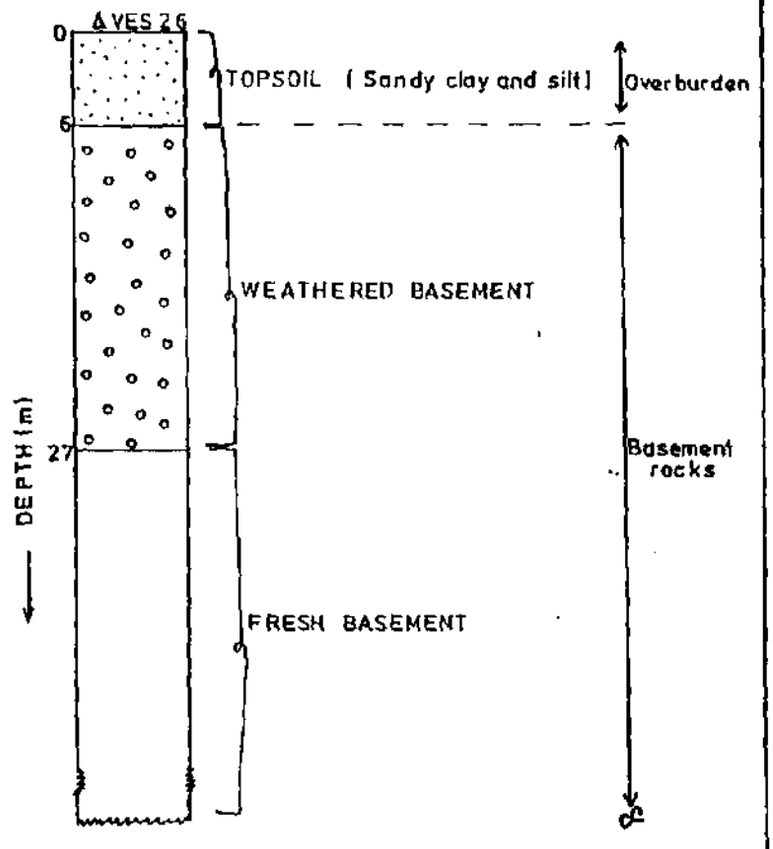


FIG. 4·5 LOG DATA FOR THE BOREHOLE LOCATED WITHIN F.C.E. ZARIA
(After Bactaves 1992)
Courtesy: Estate Department F.C.E. Zaria.

NB. VES POINT 26 OF THIS STUDY IS LOCATED BESIDE THE BOREHOLE.

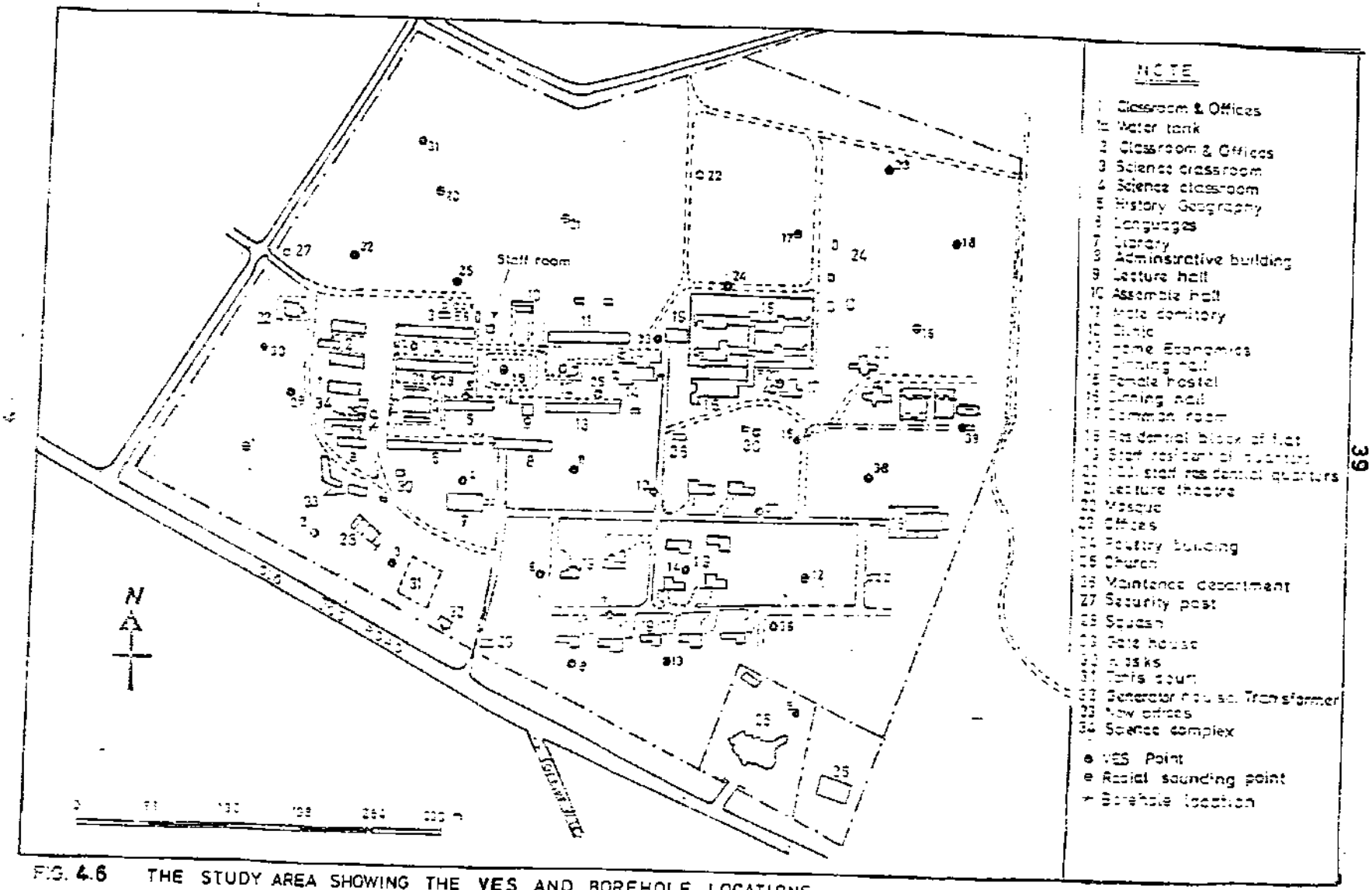


FIG. 4.6 THE STUDY AREA SHOWING THE VES AND BOREHOLE LOCATIONS

3. The rock samples collected from outcrops in the survey area were thought to be representative of the subsurface materials.

It should be noted that there is vertical exaggeration in the geologic sections along the profiles explained ahead. This is inevitable because the horizontal distance on the study area is far greater (about a kilometre) than the depth to fresh basement which is of the order of 40 meters. If the same scale were to be used for both horizontal and vertical distances, the geometry of the juxtaposition of the vertical strata along the horizontal direction will not be obvious. Thus, the vertical scale needed to be somewhat exaggerated for meaningful interpretation as shown in Figures 4.7 and 4.8.

### 4.2.2 Profile AB

The geologic section along this profile, Figure 4.7a, suggests three (3) major geologic layers in most places but two (2) layers in the area of VES 1. The top layer whose resistivity ranges from 30 to 300 ohm-meters and thickness from 4 - 12.5 m with the thickest portion in the area of VES 16 is a sandy clay and silt containing fadama loam. VES E01 is located close to a granitic outcrop. Thus, the two-layer geologic formation obtained around VES may mean that the top of the exposed rock is weathered while its freshness increases downward forming a two-layer stratum (Figure 4.7a). The study area slopes towards River Kubanni. Hence, the highest thickness of the topsoil around VES 16 may be a consequence of the above effect. The second layer has a resistivity in the range of 100 - 463 ohm -meters and extends across the entire length of the profile. Its thickness ranges from 10m around VES 17 to 35.1 m around VES 05 and 19. The geologic section suggests that the second layer is mostly weathered basement. The third layer cuts across the whole length of the profile and is fresh basement rock. This layer is shallowest

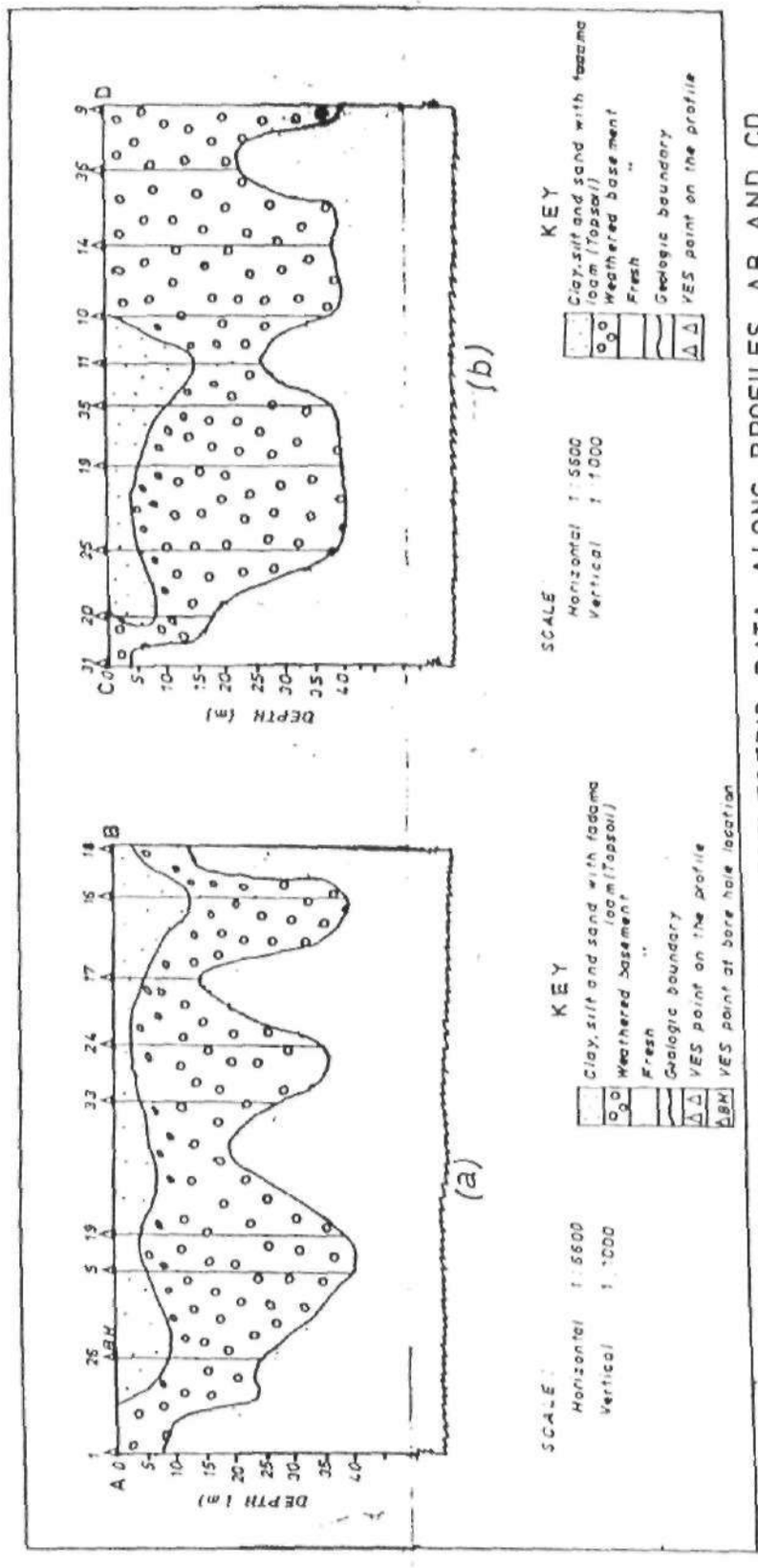


FIG. 4.7 GEOLOGIC SECTION DERIVED FROM GEOELECTRIC DATA ALONG PROFILES AB AND CD

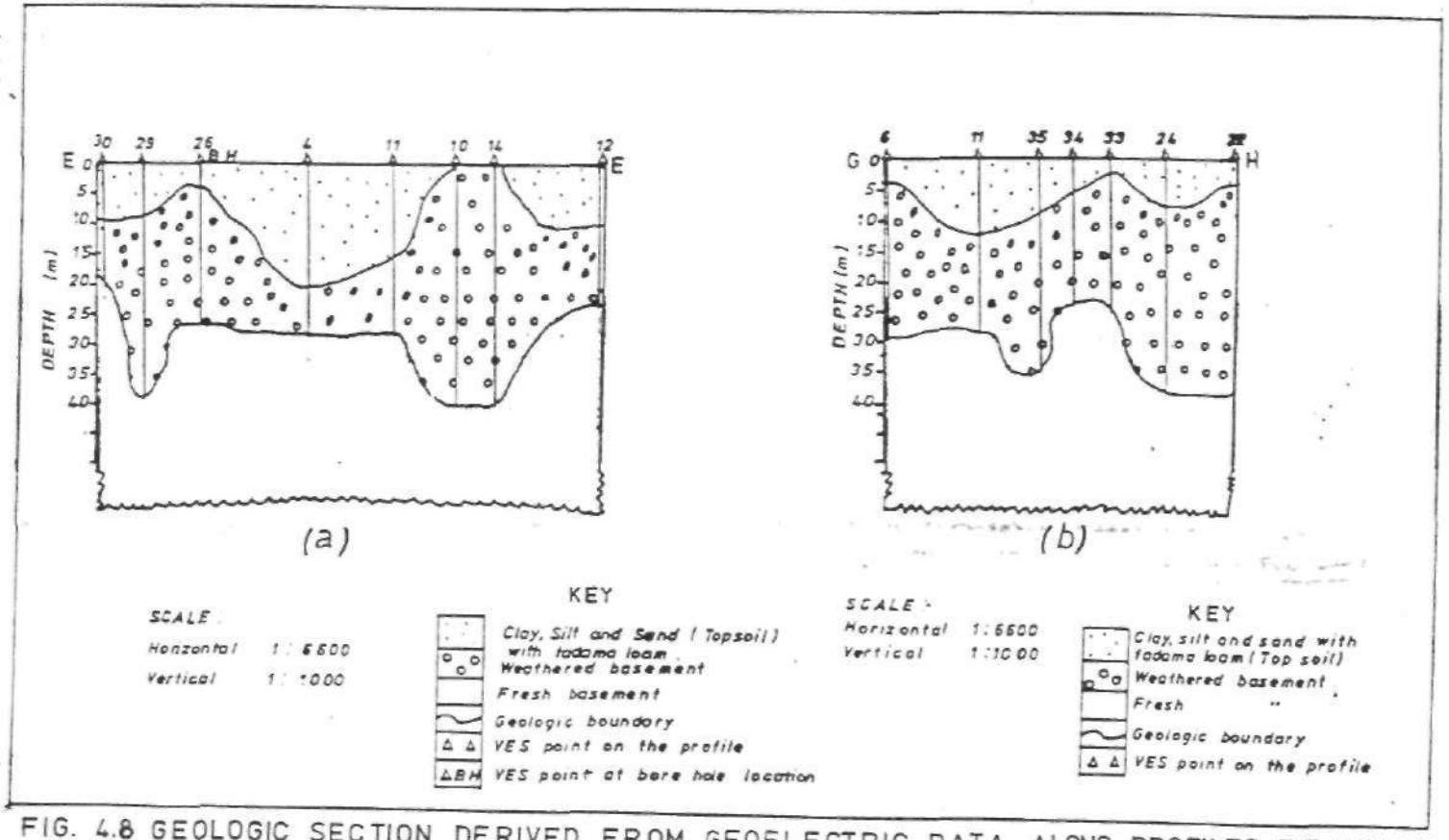


FIG. 4.8 GEOLOGIC SECTION DERIVED FROM GEOELECTRIC DATA ALONG PROFILES EF AND GH

(14m) around VES 17 and deepest (40.1 m) around VES 5 and 19. The resistivity of this layer ranges from 500 to 2000 ohm-meters. The geologic section further shows an upward extension of fresh basement into the weathered basement at depth of 14 m around VES 17 and at a depth of 18.5 m westward of VES 33.

### 4.2.3 Profile CD

The geological section along this profile, (Figure 4.7b) suggests that the subsurface is made up of 3-layers and 2-layers in some areas. The topsoil with resistivity values ranging from 70 to 300 Ω-meters and thickness ranging from 3.5 m around VES 25 to 11 m around VES 11, meets another rock type to the left- and right-hand sides of it. The second layer, assumed to be a weathered basement, has resistivity ranging from 100 to 450 -meters and thickness ranging from 10 to 35 m. The layer is thinnest towards the west of VES 25 and thickest towards the east of it. The resistivity of the third layer ranges from 500 to 1000 ohm-meters.

The fresh basement is closer to the surface around VES 31 with low resistivity value of 502 ohm-meters and its highest resistivity value appears around VES 36 with the value 1000 ohm-meters.

### 4.2.4 Profile EF

The geologic section for this profile shows the presence of 3 layers and 2 layers around VES 10 and 14 only (Figure 4.8a). The top layer is thinnest around VES 26 - 6 m and thickest around VES 4 - 16.5 m. Its resistivity range is 40 - 200 ohm-meters. Between VES 10 and 14 is another rock type which differs from the normal topsoil. The thickness of the second layer ranges from 9 to 34 m. Its resistivity is between 130 and 450 ohm -

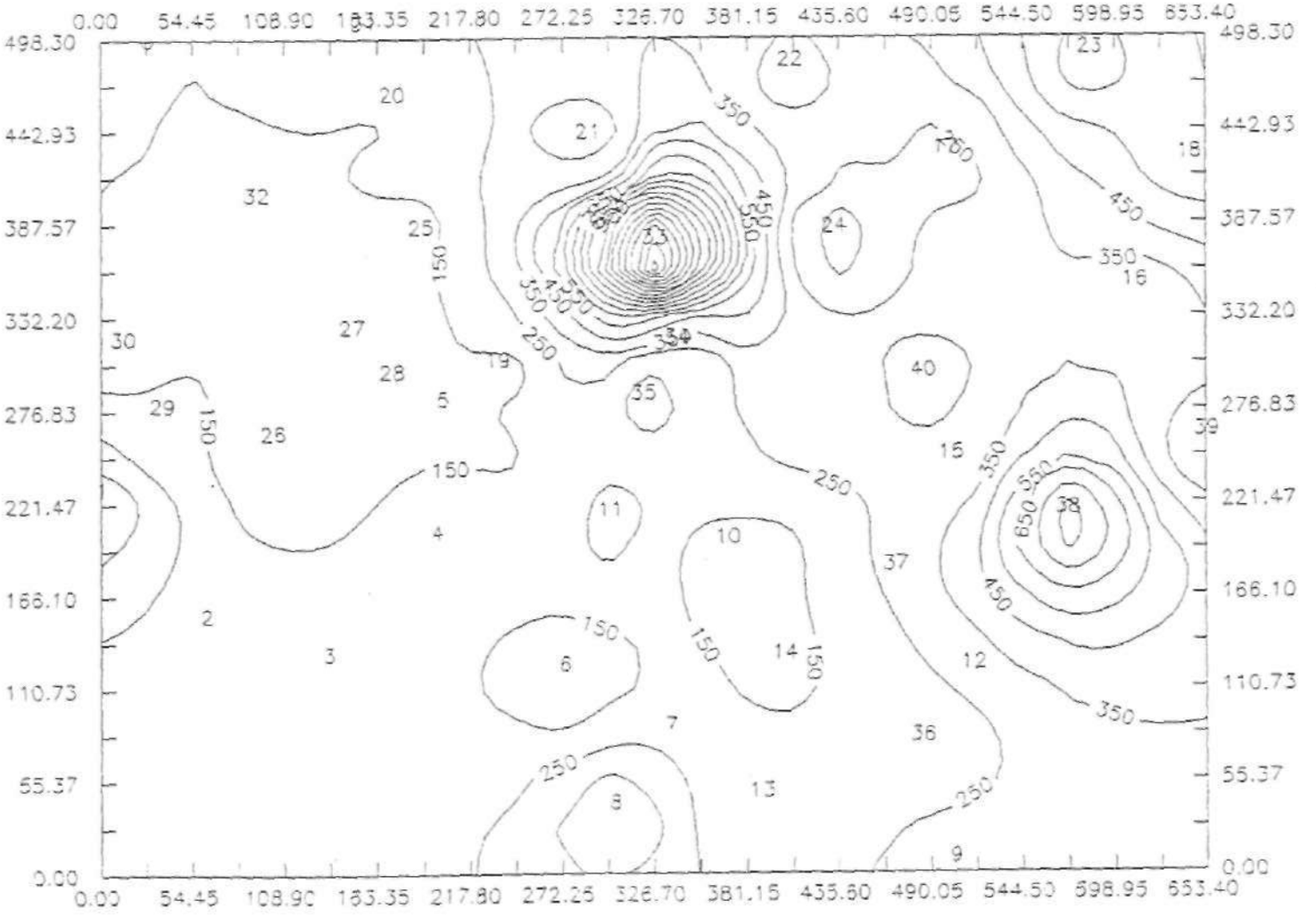


FIG. 4.9 Isoresistivity map at 1m depth con. int. 100 Ohm-meters

depth. This observation is confirmed physically on the surface at those locations. Figure 4.10 shows a high resistive value at VES 1 at depth 5 m which is an indication of outcrop of fresh basement. This situation extends towards VES 8 while other areas have very low resistivity. This indicates that topsoil has been passed, and weathered basement that are water-bearing (aquifer) have been approached in some areas. These conditions persist down 20 m depth as shown in figures 4.10, 4.11, 4.12, 4.13 and 4.14 when other areas of high resistivity are becoming prominent. Areas around VES 8 and 12 and 17 are examples of resistive spots. This situation continues as far as the last depth contoured as shown in figures 4.15, 4.16 and 4.17. This implies that VES 8, 12 and 17 are locations of encroached fresh basement. In almost all the depth contoured (Figures 4.9 to 4.17) the only outcrop located around VES 1 has its root extended towards south of the study area. Further, the weathered basement shows water content from 1.0 m to about 20 m depth (Figures 4.9, 4.10, 4.11, 4.12 and 4.13). while the weathered basement is shown dry as from about 25 m depth (Figure 4.14). Meanwhile, figures 4.15, 4.16 and 4.17 show that the fresh basement is encountered in almost all the area at a depth of 30 m. The freshness of the bedrock increases with depth as shown on figures 4.15, 4.16 and 4.17 with a progressive increase resistivity value with depth.

### 4.2.7 Results for Radial Sounding Plots

Eight (8) radial soundings of four (4) profiles per radial station were randomly established to covered the whole area as shown in figure 4.6 earlier. The resistivity values for each profile were plotted, using a linear scale, against the current electrode spread ½AB. The radial plots are shown in figures 4.18 and 4.19. These plots gave an insight into the subsurface trend of anisotropy. The presence of anisotropy sometimes depicts occurrence

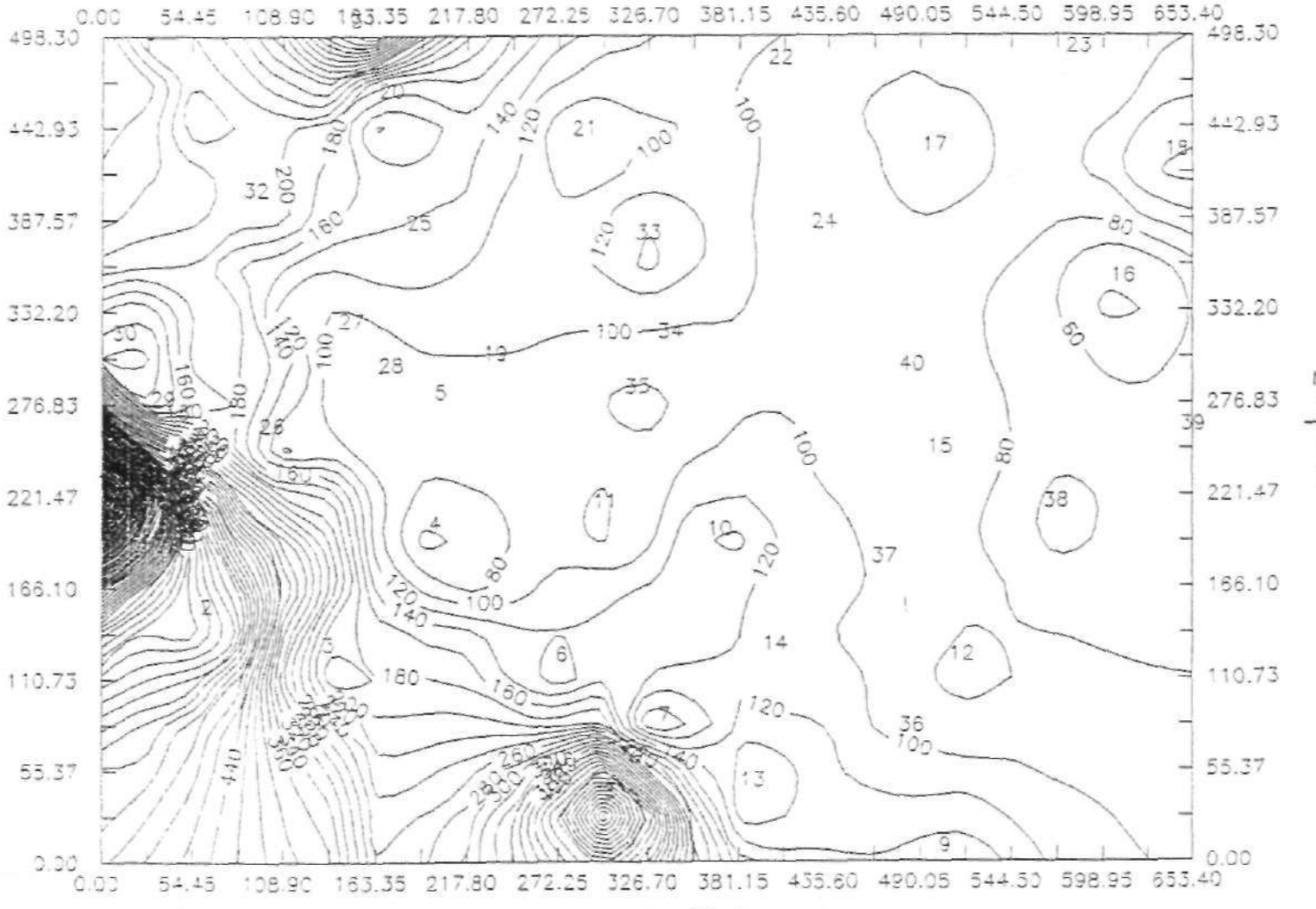


FIG. 4.10 Isoresistivity map at 5m depth con. int. 20 Ohm-meters

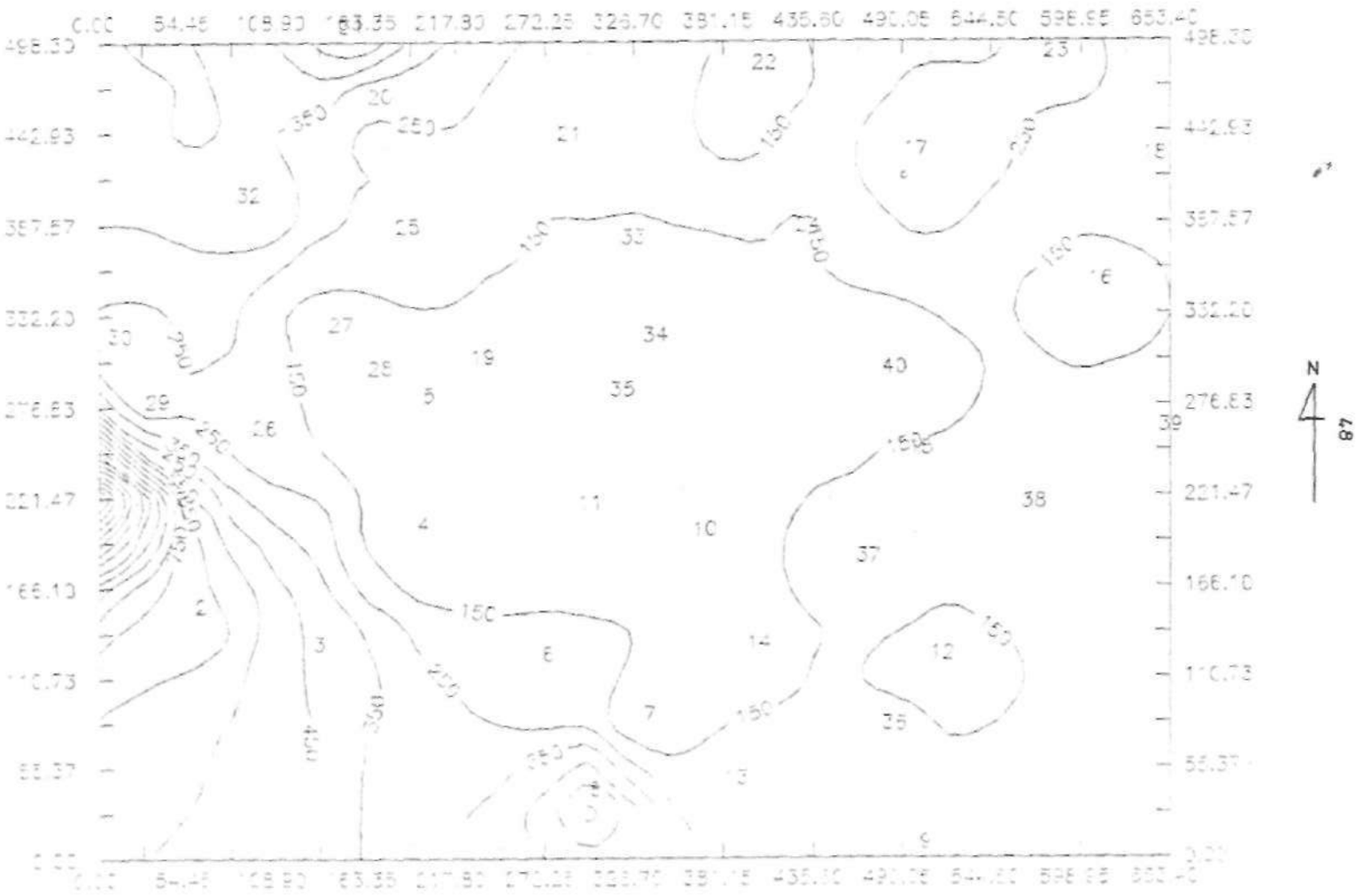


FIG. 4-11

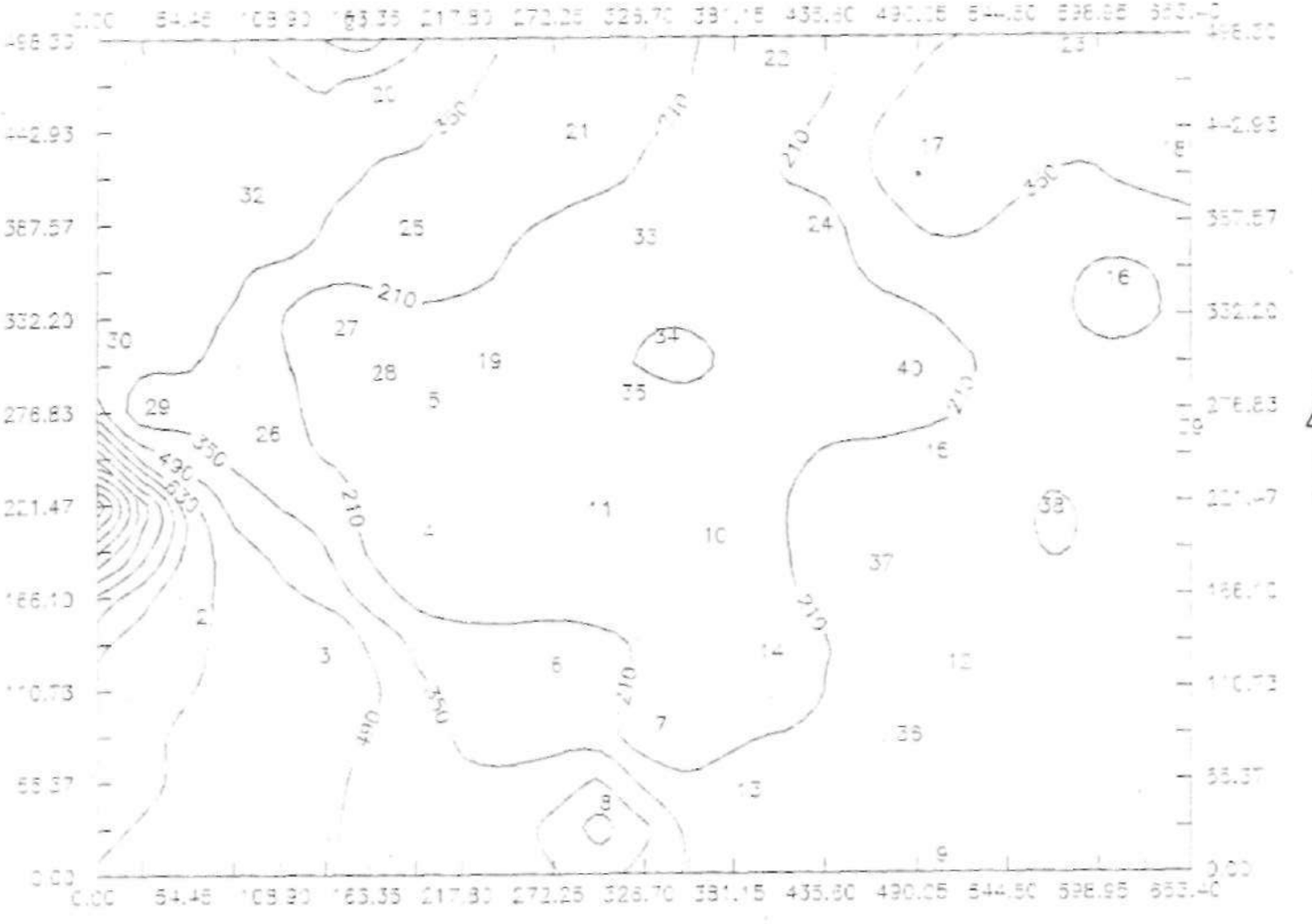


FIG. 4.12 Isoresistivity map at 15m depth btn. Int. 40 Ohm-meters

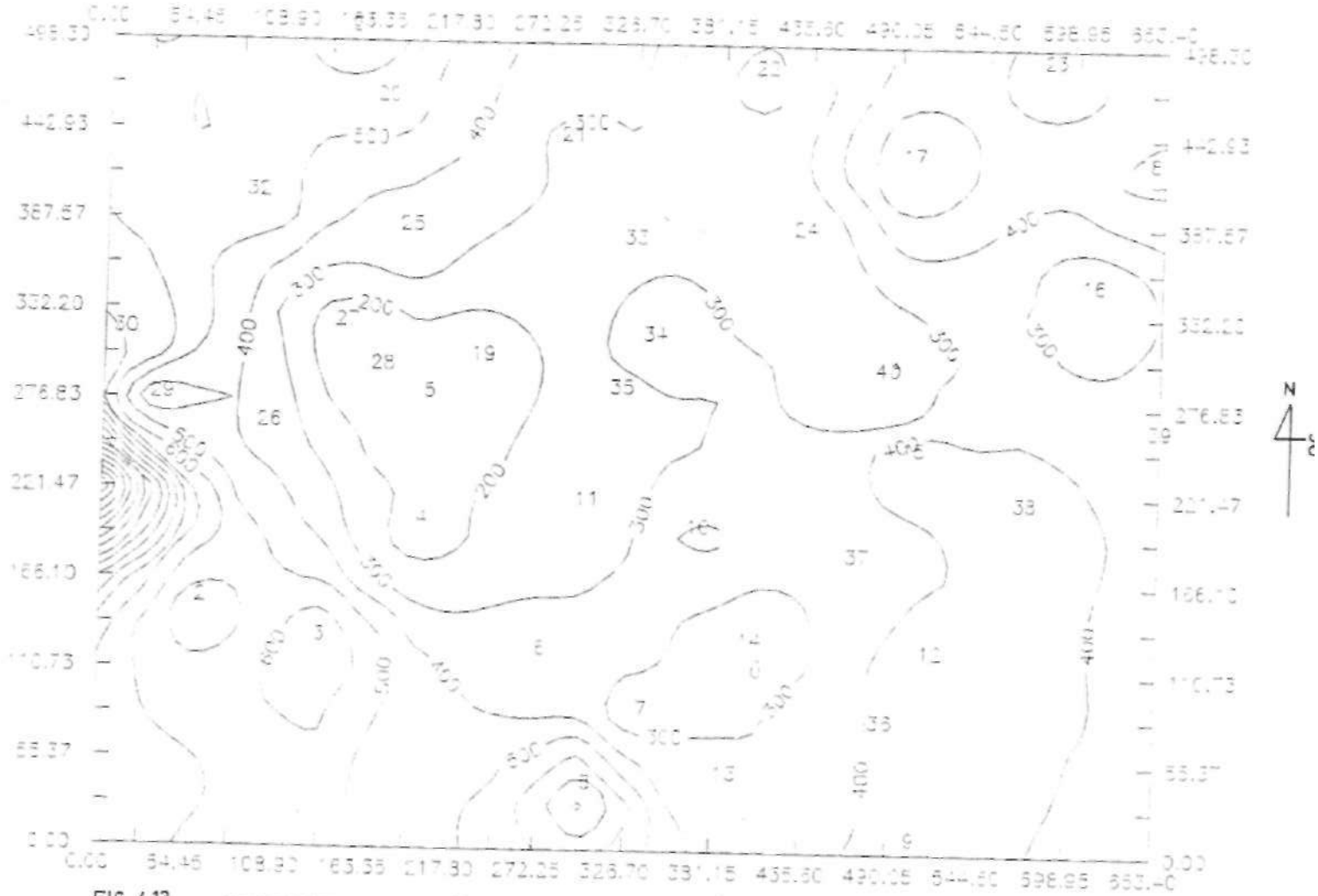

FIG. 4.13 Isoresistivity map at 20m depth equi. int. 100 Ohm-meters

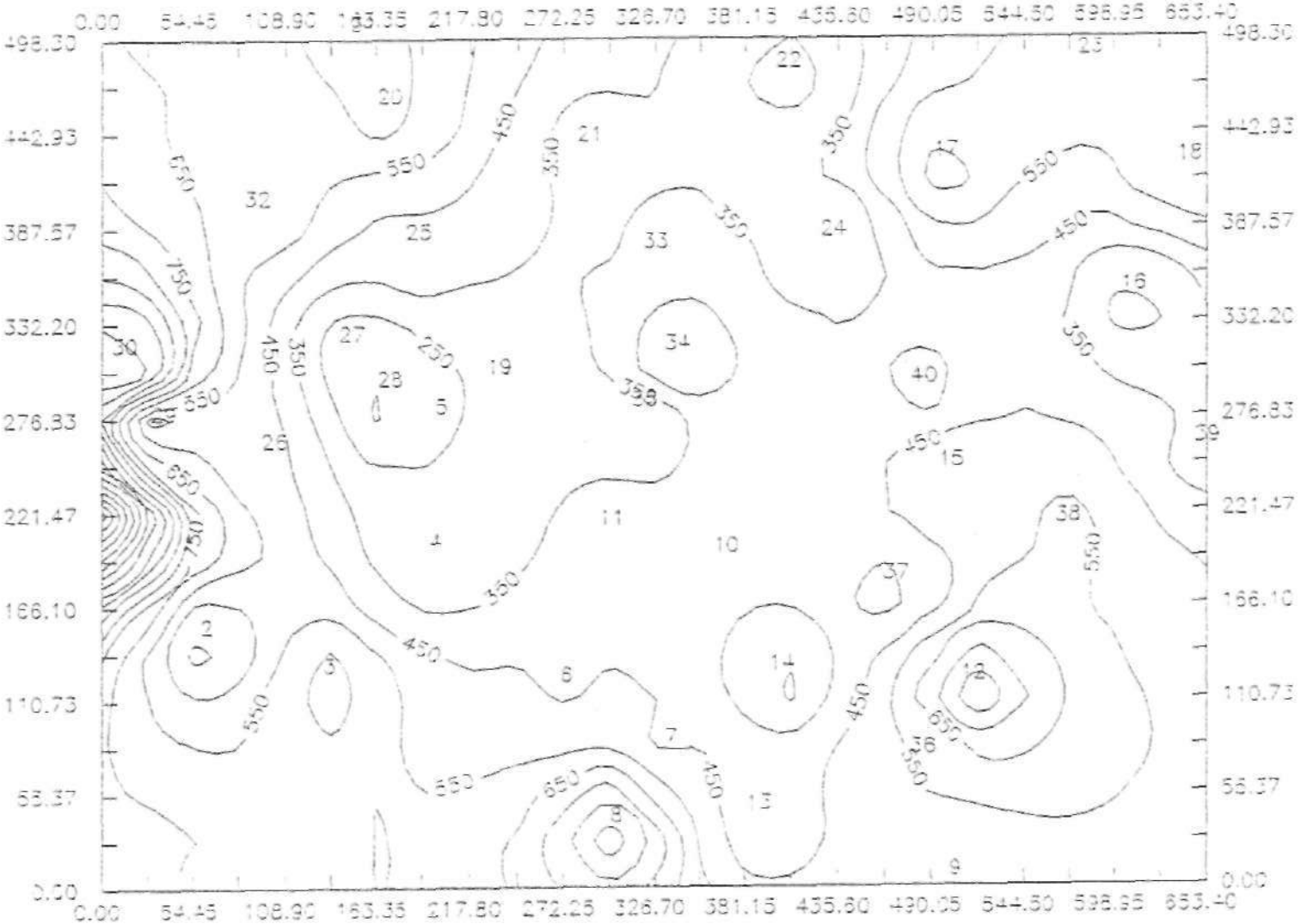


FIG. 4.14 Isoresistivity map at 25m depth con. int. 100 Ohm-meters

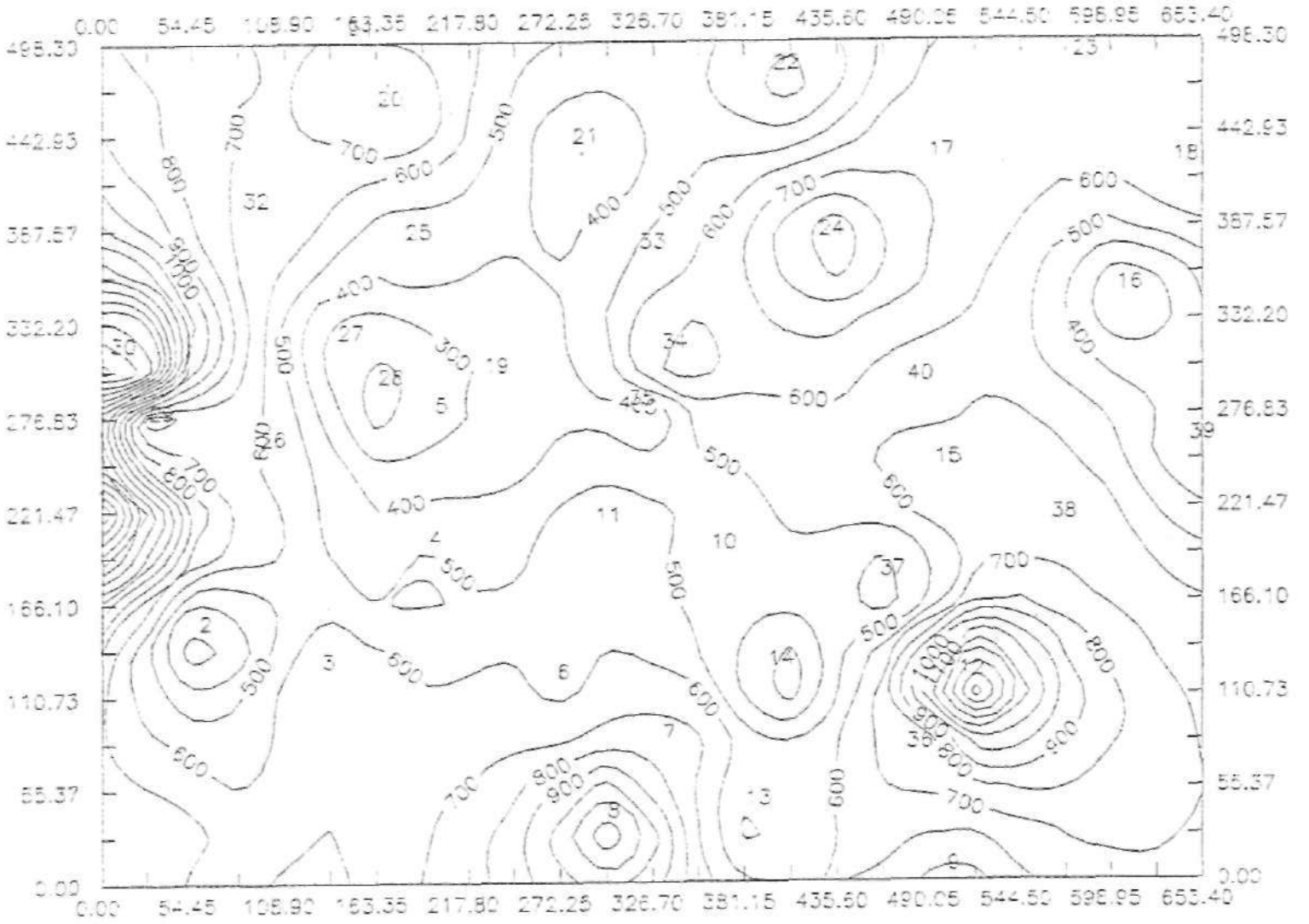


FIG. 4.15 Isoresistivity map at 30m depth con. int. 100 Ohm-meters

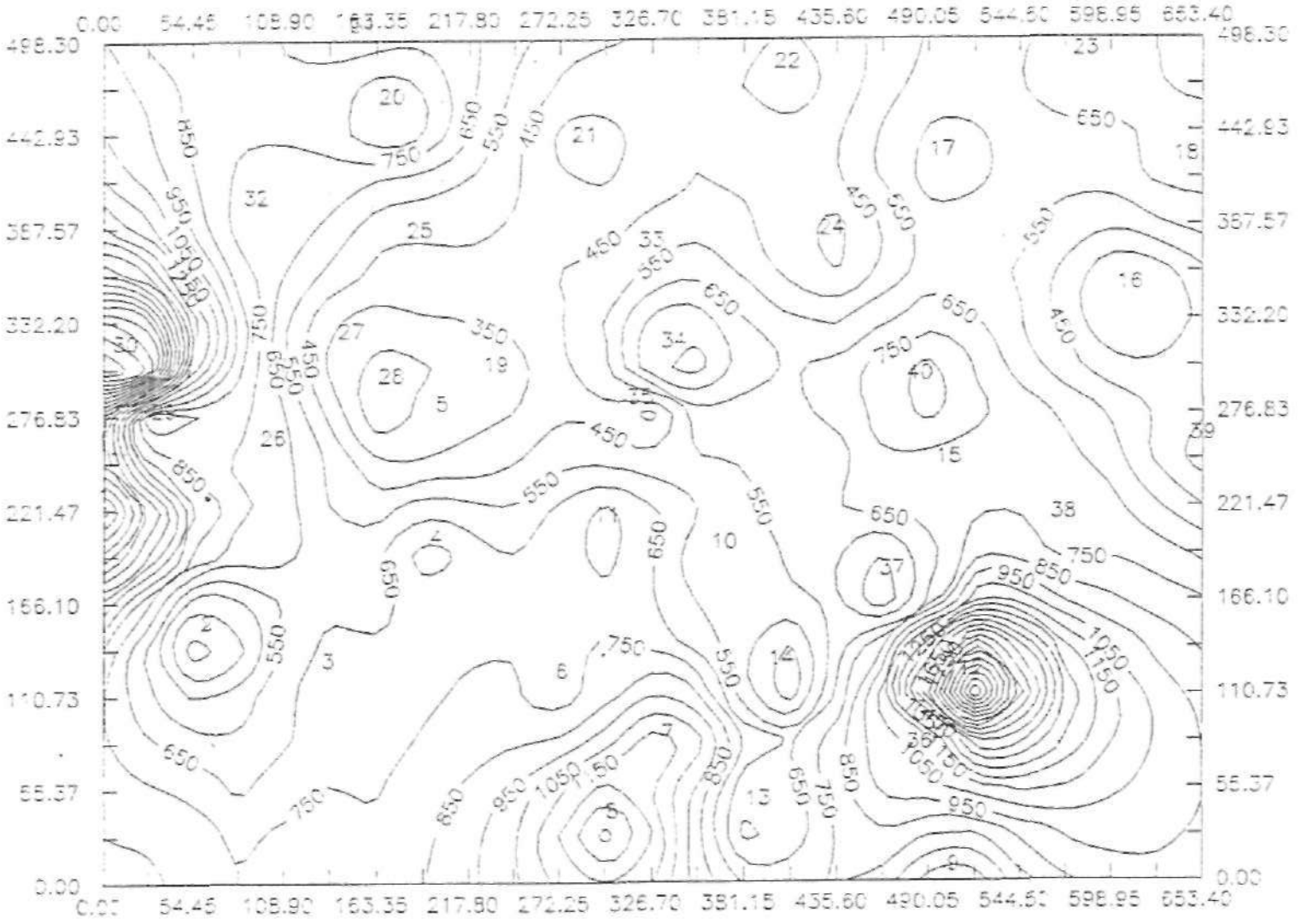


FIG. 4.16 Isoresistivity map at 35m depth con. int. 100 Ohm-meters

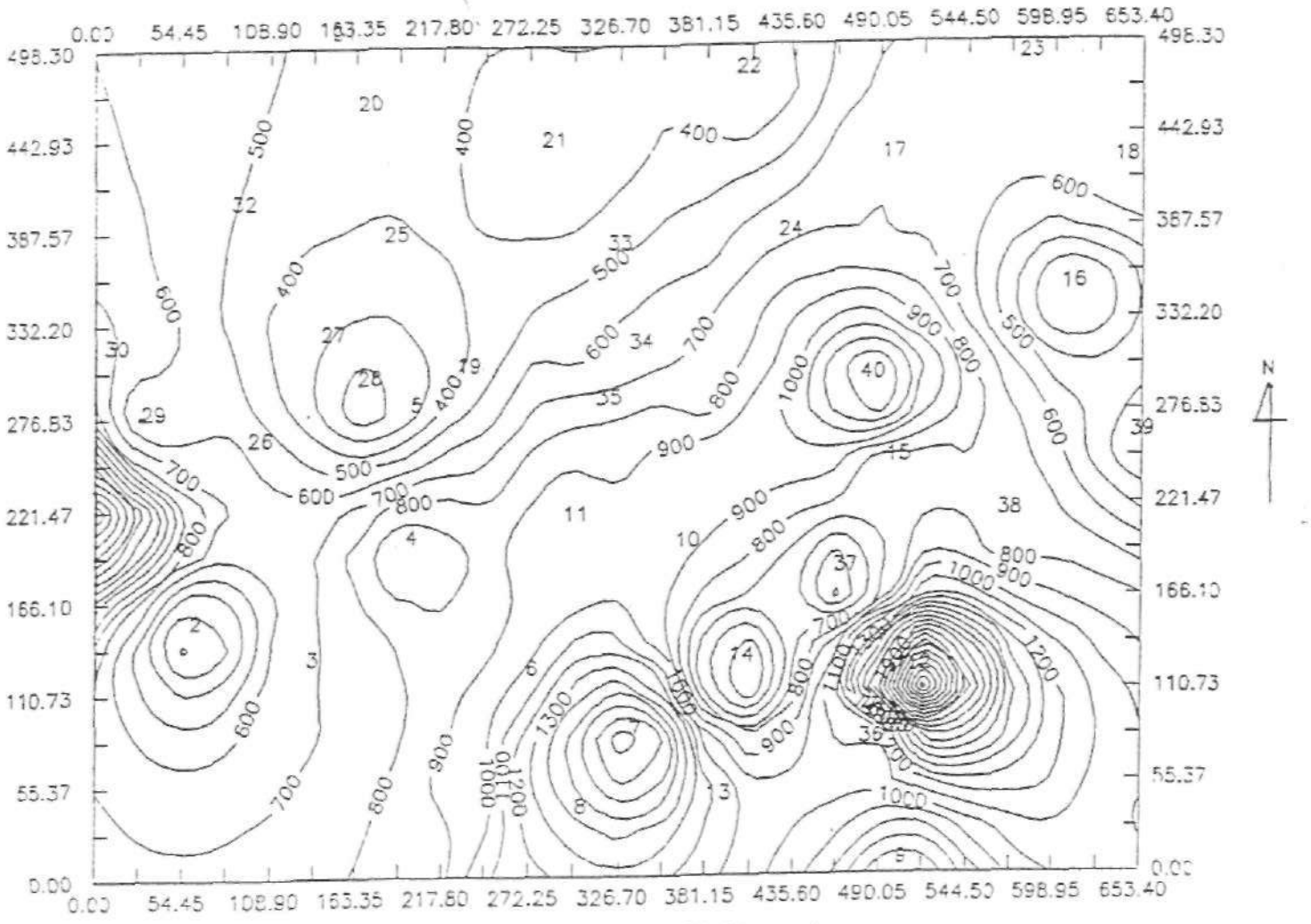


FIG 4.17 Isoresistivity map at 40m depth con. int. 100 Ohm-meters

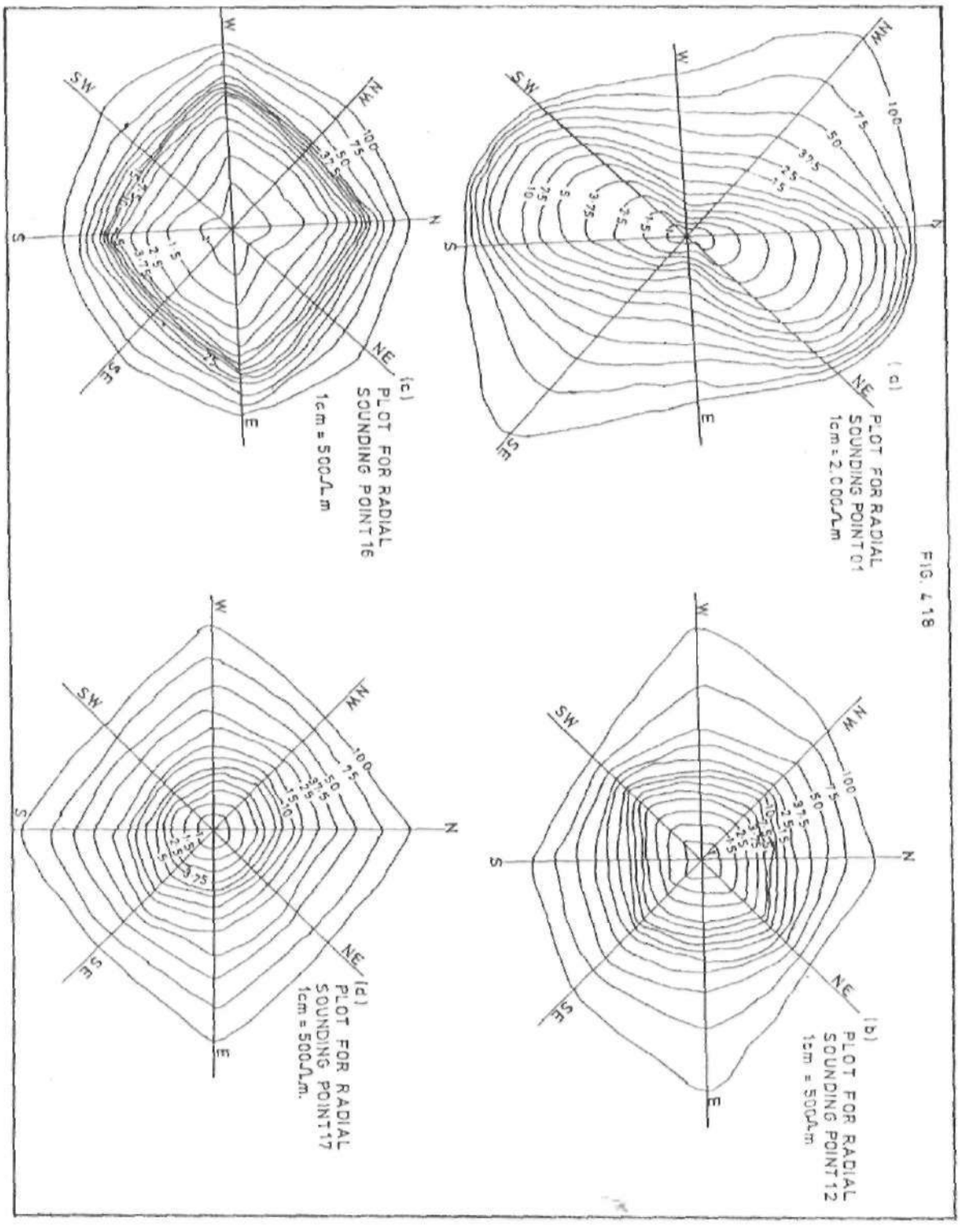
(a)
PLOT FOR RADIAL
SOUNDING POINT 01
1cm = 2.000Ωm
(b)
PLOT FOR RADIAL
SOUNDING POINT 12
1cm = 500Ωm
(c)
PLOT FOR RADIAL
SOUNDING POINT 16
1cm = 500Ωm
(d)
PLOT FOR RADIAL
SOUNDING POINT 17
1cm = 500Ωm.
N
NE
E
SE
S
SW
W
NW

FIG. 4.18

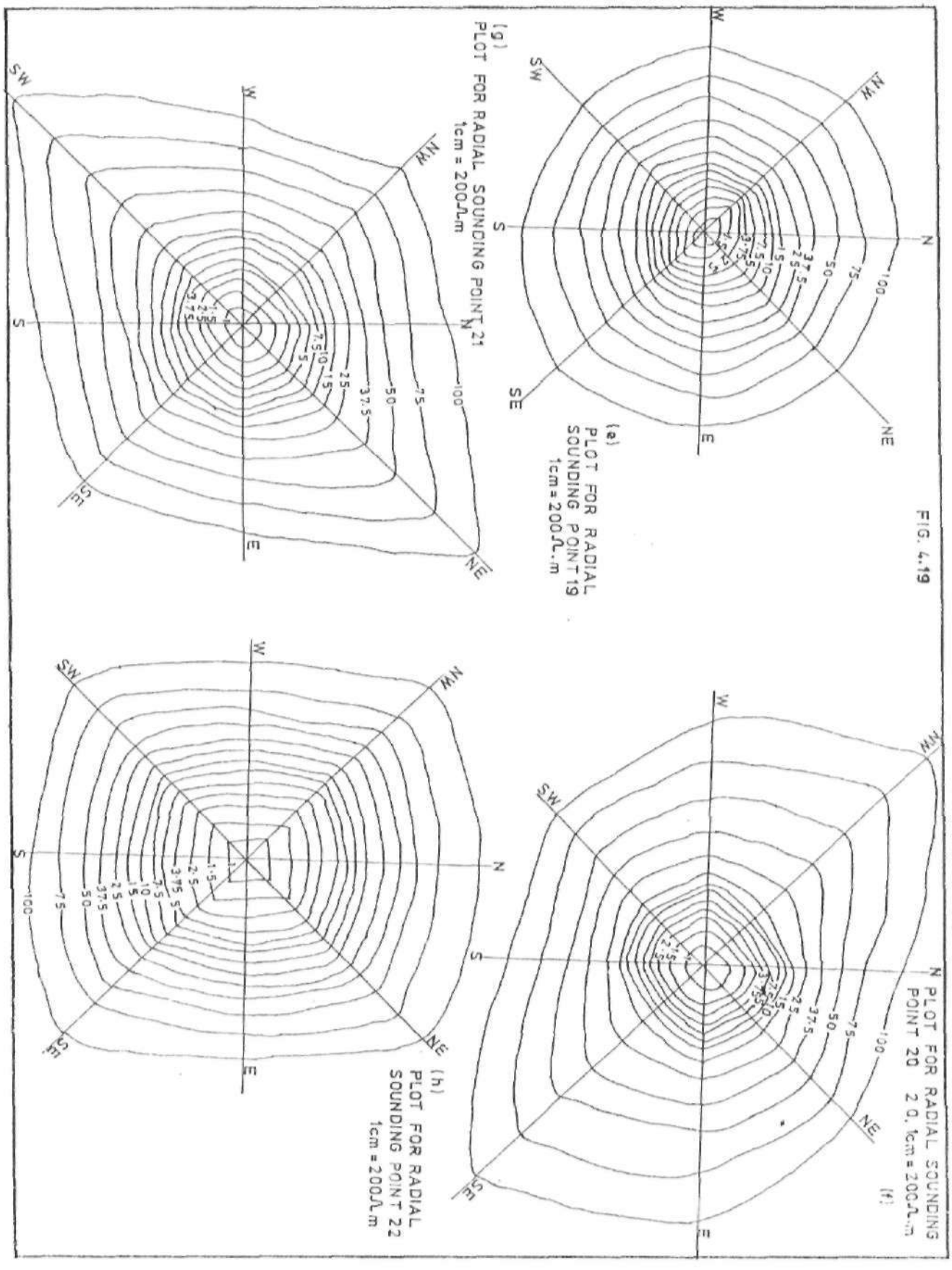
(e)
PLOT FOR RADIAL
SOUNDING POINT 19
1cm = 200Ω.m
(f)
PLOT FOR RADIAL SOUNDING
POINT 20 1cm = 200Ω.m
(g)
PLOT FOR RADIAL SOUNDING POINT 21
1cm = 200Ω.m
(h)
PLOT FOR RADIAL
SOUNDING POINT 22
1cm = 200Ω.m
N
NE
E
SE
S
SW
W
NW
1.5
2.5
3.75
5
7.5
10
15
25
37.5
50
75
100

FIG. 4.19

of fracturing and faulting (Telford *et al.*, 1976), their presence in a water bearing bed can serve as groundwater storage.

Depths of anisotropic variation are classified as shallow, intermediate and great depths. Figure 4.18a shows an existence of anisotropy which varies with depth as indicated by the ellipses of the plots. The anisotropy varies from NE-SW at shallow and intermediate depths to NW-SE at a great depth. Similarly, the direction of anisotropy for VES 12 varies from NE-SW at shallow and intermediate depths to E-W at great depth. The directions of anisotropy obtained for other stations are summarised in Table 4.4.

*Table 4.4: Trend of subsurface anisotropies as obtained from the Radial Sounding Plots*

| STATION | AT SHALLOW DEPTH | AT INTERMEDIATE DEPTH | AT GREAT DEPTH |
|---|---|---|---|
| 01 | NE - SW | NE - SW | NW - SE |
| 16 | NE - SW | E - W | E - W |
| 16 | E - W | E - W | NIL |
| 17 | NW - SE | NW - SE | E - W |
| 19 | NW - SE | NIL | NIL |
| 20 | NE - SW | NE - SW | NE - SW |
| 21 | NE - SW | NE - SW | NE - SW |
| 22 | NIL | NIL | NIL |

Table 4.4 shows a greater concentration of anisotropies at shallow and intermediate depths. It is further deduced from the table that the directions of anisotropies follow the major directions of faulting in the basement areas (NW - SE, NE - SW and E - W) as shown by Oluyide and Udoh (1986).

### 4.2.8 Depth to Bedrock Contour Map

The Zohdy's program generates a set of depths with the corresponding resistivity values from the layers. The last depths are obtained from these depth estimates. This data is used to draw the depth-to-bedrock map by picking all depth data corresponding to the resistivity values assumed for bedrock at all VES points (Figure 4.20). The VES points are posted on the contours in other to properly visualise the location of the various areas. From Figure 4.20, it could be noticed that the bedrock is shallowest around VES 1 with a depth of about 4 m and deepest around VES 4 and 11 with a depth around 36 m. A surface plot of the basement (bedrock) using the same data is shown in Figure 4.21 which presents a fair representation of the bedrock topography.

### 4.2.9 Depth to and Thickness of Weathered Basement Maps

As explained earlier, the data of depths, with the corresponding resistivity values were used to generate another set of depth to weathered basement using the resistivity value of weathered basement. The same process is followed using the resistivity range value for the weathered basement to obtain its thickness distribution. Figures 4.22 and 4.23 were obtained with the two processes above. Figure 4.22 shows that weathered basement is deepest at VES 4 with a depth of about 15 m. This corresponds to the geologic information obtained in figure 4.8a on the profile EF. Further, figure 4.23 indicates the thickest portion of weathered basement, which is about 36 m to be around VES 4, 10, 11 and 14. This is in agreement with the geologic section for profiles CD and EF (Figures 4.7b and 4.8a).

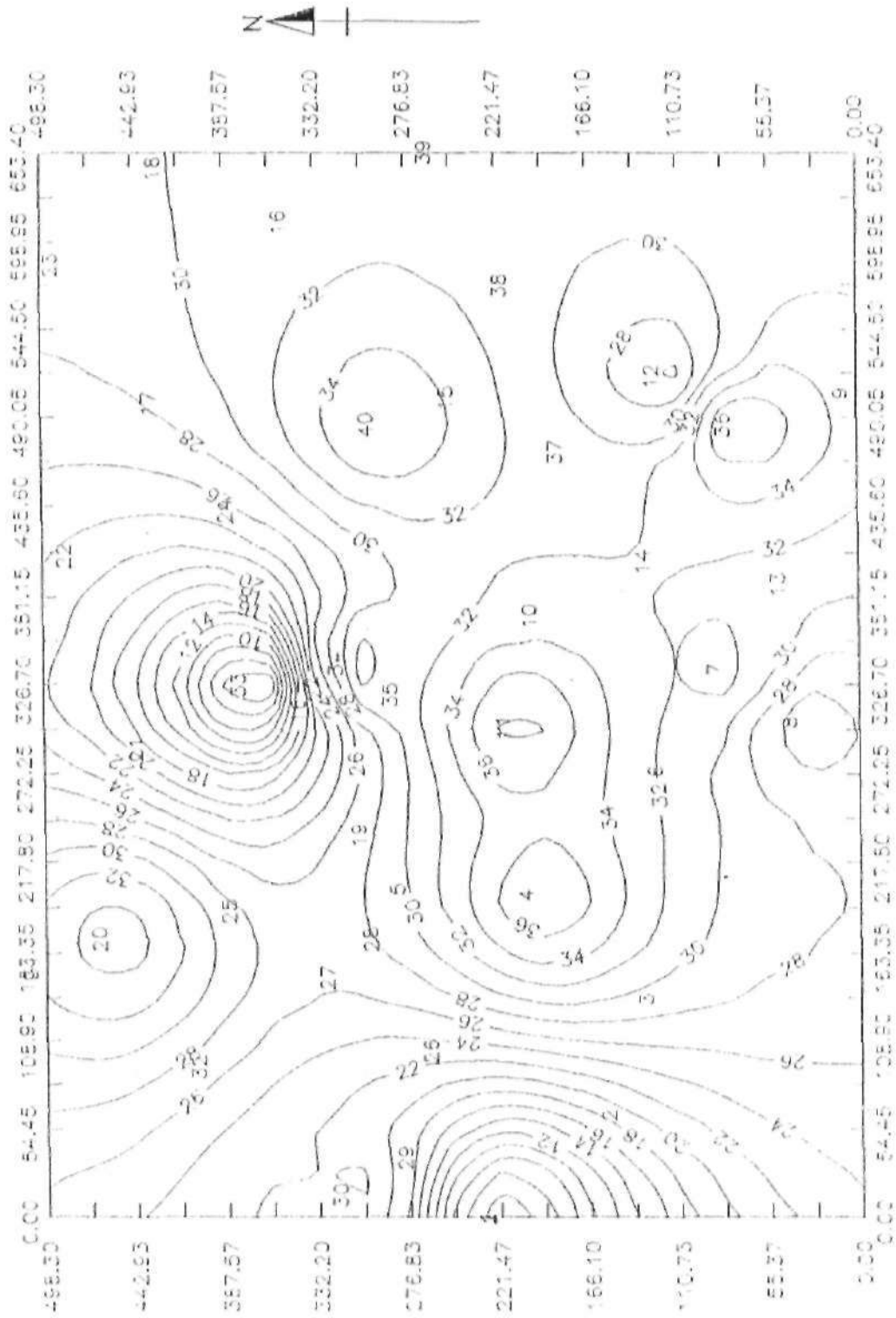


FIG. 4.20 Depth to bedrock map contour 2m

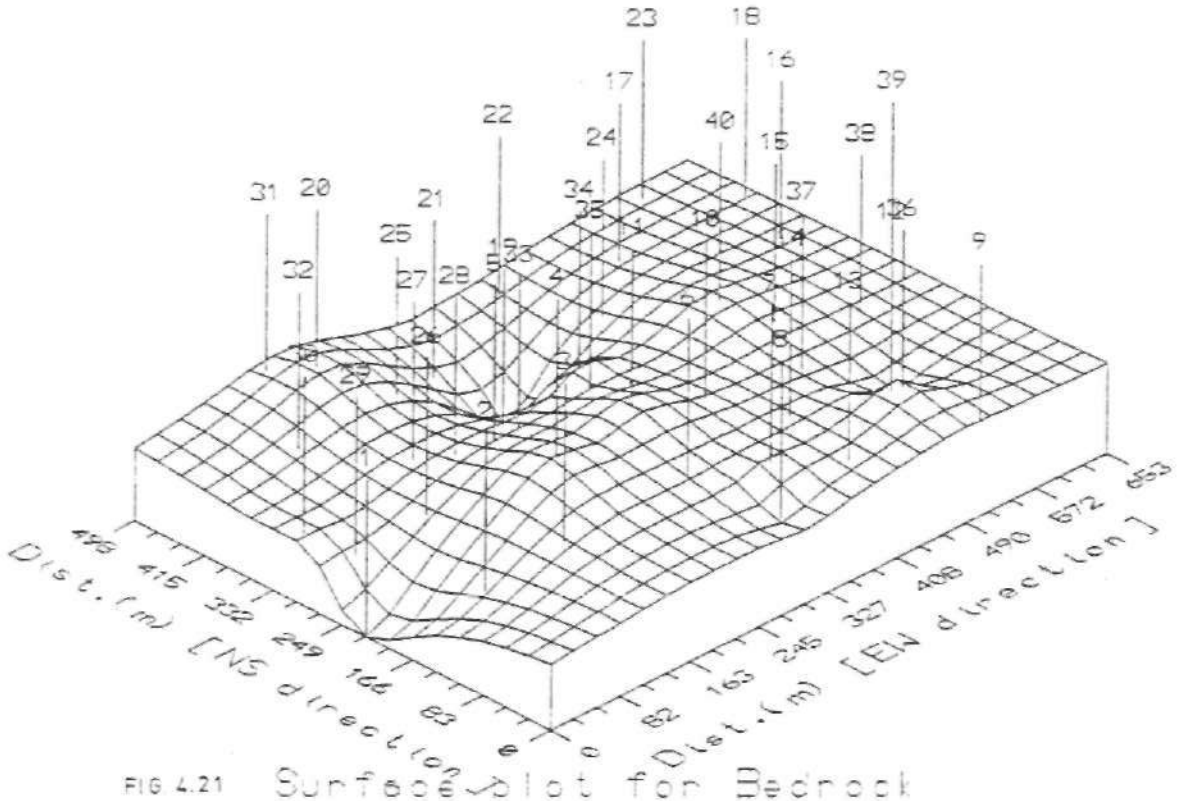


FIG 4.21 Surface Plot for Bedrock

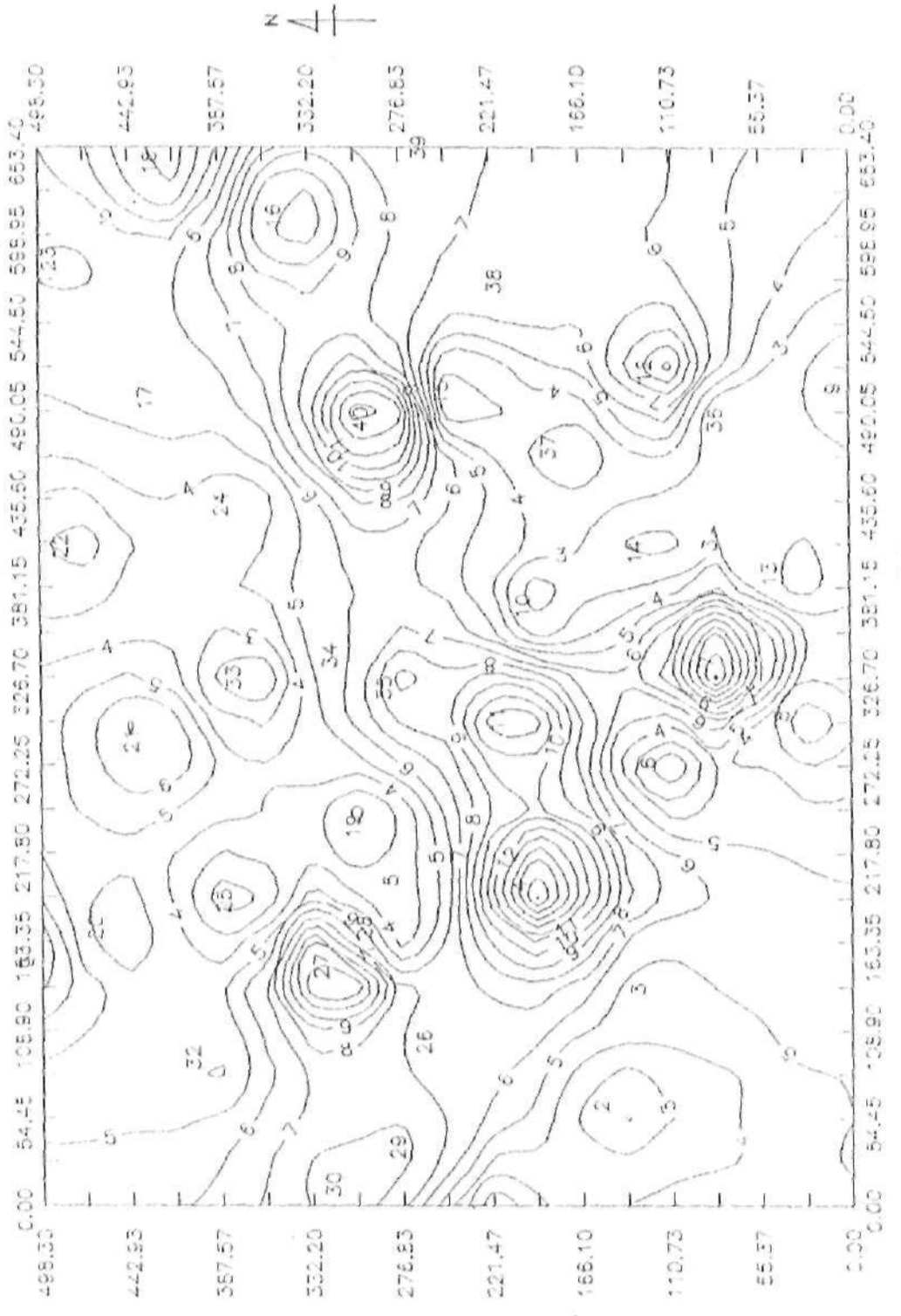


FIG. 4.22 Depth to Weathered basement map contour in m

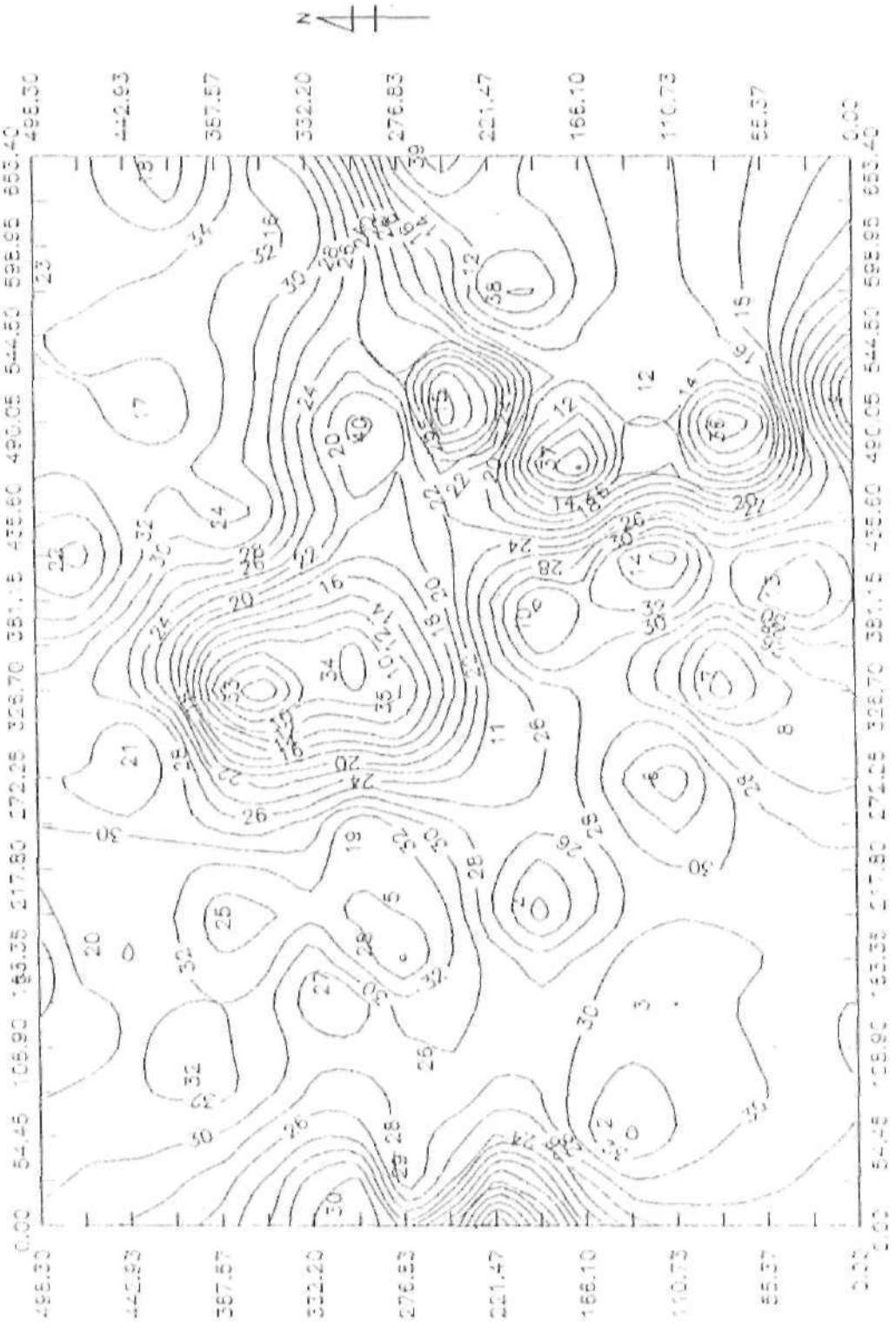

FIG. 4.23 Thickness of weathered basement map (m. Cm

### 4.2.10 Depth to and thickness of Aquifer Maps

The depth versus resistivity value data earlier obtained were also used, applying the resistivity range of aquifer to obtain the two sets of data. Figures 4.24 and 4.25 were hence drawn using the two data. The depth to aquifer map, Figure 4.24 shows that aquifer is deepest around VES 11 extending towards VES 4, with a depth of about 4.0 m. This might be accounted for by the high thickness of the topsoil as show in the geologic section of the area, Figure 4.7a. The aquifer is shallowest around VES 2 extending towards VES 1 with a depth of about 1 m. This is not to be expected, since this is the environment of the only outcrop in the study area. Figure 4.7a shows this too. The groundwater there may be retained close to the surface by the shallow underlying fresh basement. Aquifer thickness map, Figure 4.25, suggested that the surrounding of VES 4, extending towards VES 5, 27 and 28 is having the thickest aquifer of about 14 m while the thinnest portion of aquifer (1.0 m) lies around VES 2.

## 4.3 Correlation of Isoresistivity Map with Aquifer Thickness Map

It is recalled that the Isoresistivity maps seek to connect all areas with the same resistivity values at the depth considered. This helps to see at a glance the resistivity distributions over the whole study area at that depth. Similarly, Aquifer thickness map is intended at revealing the variation of the water bearing zones in the study area. A superposition of the two maps will not only show at a glance the thickest zones of Aquifer, the resistivity of such area can equally be known. The correlation maps produced at some selected depths are shown in Figures 4.26, 4.27 and 4.28.

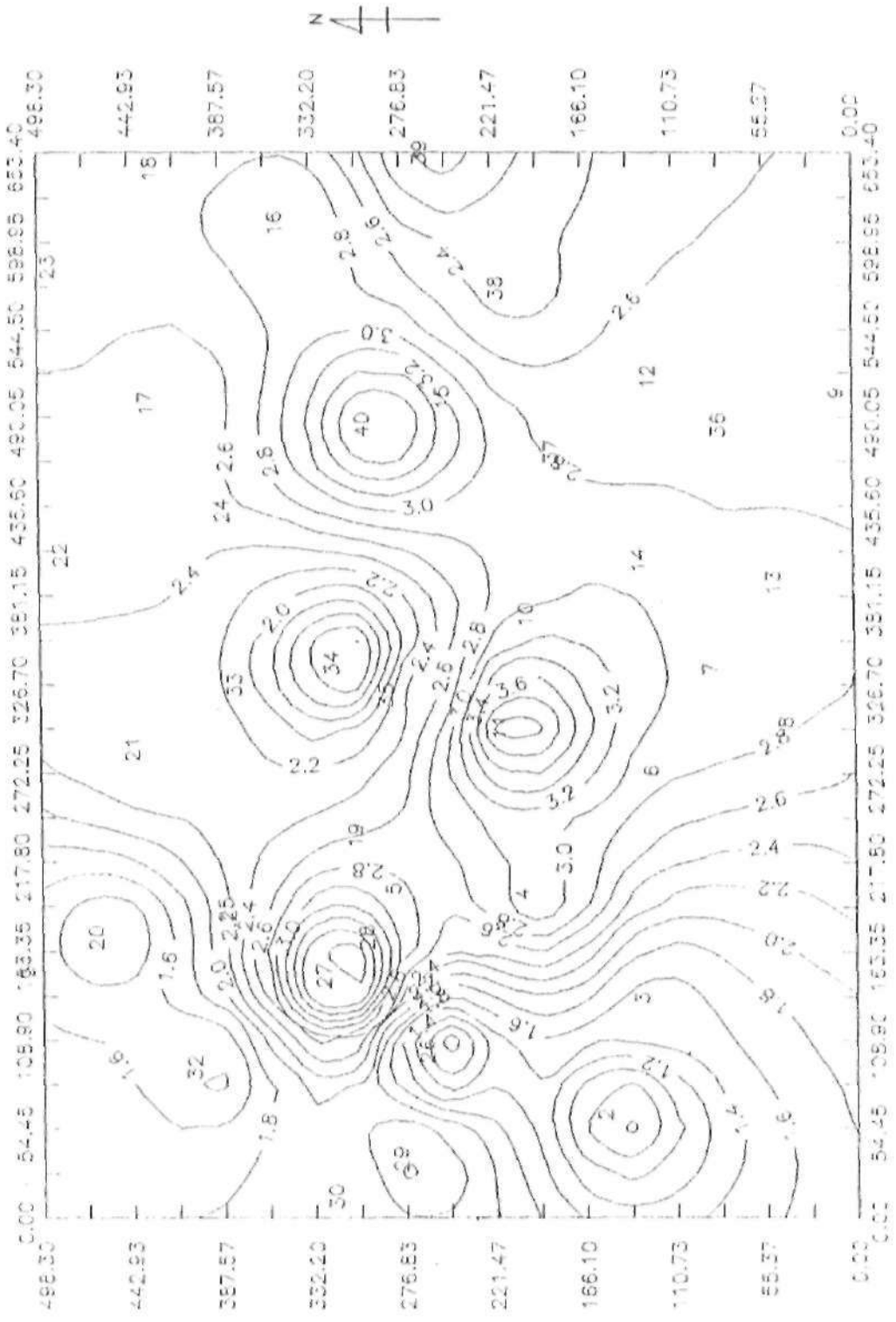

FIG.4.24 Depth to Aquifer map contours/m

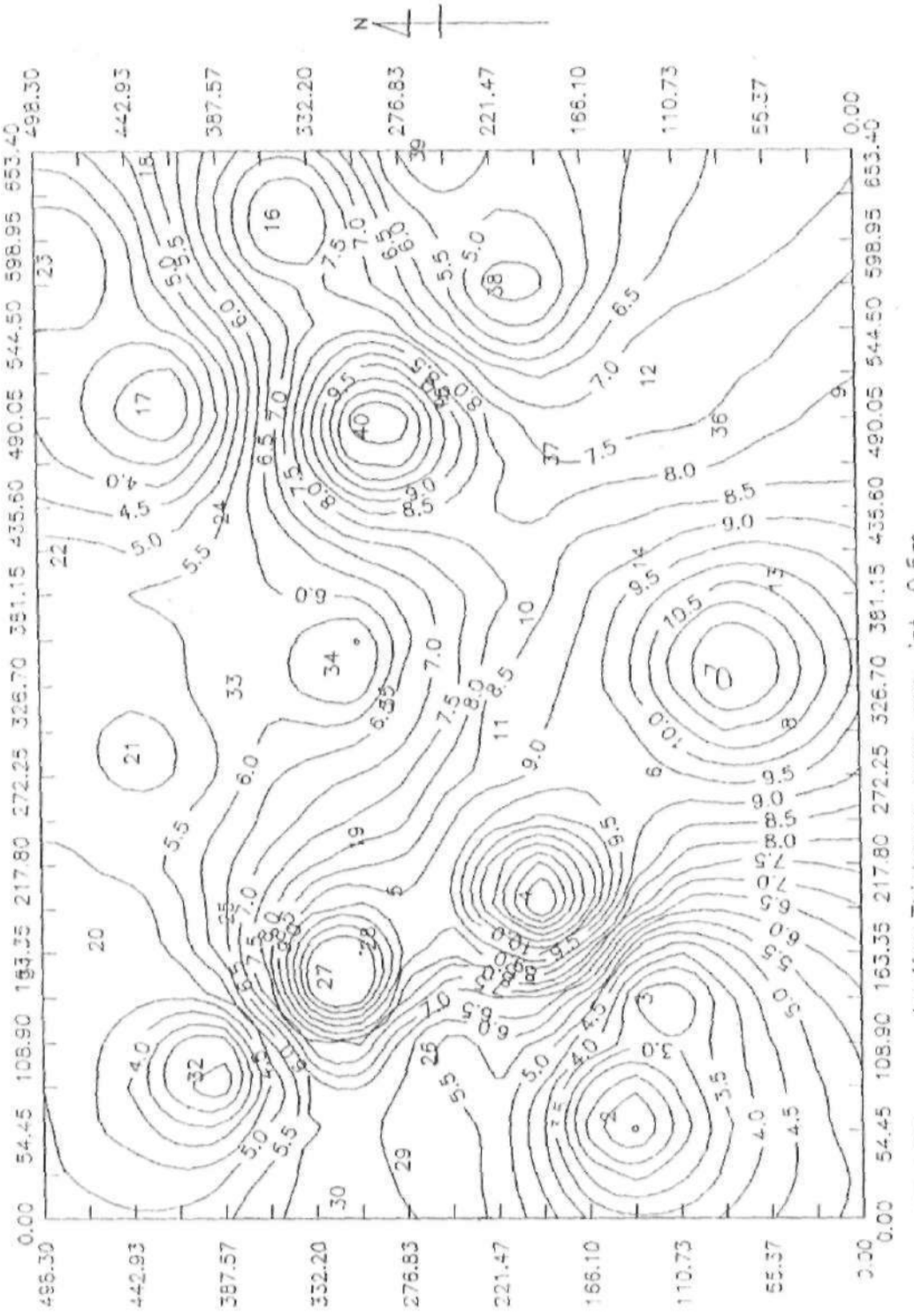


FIG. 4.25 Aquifer Thickness map con. int. 0.5m

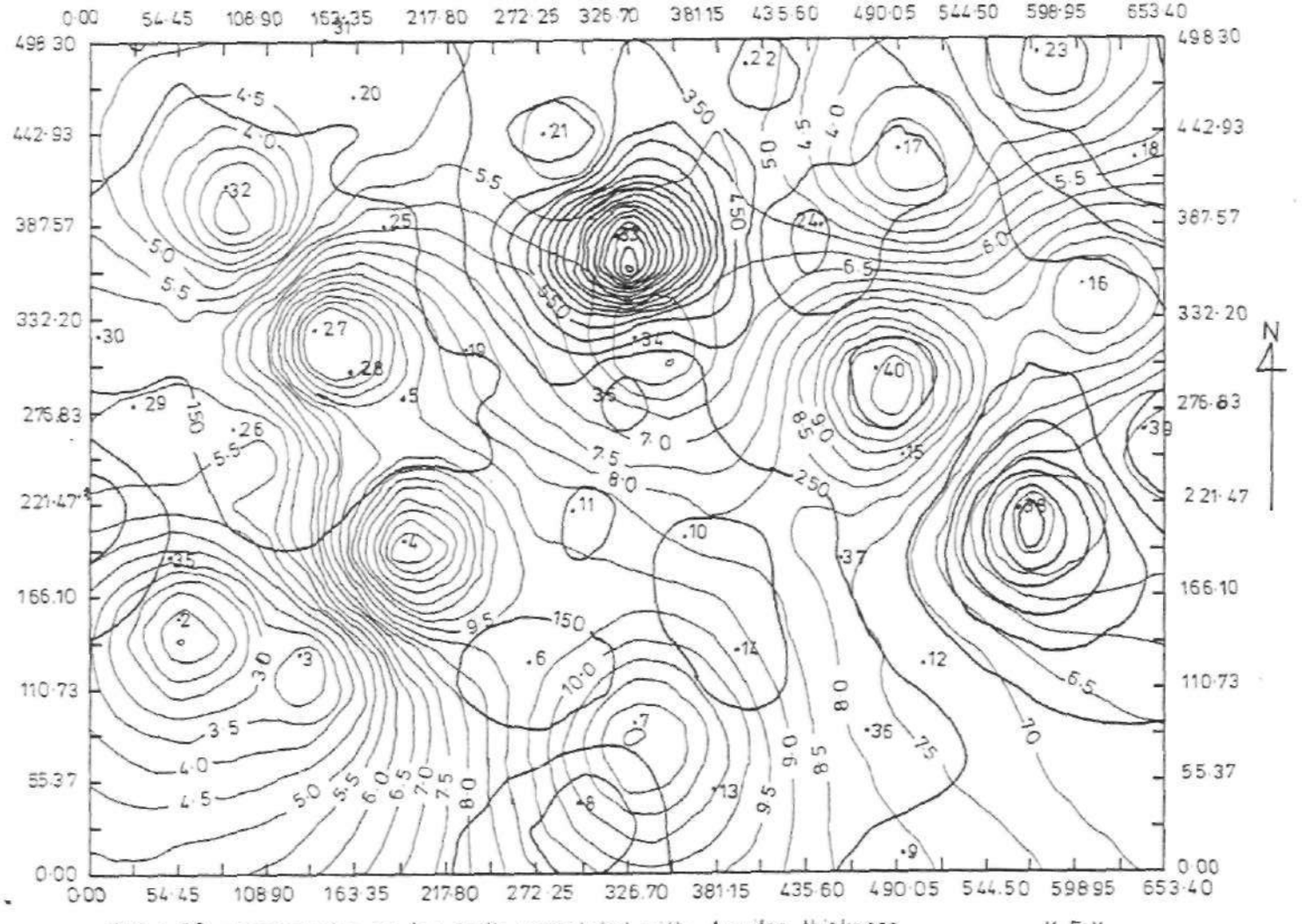


FIG. 4.26 Isoresistivity at 1m depth correlated with Aquifer thickness

KEY

— Isoresistivity contour(interval100Ωm

— Thickness " " ·5m

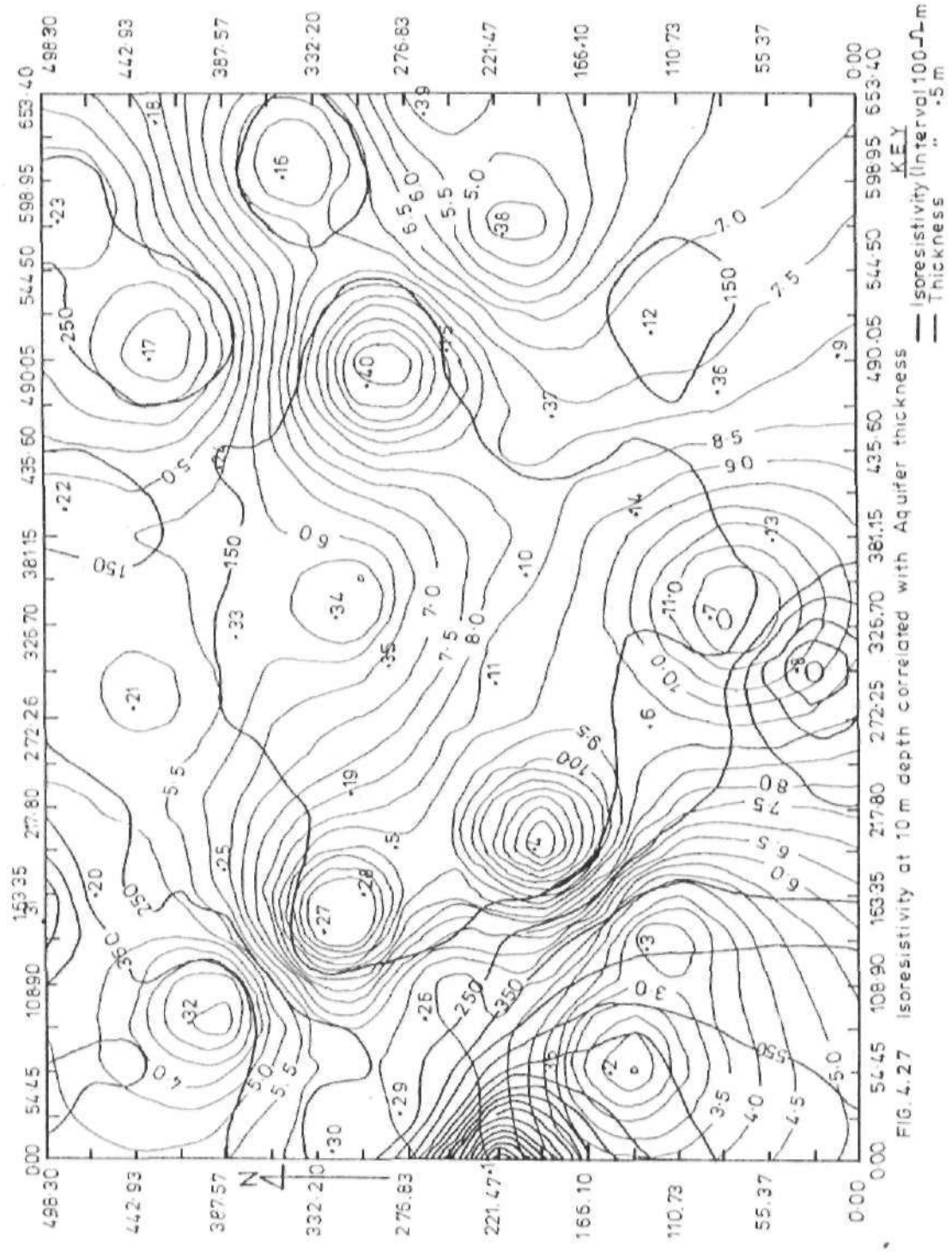


FIG. 4.27 Isoresistivity at 10 m depth correlated with Aquifer thickness

Analysis of the map (Figure 4.26) shows that the lowest resistivity value at 1 m depth is much above 100 ohm-metres along the thickest aquifer that trends NW-SE direction of the entire study area. It can be deduced that the aquifer zones shown at this depth may not be said to be reliable due to a relatively high value of minimum resistivity in that area.

Figure 4.27 shows the correlation at the depth of 10 m. It is revealed that resistivity values go below 100 ohm - metres around the aquifer zones identified especially around VES 4, 27 and 28 where the aquifer is equally thick. This effects may be due to a resourcesful aquifer around that depth.

Figure 4.28 shows a slight increase in the minimum resistivity values at 15 m depth over the values at shallower depths around the thickest aquifer zones identified (VES, 4, 27 and 28). This may indicate a slight passage of the most resourcesful aqueferous zones. It is however recalled that the thickest aquifer in that area is revealed to be 14 m as discussed in section 4.2.10.

## 4.4 INTERPRETING THE VLF DATA

The main aim of using the VLF method is to identify fractured, sheared and faulted zones. The graph of inphase and quadrature components were plotted against distance along each VLF survey lines as shown in Figures 3.1 and 4.29. The 'cross-over' points (points of intersection points of inphase and quadrature plots) sometimes indicate fracture/shear zones (Fraser 1969). It is sometimes associated with vertical contacts between intrusive materials and the country rocks (Telford *et al.*, 1976). The positive quadrature values indicated possibly fault zones (Anneke, 1988). The negative ones are likely due to earthsurface

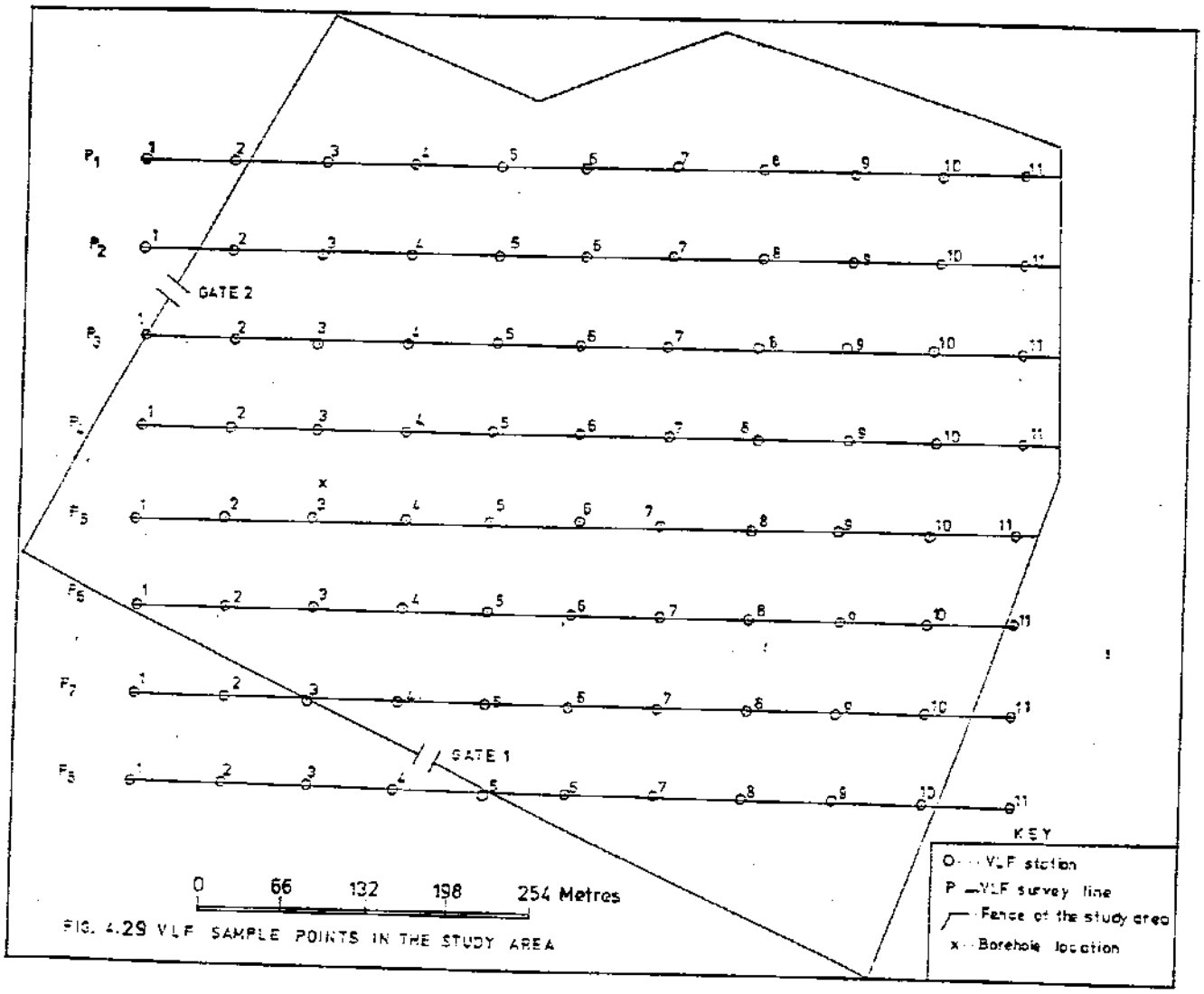


FIG. 4.29 VLF SAMPLE POINTS IN THE STUDY AREA

targets/conductors and hence can confuse the interpretation (Fraser, 1969). Thus, surface conductors are separated from the subsurface ones by separating the negative quadrature signals from positive ones.

In an effort to reduce erroneous interpretation of VLF data caused by geological noise component generated from the transmitted frequency, equation (10) was applied on the entire inphase data for numerical filtering purposes as suggested by Fraser (1969). The new set of data obtained were then contoured. This method transforms the zero crossings in the plots of Figures 4.30 and 4.31 into peaks. This filtering method reveals clearly area of high or low conductivities by improving the resolution of anomalies to ease their recognition. A positive peak indicates a conductive area (Fraser, 1969), in other words, a water bearing zone. All negative values in the filtered data were ignored as advised by Fraser (1969) as they will only confuse the expected picture.

## 4.5 Results and Deductions from the VLF Data

The results of the interpreted VLF data were obtained after analysing them as explained in section 3.3.2. In addition, the geologic information on the conductivity of the subsurface rocks in the basement area as obtained in the VLF manual and from past works, aided in the final analysis of the results in this work.

### 4.5.1 VLF Inphase and Quadrature Versus Distance/Survey line Plots for the Various Profiles

On each profile, the sample points (stations) were spaced 66 m apart. The same range was maintained all through the profiles as shown in Figure 4.29. Inpase and

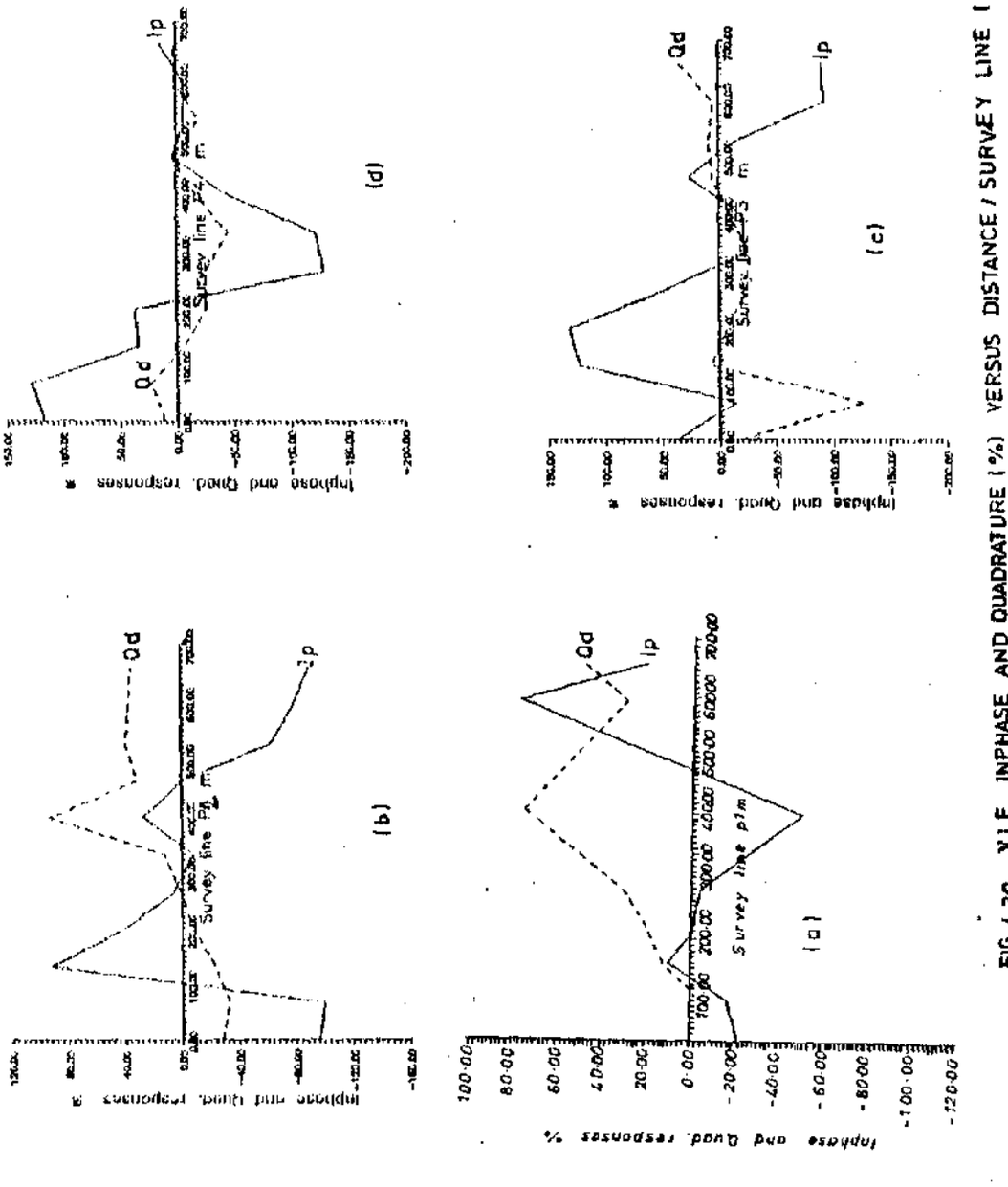


FIG. 4.30 VLF INPHASE AND QUADRATURE (%) VERSUS DISTANCE / SURVEY LINE (m)

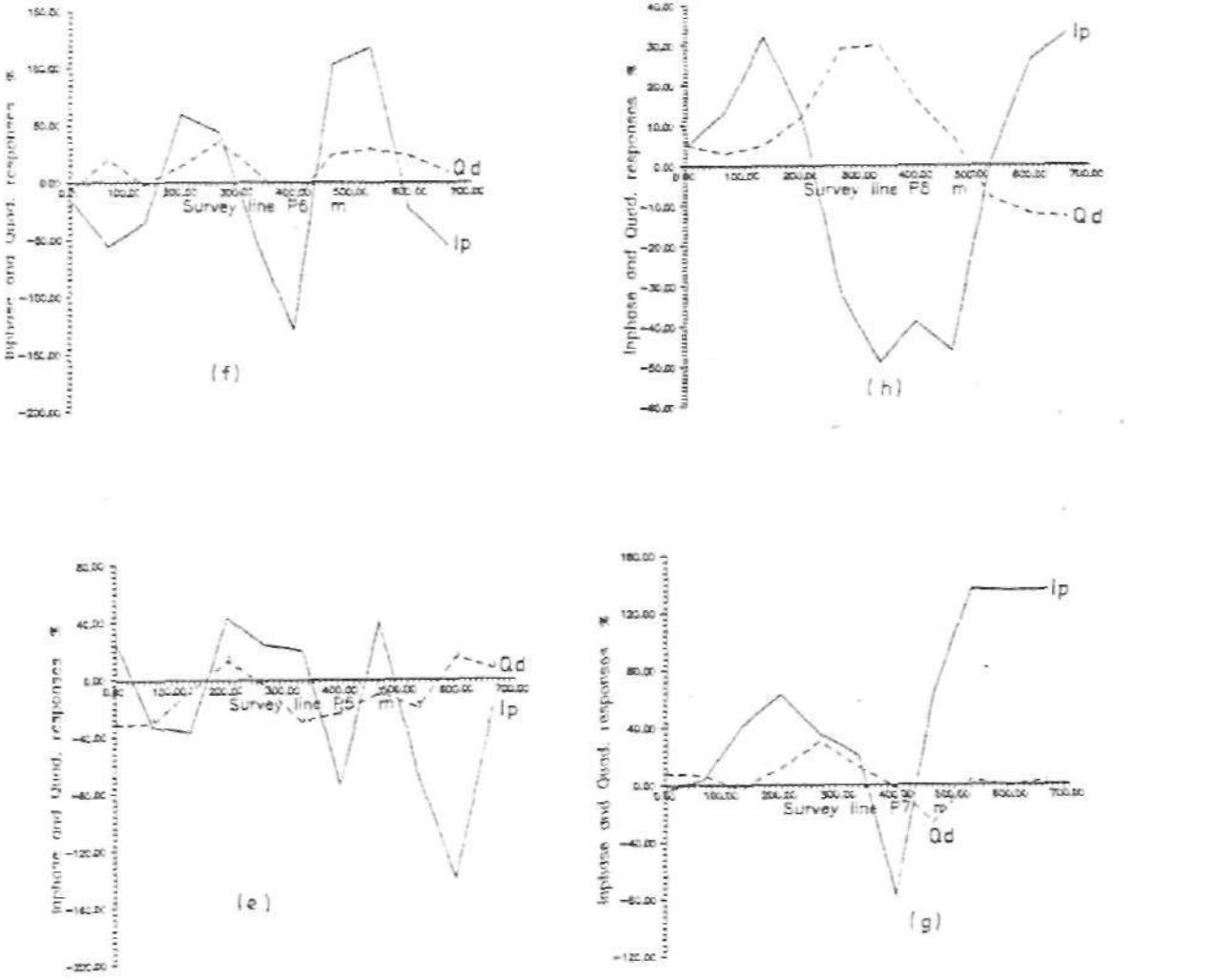


FIG. 4.31 VLF INPHASE AND QUADRATURE (%) VERSUS DISTANCE / SURVEY LINE (m)

Quadrature signal were recorded side-by-side at each station. the result of plots along each profile are discussed below.

## (a) Survey Line/Profile P1

Figure 4.30a shows the plot of Inphase and Quadrature versus distance along profile P1. The graph shows that the secondary field generated by the subsurface rock around P1 ranges from -52% to +80% while the quadrature component ranges from is -6% to +76%. The 'Cross-over'points that sometimes indicate shear zones exist in three locations along this profile: at distances 130, 540 and 640 m from the starting point. The positive quadrature values which indicate fault zones exist between 80 and 680 m along the profile. These suggest that the basement underlying between distances 130 and 640 m along profile P1 is most likely fractured to some degree. The degree of conductivity of the fractured area is expressed by the positive inphase response which exist from 110 m to 190 m and from 480 m to 670 m (Fig. 4.30a) along profile P1.

## (b) Survey Line/Profile P2

Figure 4.30b shows the plot for profile P2. On this plot the Inphase responses vary between -90% and +86% and quadrature responses vary between -36% and +86%. The two cross-over points are located 90 m and 280 m along the profile. The positive quadrature values exist from 160 to 680 m along profile P2; hence the area between 160 m and 680 m are likely fractured or sheared. The positive Inphase responses exist between 100 m and 280 m and between 350 m to 460 m along the profile. This expresses the degree of conductivities of the areas mentioned.

## (c) Survey Line/Profile P3

The plot for profile P3 is shown in figure 4.28. The values of the inphase and quadrature vary from -90% to +130% and from -125% to +30% respectively. The cross-over points exist at 340 m, 420 m and 490 m from the starting point; implying fracture or shear zones. The positive quadrature, only very mild, exists from 403 m to 660 m; implying fault zone. However, the positive responses for Inphase exist from starting point of P3 to 50 m, from 70 m to 310 m and from 420 m to 510 m from the starting point. This actually suggests that the conductive (likely water-bearing area) zone is not underlined by fractured basement, but the fractured zone exists a few meters away from there.

## (d) Survey Line/Profile P4

The Inphase and quadrature responses against the distance plot is as shown in figure 4.30d. The Inphase response value range from -130% to +130% while that of the quadrature range from -45% to +20%. The cross-overs are at 220 m, 460 m and 570 m along profile P3. The positive quadrature values lie between 120 m and the origin. The value of positive quadrature is small; this could mean a less degree of shearing or faulting around this location. The positive value of Inphase is only prominent from the starting point to 210 m distance.

## (e) Survey Line/Profile 5

The plot of the Inphase/quadrature against the station positions for profile 5 is shown in Figure 4.31a. This graph shows variation of Inphase responses, between -140% and +44% and quadrature responses vary between -32% and +16%. The cross-over points are located 70 m, 160 m, 370 m and 500 m along profile P5. This implies the presence of

fractures in the underlying bedrock. However, a low value of positive responses of quadrature that occur suggests mild faulting or shearing. The positive Inphase responses lie between the origin and a point 30 m away, between 160 and 360 m, and between 400 m and 490 m along profile P5.

**(f) Survey Line/Profile 6**

The inphase and quadrature response values vary from -130 to +115% and from -20 to +40% as shown in figure 4.31b. The cross-over occurs at, from the starting point, 160m, 270m, 440m and 560 m. This may mean series of fractures. Positive inphase exists between 150 m and 290 m, and between

430 m and 580 m from the starting point along the profile. This shows a probable water bearing zones.

## (g) Survey Line/Profile 7

The values of Inphase and quadrature components lie between -76% and +14% and -24% and +32%. Cross-overs occur at 70 mm 340 m and 410 along of profile P7 as shown in Figure 4.31c. The positive quadrature exist from the origin to a point 380 m along the profile. From this plot it can be inferred that the underlying basement along this profile may have been fractured or faulted. The positive inphase covers a large length on this profile with a very high value starting from 410 m and extends to the end of the profile. This indicates the presence of water bearing zone especially within the fractures.

## (h) Survey Line/Profile 8

Figure 4.30b shows the Inphase/quadrature plots against distance for profile P8. The Cross-over points exist on this profile at the origin, 200 m and 520 m along the origin. This indicates fracturing at depth. The positive quadrature covers from the origin to a point 520 m along the profile, indicating large scale faulting. However, the positive inphase response covers from the origin to a point to 220 m away and from 530 m to the end of the profile. Meanwhile, the Inphase response components vary between -50% and +32% while the quadrature components vary from -16% to 29%.

## 4.6 The VLF Positive Inphase Map for filtered Data

Figure 4.32 is the map obtained from the filtered data of the Inphase responses and Figure 4.33 represents the surface plot from the same data showing the surface reflection of the subsurface features (topography) as detected by the VLF survey. As Fraser (1969) suggested,

only the positive filtered values were used in the plots. This contour map is intended to reveal clearly the areas of high or low conductivities obtained in Figures 4.30 and 4.31. The zero crossings are transformed into peaks. This can aid a clearer identification of subsurface zones with greater underground water potentials. The process also helps to delineate surface conductors from the subsurface ones. Figure 4.32 shows a tendency to form closures of high positive Inphase values towards western part of the study area with greater concentrations around North-western corner of the area. This extends toward South East of the study area. This is an indication of high subsurface conductivity. The only existing borehole in this study area is located few meters away from the western part toward the

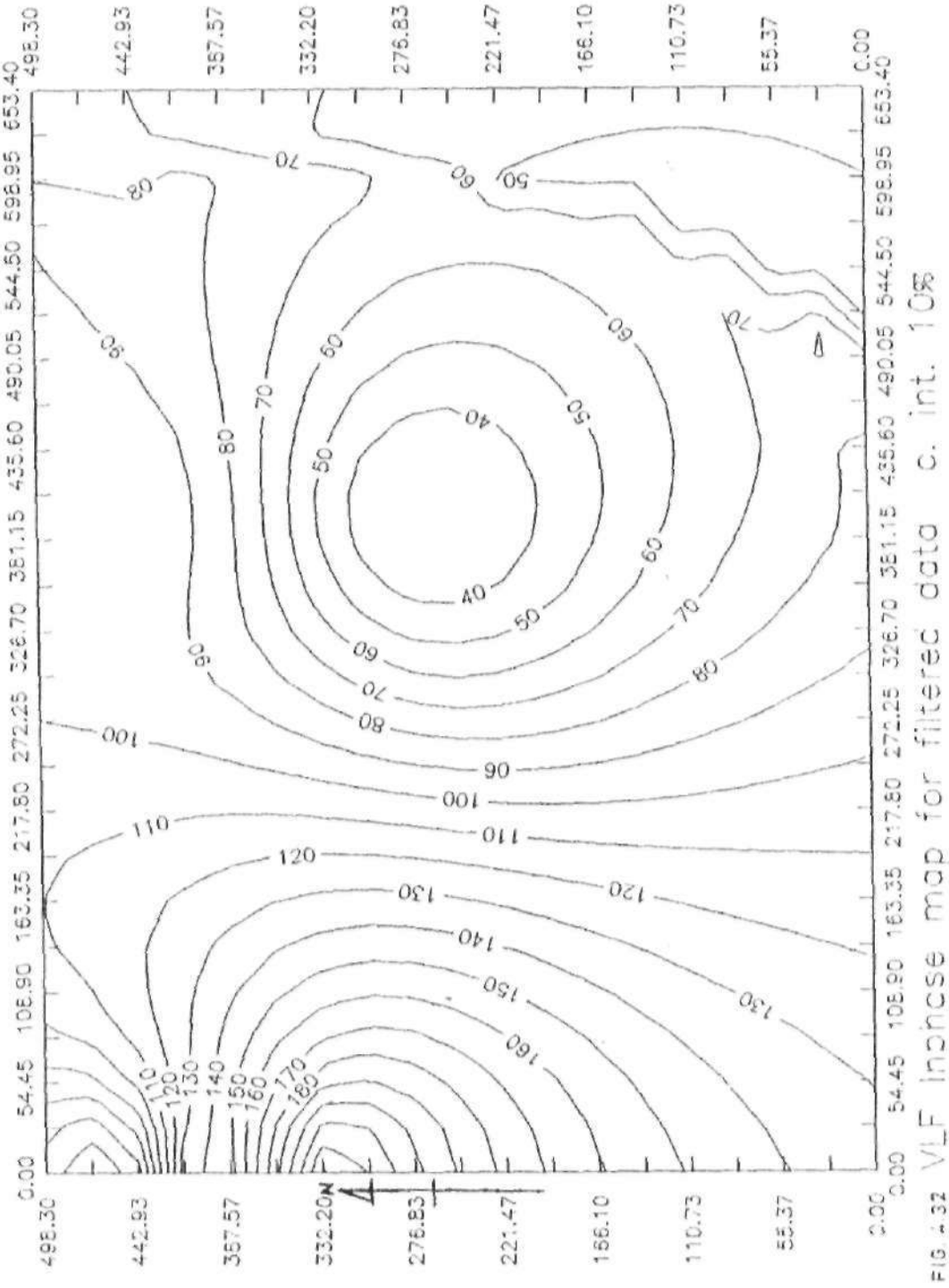


FIG. 4.32 VLF inphase map for filtered data c. int. 10%

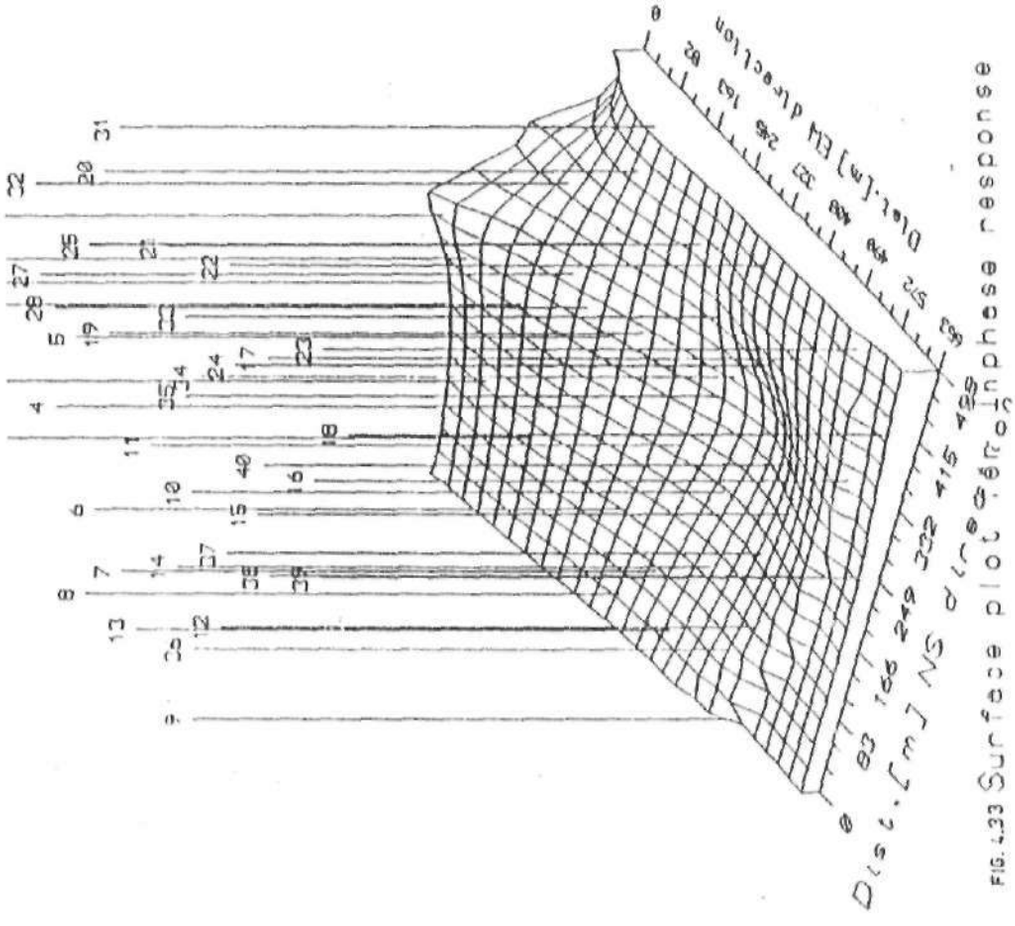


FIG. 4.33 Surface plot of broadband response

central part of the area. A hand-dug Well located closer westward, than the borehole near the school mosque (shown in figure 1.3), is also very resourceful. Also, the thickest part of the aquifer in the area as suggested by the aquifer thickness map (Figure 4.25) is located in the western part of the study area. However, the thickness reduces towards southwest (SW). This indicates low conductivity. Meanwhile, the only outcrop of granite in the area is located toward west but close to the central part of the area. A closure of a very low positive Inphase values is formed around the Eastern part of the area (Figure 4.32). This implies low conductivity. This explains why a hand-dug well located near the College poultry within this area has not been resourceful. However, the contour lines increase in value around North-Eastern part of the area. The survey area is indeed close to the confluence of Rivers Galma and Kubanni. This could have contributed to the high conductivity of the subsurface highlighted in the North-western corner of the area. The 3-D plot for inphase responses in figure 4.33 is a replica of the contour in figure 4.32 at a glance. The Figure shows a progressive decrease in the conductivity of the subsurface conductors from West to the East.

## 4.7 Correlation of Isoresistivity map with the VLF inphase Map

The VLF inphase map identifies areas where the subsurface is highly conductive as the isoresistivity map links the areas with equal resistivity values thereby presenting the resistivity distribution of the study area. This correlation will therefore show the subsurface areas with low or high conductivities. The reliability of the above will be observed by the corresponding resistivities of the areas identified through the corresponding isoresistivity plot at that point.

The correlation map produced is shown is figure 4.34. From this figure the Eastern part of the Study area have very high resistivity values. The resistivity decreases westward with lowest values along NW-SE. Coincidentally, a low conductivity is revealed towards the Eastern part of the study area by the VLF superposed map. The high conductivity originating from the Northwest extends towards South east.

## 4.8 Correlation of Aquifer thickness map with the VLF Inphase map

Figure 4.35 shows the map produced by superposition of the VLF inphase map on the Aquifer thickness map. The map is expected to show the areas of low or high conductivities as well as the thickiness of the aquifers within such area.

From figure 4.35, the high conductivity contours appear crowded towards the North-western corner of the study area dispersed southward and crowded more around VES 4, 19, 27 and 28. This area is indicated as the location of the thickest aquifer (14 m) by the Aquifer thickness contours shown on the same map.

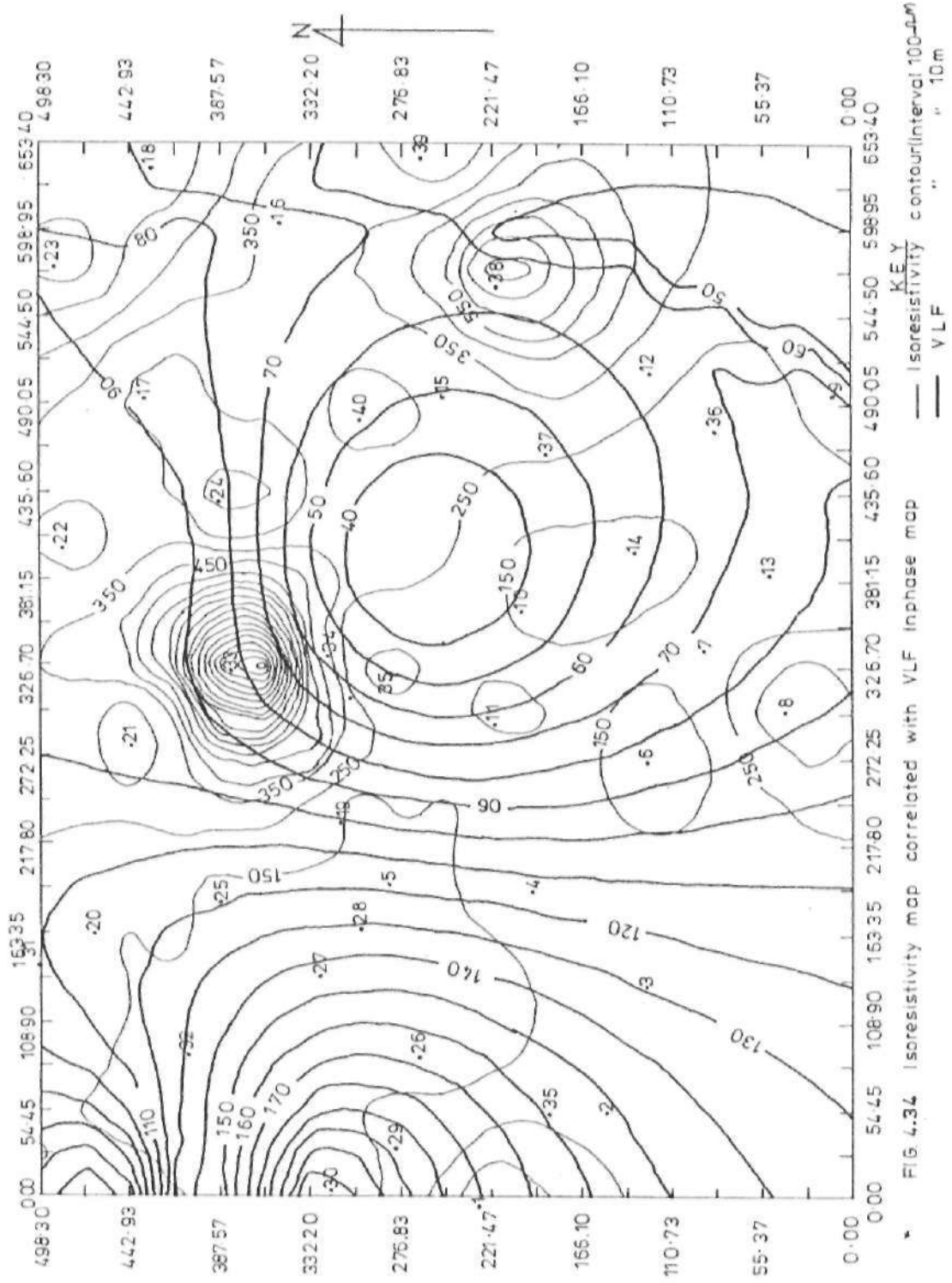


FIG. 4.34 Isoresistivity map correlated with VLF Inphase map

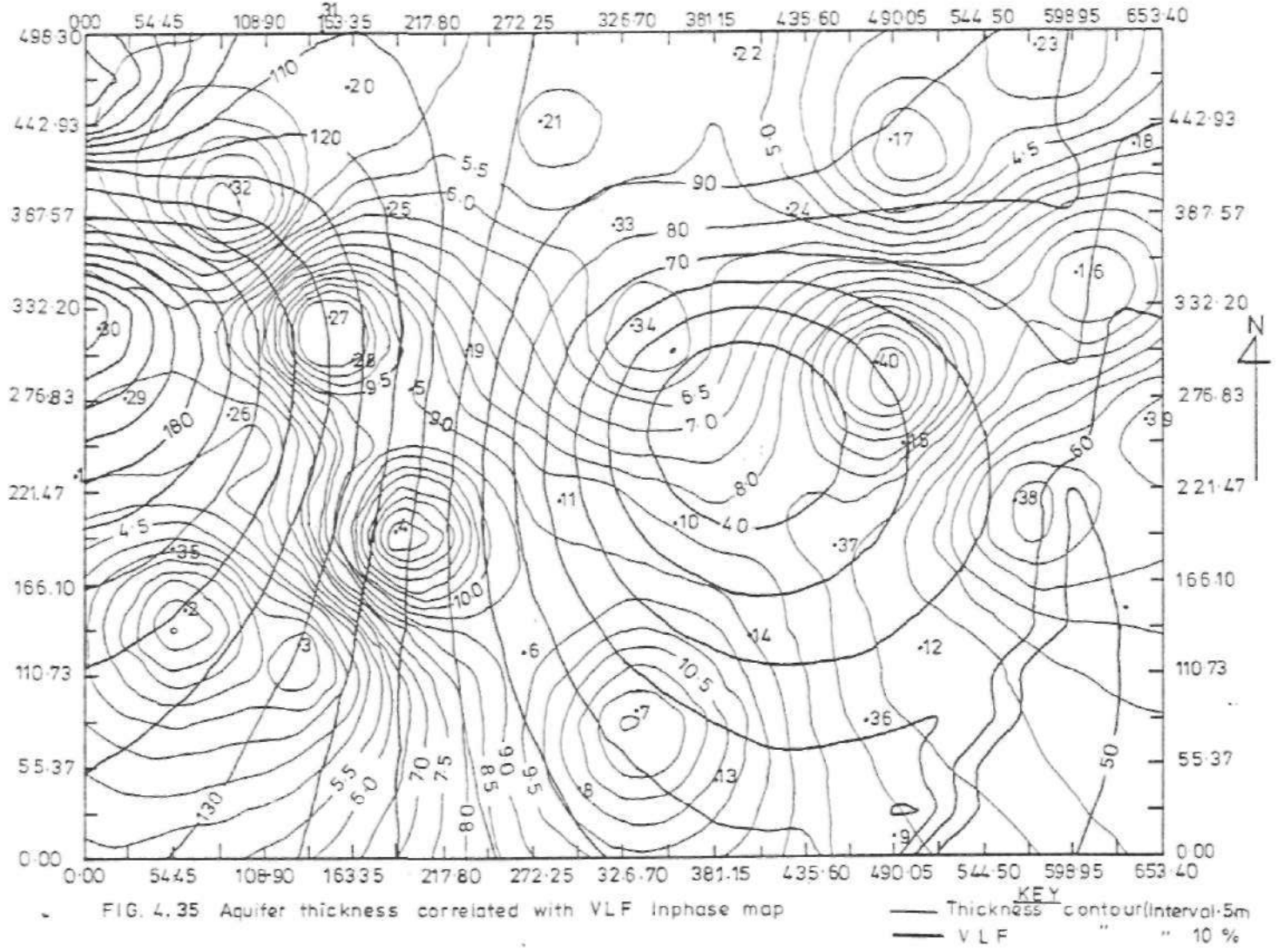


FIG. 4.35 Aquifer thickness correlated with VLF Inphase map

# CHAPTER FIVE

## DISCUSSION, CONCLUSION AND RECOMMENDATION

### 5.1 General Discussions

The aim of this work is to investigate depth to the bedrock, depth to and thickness of aquifer, depth and thickness of weathered basement, and fracture systems in the area. The two geophysical methods used (the vertical electrical sounding and electromagnetic, the VLF) were found sufficient to achieve this aim.

On the structural analysis, the vertical electrical soundings carried out at 40 stations have aided in deriving geologic sections equivalent to some geoelectric sections on chosen profiles. These revealed that there are, mostly three geologic layers beneath each VES station. A few two geologic layers were also found in some places. The predominant layers are: the topsoil consisting of clay, silt, sand and Fadama loam soil. The resistivity of this layer is as low as 30 Ohm-meters on some profiles while the thickness range is 5 to 14 m. The weathered basement forms the second layer in most of the profiles with resistivity value as low as 84 Ohm-meters on some profiles. The thickness ranges from 9 to 36.5 m. The shallowest depth is 5 m and the deepest is 14 m. The third layer is the fresh basement whose resistivity is as high as 3000 Ohm-meters.

These findings agree with the report of Bactaves Geo-Technical Services Nigeria Limited in their search for suitable location for borehole facility on the study site. Figures 4.7, 4.8 and 4.21 suggest that the basement structure is partly erosional and partly basement

depression caused by block-faulting. This agrees with earlier findings, which Shemang (1990), reported to be the existence of buried structures such as faults and fractures around west to South-western part of Kubanni basin where this present work was carried out. In the views of Hassan *et al.*, (1988) the deep seated structure is either a basement subsidence due to faulting, or an erosional surface.

The radial sounding results (Figures 4.18 and 4.19) show some prevalent structural patterns and trends which are NE-SW, NW-SE and E-W. This is evident from the changing directions of anisotropies with depth, a phenomenon which is likely to be due to faulting because one of the structural patterns, trending NE-SW, is parallel to the Funtua trans-current fault pattern which was reported by McCurry (1970) (Table 4.4). The changes in the direction of anisotropies with depth as revealed by the radial sounding results may be due to stages of tectonic activities. This can be classified as the upper anisotropy. This is associated with the upper layers (Table 4.4) and may be neotectonic in origin. Those occurring at great depth (though this did not appear in all stations, Table 4.4) can be termed lower anisotropy.

The resistivity method further revealed that the area with the shallowest depth to aquifer corresponds to the thickest aquifer, and the area with the thickest weathered basement coincides also with the area with the thickest aquifer which trends NW-SE in the western boarder of the survey area (Figures 4.23, 4.24 and 4.25). This area is likely to have the highest ground water potentials.

The VLF survey results agreed with some findings obtained with the resistivity method. The graphs of Inphase/quadrature response versus distance for all the VLF profiles

(Figures 4.30 and 4.31) suggest the presence of fractures and faults in the area. The orientations of the fractures are similar to those revealed by radial sounding results (Figure 4.25). The VLF maps revealed areas of high and low conductive subsurface materials. The most conductive area correlates well with that obtained in resistivity method, that is, NW-SE in the western part of the survey area. This corresponds to the area with highest ground-water potential (Figure 4.32). Therefore the two methods employed in this work correlate, and complement with each other.

## 5.2 Physical Events Confirming the findings in this Study

A number of events are observable in the study area which correlate with some results of this work.

The College lecture theatre is located within VES 5, 26 and 28 (Figure 4.6). The aquifer depth is about 2.6 m in this area and is about 10 m thick (Figures 4.24 and 4.25). This implies that the theatre is seated on a shallow aquifer. This is confirmed by the fact that the undergroundwater was diverted with a pipe in various directions when the construction was done. There is annual undergroundwater flow in one of the pipes left open to the surface, up to February in a year before it ceases. Also, the cement slabs on the floor of the building are usually wetted especially during the raining season.

A hand-dug well located at the back of the block of offices 2 (Figure 4.6) is 5.6 m deep. It bears water throughout the year. The greatest depth of aquifer in this area is about 4.0 m (Figure 4.24).

Figures 4.24 and 4.25 show that aquifer is almost disappearing around VES 17 and 23. Consequently, a hand-dug well belonging to Agriculture Department of the College is 11.3 m and only bears water during the rainy season yearly. Also, a borehole which is 48 m deep was recently sunk in February by the Petroleum Trust Fund (PTF) around VES 17. It is also unresourceful

## 5.3 Conclusions

In this work two methods were used; D.C. resistivity method with 40 VES points, out of which 8 were radial soundings, and VLF E-M method. The two methods correlate well going by their findings. Thus they offered complimentary solution to the problem of this investigation. Therefore, the following conclusions are drawn from this work:

The study area is mostly three-layer formation viz:- the topsoil (clay, silt, sand with fadama loam), the weathered basement and the fresh basement. This is shown in Figures 4.7 and 4.8. The topsoil has resistivity ranging from 30 to 300 Ohm-meters. The weathered basement has resistivity ranging from 84 to 480 Ohm-meters with depth ranging from 5 to 14 meters in some parts of the study area (Figures 4.23). The weathered basement is deepest around VES 4, close to the west-central part of the study area. The thickness of the weathered basement ranges from 4 m around VES 33, to 36 m around VES 4, 10, 11 and 14 (Figure 4.23). The fresh basement is 40.1 m at its deepest part. This occurs towards the eastern part of the study area.

The aquifer with the resistivity ranging from 30 to 100 Ohm-meters lies partly in the topsoil and partly in the weathered basement. Also, not all the weathered zones in the area

contain appreciable quantity of groundwater. This inference is drawn from the fact that the thickest weathered basement that occurs around VES 14 as explained in section 4.2.9 did not correspond to the thickest aquifer located around VES 4, 5, 27 and 28 as earlier explained in section 4.2.10 and shown in Figures 4.23 and 4.25.

The presence of fracturing and faulting were revealed by the existence of anisotropies in the subsurface rocks. These vary with depth and thus confirm the occurrence of tectonic activities in the study area: The major anisotropic directions are NE-SW, NW-SE and E-W. These trends are caused by near-surface features than at great depth (Table 4.4). VLF survey equally confirmed that the western part of the study area is the most promising zone for groundwater exploration. The zone is characterized by high conductivity on the VLF map (Figure 4.32). Further, fracturing and faulting were also detected as shown in Figures 4.30 and 4.31.

## 5.4 Recommendation

The investigation was accomplished on profiles at stations which are randomly chosen at areas that are yet to be physically developed. The VES profiles were sometimes oriented in the N-S direction and other times in the E-W direction. Series of extrapolations were consequently carried out in order to make some deductions. This will no doubt introduce some level of errors into the results. A more adequate process would have been to regularly grid the entire premises and locate the stations at the grids cross-over points. Two profiles trending N-S and E-W directions would have been established at each station. Average of the two data for each current electrode spacing (AB/2) would have been taken and recorded as the final data in resistivity method. A regular grid enhances good result in

VLF method too. In the alternative, profiles would have been chosen perpendicular to the commonest anisotropic direction which would have been deduced from preliminary radial sounding results. This would reduce the error due to changes in direction caused by anisotropy.

Other geophysical methods such as, seismic refraction and magnetic methods which are found to be greatly adequate in investigating the nature of subsurface materials and in determining depth to bedrock can be used to complement the methods used in this study.

Finally, the computer program used finds its unique value in the fact that the lateral extent of a target subsurface structure is readily obtained and viewed with Schlumberger array at various depth. This has eluded the necessity for resistivity profiling which would have necessitated the use of Wenner array whose field procedure is more cumbersome than Schlumberger array. However, the program only employs the apparent resistivity values for interpretation. This requires additional manual calculation of apparent resistivity using the appropriate geometric factors (K) and the resistance obtained from the Terrameter. A computer sub-routine is therefore recommended as a modification, to be incorporated in the program to automatically calculate the apparent resistivity. This will obviously reduce human errors that may occur during manual calculation.

# REFERENCES


Akpoborie, I. A. (1973): *Hydrological Control of Structures along Samaru Creek.* Unpublished B.Sc. Thesis A.B.U., Zaria.

Anneke, S. C., (1988): *A composite Geophysical Investigation of Burum Dolomitic Marble, F.C.T., Abuja.* Unpublished M.Sc. Thesis, A.B.U., Zaria.

Bactaves Geo-Technical Services Nigeria Limited, (1992): Log data for the borehole located within Federal College of Education, Zaria. Unpublished report. Nigeria.

Barker, R. D., (1989): Depth of Investigation of Collinear Symetrical four-electrode arrays. Geophysics. Vol. 54, No. 6. P. 1031 - 1037.

Danladi, G. G., (1985): *Appraisal of Hydrological Investigation in Shallow Basement Area of Zaria.* Unpublished M.Sc. Thesis, A.B.U., Zaria.

Dobrin, M. B. and Savit, C. H., (1988): *Introduction to Geophysical Prospecting. Fourth Edition.* McGraw-Hill Book Co.

Du. Preez, J. W. (1952). *The Regional Technical College Site, Zaria Water Supply.* Unpublished report. Geological Survey of Nigeria. No. 1005.

Eigbefo, C., (1978): *Hydrology of Kubanni Drainage Basin, Zaria.* Unpublished M.Sc. Thesis A.B.U., Zaria.

Fraser, D. C., (1989): *Contouring of VLF-EM Data,* Geophysics. Vol. 54. No. 2. P. 245 - 253.

Harold, E. D., (1970): *Arid Lands in Transition,* The Hornshafer Company Division of G.D.W. King Printing Co., U.S.a.

Hassan, M., (1987): *Geoelectrical Investigation of the Western Half of the Kubanni Basin, Zaria.* Unpublished M.Sc. Thesis A.B.U., Zaria.

Hassan, M., Ajayi, C. O. and Ojo, S. B., (1988): *A Basement Structure Determined from Geoelectric Mapping of the Kubanni Basin, Zaria.* Nigerian Journal of Physics.

Hockney, R. D. (1986): *The Geology of the Lokoja - Auchi Area,* Sheet 62 G.S.N. Bulletin No. 39.

Hore, P. N. (1970): *Weather and Climate: Zaria and its Region.* Ed. by M. J. Mortimore. Department of Geography, Occasional Paper No. 4 A.B.U., Zaria. P. 41 - 54.

Keary, P. and Brooks, M., (1984): *An Introduction to Geophysical Exploration Geoscience.* Text, Published by Blackwell Scientific Publications.

Klinkenbara, K., (1970): *Soil of Zaria Area.* Ed. By M. J. Mortimore. Department of Geography, Occasional Paper No. 4. A.B.U., Zaria.

Kunetz, G., (1966): *Principles of D.C. Resistivity Prospecting Geoexploration Monographs.* Series/No. 1 Gebruder Borntraeger, Berlin.

McCurry, P, (1970): *The Geology of Degree Sheet 21, Zaria.* Unpublished M.Sc. Thesis A.B.U., Zaria.

Olowu, J., (1967): *Preliminary Investigations of the Groundwater conditions in Zaria, Sheet 102 SW.* G.S.N. Report No. 1462.

Ologe, M. (1971): Geomorphology of Zaria and its region. Department of Geography Occasional Paper, A.B.U., Zaria.

Olufemi, R. O., (1985): *Hydrology of Jama'a Kubanni Area, Zaria Sheet 102 SW.* Unpublished B.Sc. Thesis A.B.U., Zaria.

Oluyide, P. O. and Udoh, A., (1986): *In Major Fracture System of Nigeria.* In Press.

Oyawoye, M. O., (1964): *Geology of Nigerian Basement Complex.* Journal of Mining and Geology. Vol. 1.

Parasnis, D. S., (1962): *Principles of Applied Geophysics,* Chapman and Hall Ltd., London.

Peter, L. J. and Bardeen, J., (1930): *Some Aspects of Electrical Prospecting Applied in Locating Oil Structures* Physics. Vol. 2. Society of Exploration Geophysicists, Tulsa Okla.

Shemang, E. M. (1990): *Electrical Depth Soundings at Selected Well Sites within Kubanni River Basin, Zaria.* Unpublished M.Sc. thesis, A.B.U., Zaria.

Telford, W. M. et. al., (1976): *Applied Geophysics.* Cambridge University Press, London.

Thorp, M. B., (1970): *Land forms and Land Scape Evolution, Zaria and its Region.* Department of Geography Occasional Paper, No. 4, A.B.U., Zaria.

Van, N.R.G. and Cerk, K. L., (1966): *Interpretation of Resistivity Data.* U.S. Geological Survey Professional papers P. 499.

Webb, P. K., (1972): *Notes on Recent Research on the Geology between Zaria and Kaduna,* Savannah, Vol. 1, No. 2.

Worthington, P. F., (1977): *Geophysical Investigation of Groundwater Resources in the Kalahari Basin,* Geophysics. Vol. 42, P. 838 - 849.

Wright, J. B. and McCurry, P. (1970): *The Geology of the Zaria Sheet 102 SW,* Zaria and its region, Ed. By M. J. Mortimore.

Zohdy, A.A.R., (1989): *A New Method for the Authomatic Interpretation of Schlumberger and Wenner Sounding Curves.* Geophysics, Vol. 54. No. 2. P. 245 - 253.